Macromolecular interactions in vitro, comparing classical and novel approaches

Christophe Velours, Magali Aumont-Nicaise, Stephan Uebel, Patrick England, Adrian Velazquez-Campoy, David Stroebel, Guillaume Bec, Pierre Soule, Christophe Quétard, Christine Ebel, et al.

European Biophysics Journal

Macromolecular interactions in vitro, comparing classical and novel approaches

--Manuscript Draft--

Manuscript Number:	EBJO-D-20-00187R1
Full Title:	Macromolecular interactions in vitro, comparing classical and novel approaches
Article Type:	S.I. : COST Action CA15126, MOBIEU: Between atom and cell
Keywords:	Molecular scale biophysics; macromolecular interactions; artificial binders; double-stranded DNA breaks repair factors
Corresponding Author:	PALOMA FERNANDEZ VARELA, Ph.D Centre National de la Recherche Scientifique FRANCE
Corresponding Author Secondary Information:	
Corresponding Author's Institution:	Centre National de la Recherche Scientifique
Corresponding Author's Secondary Institution:	
First Author:	PALOMA FERNANDEZ VARELA, Ph.D
First Author Secondary Information:	
Order of Authors:	PALOMA FERNANDEZ VARELA, Ph.D
	Christophe Velours, PhD
	Magali Aumont-Nicaise, PhD
	Stephan Uebel, PhD
	Patrick England, PhD
	Adrian Velazquez-Campoy, PhD
	David Stroebel, PhD
	Guillaume Bec, PhD
	Pierre Soule, PhD
	Christophe Quétard, PhD
	Christine Ebel, PhD
	Alain Roussel, PhD
	Jean-Baptiste Charbonnier, PhD
Order of Authors Secondary Information:	
Funding Information:	ANR (ANR-12-SVSE8-012) — Mr Jean-Baptiste Charbonnier
	ARC (SLS220120605310) — Mr Jean-Baptiste Charbonnier
	INCA DomRep (PLBIO 2012-280) — Mr Jean-Baptiste Charbonnier
	French Infrastructure for Integrated Structural Biology (ANR-10-INBS-05) — Mr Jean-Baptiste Charbonnier
Abstract:	Biophysical quantification of protein interactions is central to unveil molecular mechanisms of cellular processes. Researchers can choose from a wide panel of biophysical methods, including classical and more novel ones. A real-life proof-of-concept was carried out during an ARBRE-MOBIEU training school held in June 2019 in Gif-sur-Yvette, France. Twenty European students benefited from a one-week

	training with lessons and practical sessions on six complementary approaches: (i) Analytical UltraCentrifugation with or without a Fluorescence Detector System (AUC-FDS), (ii) Isothermal Titration Calorimetry (ITC), (iii) Size Exclusion Chromatography coupled to Multi-Angle Light Scattering (SEC-MALS), (iv) Bio-Layer Interferometry (BLI), (v) MicroScale Thermophoresis (MST) and, (vi) switchSENSE. They implemented all these methods on two examples of macromolecular interactions: firstly, a protein-protein interaction between an artificial alphaRep binder, and its target protein, also an alphaRep; secondly, a protein-DNA interaction between a DNA repair complex, Ku70/Ku80 (hereafter called Ku), and its cognate DNA ligand. The students acknowledged that the workshop provided them with a clearer understanding of the advantages and limitations of the different techniques and will help them in the future to choose the approaches that are most relevant or informative to their projects.
Response to Reviewers:	Reviewer #1: We have incorporated all of your suggestions into our revised manuscript they were very helpful. You will find below the answer to your specific comments: 1)Despite the interest of some of the drawn conclusions—and their indubitable didactical value—, the strongly promotional content of the manuscript should be tempered. For instance, Figure S1 should be removed from the paper—maybe it can be substituted for a link to the website of the course in the main text. As required Figure S1 has been removed and substituted by a link to the website of the course in the main text. 2)The need of in vitro validation of demonstrated interactions in cell is suggested in two occasions (lines 48 and 630). However, the in cell detection of an interaction constitutes a stronger evidence of its specificity. It would be more adequate to talk about in vitro characterisation, which provides structural, physical and thermodynamical details that cannot be obtained in cell (especially in a quantitative way) and are also important to understand macromolecular interactions. Now lines 49 and 688 have been corrected to describe in vitro characterization instead of validation of macromolecular interactions observed in cell. 3)More detailed explanations about the followed procedures in "Materials and methods" section would be desirable rather than general descriptions of the used techniques, so the exposed experiments can be easily reproduced. Similarly, "Samples preparation" subsection barely contains information about experimental procedures. We agree with the reviewer that more detailed explanations about the procedures are missing. A few important details have been included in the revised version. 4)Line 124 states that only the interaction between A3 and Rep17 has been studied due to its stronger character versus the one between A3 and Rep2. However, measurements on the A3-Rep2 complex are commented (312). This should be clarified. Now line 134 as required has been clarified in the text, both A3/Rep2 and A3/Rep17 interactions were measured by different methods during the preparation of the training. We chose to measure only the latter during the training because of its higher affinity. 5)Regarding binding experiments with labelled AlphaReps, some aspects about methodology and the results should be clarified. We clarified the following questions regarding coupling or labelled A3: - It seems plausible that the coupling of A3 to the DNA strand for switchSENSE (line 364) could affect the A3 binding with Rep2, positive or negatively. Has it been tested? -Now line 415: Binding of coupled A3-DNA to Rep2 was tested during the preparation of the training. The measured affinity was comparable with the values obtained previously with other methods, i.e. ITC, SPR (Léger et al., 2019). - Authors state that the used dye for MST experiments substantially improves the signal detection and protein integrity versus the one used in AUC-FDS (line 400). Then, does the latter produce protein instability? In this case, could the His-Tag Red-tris-NTA labelling used for both techniques? -Now line 448: His-Tag Red-tris-NTA labelling cannot be used for AUC-FDS

experiment, because we are out of the excitation and emission wavelengths range of the detector (488 nm and 505-565 nm, respectively).
- Authors suggest that the higher KD obtained by AUC-FDS and MST for the AlphaReps interaction could be explained by a hindrance of the interaction site caused by the fluorophore (lines 441-444). However, the KD measured by MST suffers a considerably much bigger change, in spite of the suggested greater "respect to protein integrity". Can this point be really explained by any other details? Please, discuss this point deeper.
-Upon closer inspection we would like to omit the data set on A3-Rep17 from the blue channel, this measurement does not fulfil the quality criteria applicable to MST data (S/N) and the measured KD cannot be trust it under these conditions.

6)Regarding measurements on the Ku-DNA interaction, some points about the obtained results should be clarified.

We clarified the following points regarding Ku-DNA interactions:

- Authors suggest that SEC-MALS provide peaks corresponding to Ku binding to a 42 bp DNA with both 2:1 and 1:1 stoichiometry (lines 452-459). However, in consistency with the statement of that a 42 bp DNA should bind 2 Ku heterodimers (lines 144-146), a 1:1 binding should be barely o not observed. Could this result be explained by the use of an insufficient Ku concentration (not saturating) for the complexation reaction prior to SEC?

-Now lines 153-155/lines 495-504: SEC-MALS experiments were carried out with an excess of DNA, which corresponded to the last elution peak of the chromatograms. Because, we used a sub-saturating Ku concentration, we observed two types of complexes with the 42bp DNA, comprising one or two Ku heterodimers.
- Authors expose that they were not able to obtain a well fitted model for experimental data obtained by BLI, arguing the low capability of the used model to explain a more complex binding mechanism (lines 485-489). Should the obtained binding constants be taken into account? Or measurements are only qualitative...
-Now lines 528-534: The first BLI experiments were not conclusive, as a result the obtained binding constants are only qualitative in the presented conditions. We added a sentence at the end of the corresponding paragraph to precise this point (lines 537-538).
-
7)Authors suggest that the deployed approaches allow them to "characterize the architecture" of the interactions (lines 555-557). However, no structural details or predictions about the studied complexes are provided in this article.

Now line 601: We specified the term architecture by adding “(in term of size and stoichiometry)” in the text as required.

8)In spite of the data provided by the results, a comparative discussion of the obtained KD values is not present in the manuscript. It seems essential in order to evaluate the scope of each of the presented biophysical techniques, as well as consider the use of one or another for each particular case.

We add a comparative discussion of the KD measured by the students and highlight that in the two systems studied the approaches tested allow to measured KD. We compare the difference between the maximal and minimal values obtained for each system (lines 622-630).

9)Some aspects about figures should be noted.

The following figures have been corrected:

- Abbreviations defined in the caption to figure 1 need to be revised. It contains definitions for abbreviations that are not present in the figure (i. e. MT) and it lacks definition for abbreviations that are present (i. e. MM).

-Figure 1: Abbreviations have been updated.
- Graphs in figure 3b should be more understandable. Line grids and marks have be

enlarged.
-Figure 3b: A new figure is proposed with larger line grids and marks.
- Information displayed by figure 4 should be better organised. Sample quantities have to be displayed separated for the measurable parameters or further observations.
-Figure 4: Sample quantities have been displayed separated for the measurable parameters or further observations as suggested.
- Reference to figure 2e in line 398 should be changed by figure 2f.
-Figure 2e/2f references have been corrected.

10)Overall, the use of English should be revised. For instance, some informal expressions have to be changed in order to become more polished or precise. Specially, the repeated use of "amount of material" (lines 436, 569, 579, 589) referring to quantity of sample or expressions like "the same column as above" (line 452) rather than specifying the used material should be avoided.

The use of English has been revised.
Now lines 481, 591, 633, 642 have been corrected with quantity of sample instead of amount of material.
Now line 495 has been corrected with the use material.

Reviewer #2: We thank you very much for your comments and we follow all your recommendations.
1)Several of these techniques require a concentration series - the authors have chosen well-characterised systems from their own laboratories, and so the concentration ranges employed to accurately determine binding parameters are already known. However, it might be useful for new users if the authors were to summarise (in a sentence or two) how these concentration ranges were determined. Equally, when discussing AUC the authors mention that dn/dc and UV extinction coefficients are required. Again, it might be useful for novice users if the authors summarised how these values were determined.

We summarized in a paragraph at the end of section “Sample preparation” how concentration ranges can be determined (lines 356-362).
AUC required values, dn/dc and UV extinction coefficients are now described in Materials and Methods section (lines 280-282).

2)I believe that the use of screenshots from analysis software in the figures, whilst often not appropriate, is appropriate in a review of this type. However, the authors should ensure that the resolution of the images is high enough to allow readers to read the axis labels, etc where necessary. Where this isn't possible, legible labels should be added to the figure though other means (illustrator, Inkscape etc).

A higher resolution Figure3b (SECMALS) is proposed with labels that are more legible. In MST figures, legible labels have been added.

Specific minor comments.

Minor comments have been corrected:

Figure 1 typo - Limitated -> Limited.
Figure 1 typo has been corrected.

Line 116 missing word - "New applications of these artificial binders are currently *being* explored in relation to their ability to be expressed in eukaryotic cells".

Now line 126 missing word has been added.

Line 153 typo - feedbacks -> feedback

Now line 163 typo has been corrected.

Line 283 - "In the conditions used, we assumed A3 is a monomer, as the simultaneous presence of the monomeric and dimeric forms would make the analysis difficult." - for completeness maybe expand on this with a sentence explaining how and/or why

	analysis would be difficult. An explanation about how and why the analysis of an interaction A3/Rep17 in the presence of monomeric and dimeric forms of A3 has been included in the text. (now lines 328-332) Line 301 missing words- "such as 0.1 % Tween-20, to reduce surface tension (*in the* capillaries, chip, *and* biosensors)." Now line 347 missing word has been added. Line 619 - "The MoSBio training school over a week with 20 students proved to be a very rich occasion for such discussions." - this sentence seems out of place. Perhaps it was intended to be added to the following section (Line 628)? The sentence “The MosBio training school…” has been moved to the following paragraph as suggested (now line 683). Line 636 - NMR shift mapping can also reveal residues involved in interaction surfaces. Now line 692, NMR shift mapping has been added to the text. Line 644 typo - feedbacks -> feedback Now line 701 typo has been corrected.

Dear Editors,

We are grateful that you and the reviewers appreciate the study presented in our article and give us the opportunity to send a revised version of our manuscript following the recommendations of the reviewers. You will find below a point-by-point response to the corrections asked by the reviewers. The corresponding changes in the manuscript are coloured in red in the clean version to help visualization. We would like to thank them for their careful analysis of the manuscript and their suggestions that improve the article

Reviewer #1: We have incorporated all of your suggestions into our revised manuscript they were very helpful. You will find below the answer to your specific comments:

1) *Despite the interest of some of the drawn conclusions—and their indubitable didactical value—, the strongly promotional content of the manuscript should be tempered. For instance, Figure S1 should be removed from the paper—maybe it can be substituted for a link to the website of the course in the main text.*

   As required Figure S1 has been removed and substituted by a link to the website of the course in the main text.

2) *The need of in vitro validation of demonstrated interactions in cell is suggested in two occasions (lines 48 and 630). However, the in cell detection of an interaction constitutes a stronger evidence of its specificity. It would be more adequate to talk about in vitro characterisation, which provides structural, physical and thermodynamical details that cannot be obtained in cell (especially in a quantitative way) and are also important to understand macromolecular interactions.*

   Now lines 49 and 688 have been corrected to describe in vitro characterization instead of validation of macromolecular interactions observed in cell.

3) *More detailed explanations about the followed procedures in "Materials and methods" section would be desirable rather than general descriptions of the used techniques, so the exposed experiments can be easily reproduced. Similarly, "Samples preparation" subsection barely contains information about experimental procedures.*

   We agree with the reviewer that more detailed explanations about the procedures are missing. A few important details have been included in the revised version.

4) *Line 124 states that only the interaction between A3 and Rep17 has been studied due to its stronger character versus the one between A3 and Rep2. However, measurements on the A3-Rep2 complex are commented (312). This should be clarified.*

Now line 134 as required has been clarified in the text, both A3/Rep2 and A3/Rep17 interactions were measured by different methods during the preparation of the training. We chose to measure only the latter during the training because of its higher affinity.

5) *Regarding binding experiments with labelled AlphaReps, some aspects about methodology and the results should be clarified.*

We clarified the following questions regarding coupling or labelled A3:

- It seems plausible that the coupling of A3 to the DNA strand for switchSENSE (line 364) could affect the A3 binding with Rep2, positive or negatively. Has it been tested?

- Now line 415: Binding of coupled A3-DNA to Rep2 was tested during the preparation of the training. The measured affinity was comparable with the values obtained previously with other methods, i.e. ITC, SPR (Léger et al., 2019).

- Authors state that the used dye for MST experiments substantially improves the signal detection and protein integrity versus the one used in AUC-FDS (line 400). Then, does the latter produce protein instability? In this case, could the His-Tag Red-tris-NTA labelling used for both techniques?

- Now line 448: His-Tag Red-tris-NTA labelling cannot be used for AUC-FDS experiment, because we are out of the excitation and emission wavelengths range of the detector (488 nm and 505-565 nm, respectively).

- Authors suggest that the higher KD obtained by AUC-FDS and MST for the AlphaReps interaction could be explained by a hindrance of the interaction site caused by the fluorophore (lines 441-444). However, the KD measured by MST suffers a considerably much bigger change, in spite of the suggested greater "respect to protein integrity". Can this point be really explained by any other details? Please, discuss this point deeper.

- Upon closer inspection we would like to omit the data set on A3-Rep17 from the blue channel, this measurement does not fulfil the quality criteria applicable to MST data (S/N) and the measured K_D cannot be trust it under these conditions.

6) *Regarding measurements on the Ku-DNA interaction, some points about the obtained results should be clarified.*

We clarified the following points regarding Ku-DNA interactions:

- Authors suggest that SEC-MALS provide peaks corresponding to Ku binding to a 42 bp DNA with both 2:1 and 1:1 stoichiometry (lines 452-459). However, in consistency with the statement of that a 42 bp DNA should bind 2 Ku heterodimers (lines 144-146),

a 1:1 binding should be barely o not observed. Could this result be explained by the use of an insufficient Ku concentration (not saturating) for the complexation reaction prior to SEC?

- Now lines 153-155/lines 495-504: SEC-MALS experiments were carried out with an excess of DNA, which corresponded to the last elution peak of the chromatograms. Because, we used a sub-saturating Ku concentration, we observed two types of complexes with the 42bp DNA, comprising one or two Ku heterodimers.

- Authors expose that they were not able to obtain a well fitted model for experimental data obtained by BLI, arguing the low capability of the used model to explain a more complex binding mechanism (lines 485-489). Should the obtained binding constants be taken into account? Or measurements are only qualitative...

- Now lines 528-534: The first BLI experiments were not conclusive, as a result the obtained binding constants are only qualitative in the presented conditions. We added a sentence at the end of the corresponding paragraph to precise this point (lines 537-538).
-

7) *Authors suggest that the deployed approaches allow them to "characterize the architecture" of the interactions (lines 555-557). However, no structural details or predictions about the studied complexes are provided in this article.*

Now line 601: We specified the term architecture by adding "(in term of size and stoichiometry)" in the text as required.

8) *In spite of the data provided by the results, a comparative discussion of the obtained KD values is not present in the manuscript. It seems essential in order to evaluate the scope of each of the presented biophysical techniques, as well as consider the use of one or another for each particular case.*

We add a comparative discussion of the K_D measured by the students and highlight that in the two systems studied the approaches tested allow to measured K_D. We compare the difference between the maximal and minimal values obtained for each system (lines 622-630).

9) *Some aspects about figures should be noted.*

The following figures have been corrected:

- Abbreviations defined in the caption to figure 1 need to be revised. It contains definitions for abbreviations that are not present in the figure (i. e. MT) and it lacks definition for abbreviations that are present (i. e. MM).

- Figure 1: Abbreviations have been updated.

- Graphs in figure 3b should be more understandable. Line grids and marks have be enlarged.

- Figure 3b: A new figure is proposed with larger line grids and marks.

- Information displayed by figure 4 should be better organised. Sample quantities have to be displayed separated for the measurable parameters or further observations.

- Figure 4: Sample quantities have been displayed separated for the measurable parameters or further observations as suggested.

- Reference to figure 2e in line 398 should be changed by figure 2f.

- Figure 2e/2f references have been corrected.

10) *Overall, the use of English should be revised. For instance, some informal expressions have to be changed in order to become more polished or precise. Specially, the repeated use of "amount of material" (lines 436, 569, 579, 589) referring to quantity of sample or expressions like "the same column as above" (line 452) rather than specifying the used material should be avoided.*

The use of English has been revised.
Now lines 481, 591, 633, 642 have been corrected with quantity of sample instead of amount of material.
Now line 495 has been corrected with the use material.

Reviewer #2: We thank you very much for your comments and we follow all your recommendations.

1) *Several of these techniques require a concentration series – the authors have chosen well-characterised systems from their own laboratories, and so the concentration ranges employed to accurately determine binding parameters are already known. However, it might be useful for new users if the authors were to summarise (in a sentence or two) how these concentration ranges were determined. Equally, when discussing AUC the authors mention that dn/dc and UV extinction coefficients are required. Again, it might be useful for novice users if the authors summarised how these values were determined.*

   We summarized in a paragraph at the end of section "Sample preparation" how concentration ranges can be determined (lines 356-362).
   AUC required values, dn/dc and UV extinction coefficients are now described in Materials and Methods section (lines 280-282).

2) *I believe that the use of screenshots from analysis software in the figures, whilst often not appropriate, is appropriate in a review of this type. However, the authors should ensure that the resolution of the images is high enough to allow readers to read the axis labels, etc where necessary. Where this isn't possible, legible labels should be added to the figure though other means (illustrator, Inkscape etc).*

   A higher resolution Figure3b (SECMALS) is proposed with labels that are more legible.
   In MST figures, legible labels have been added.

   Specific minor comments.

   Minor comments have been corrected:

   Figure 1 typo – Limitated -> Limited.
   Figure 1 typo has been corrected.

   *Line 116 missing word – "New applications of these artificial binders are currently *being* explored in relation to their ability to be expressed in eukaryotic cells".*

   Now line 126 missing word has been added.

   Line 153 typo – feedbacks -> feedback

   Now line 163 typo has been corrected.

Line 283 - "In the conditions used, we assumed A3 is a monomer, as the simultaneous presence of the monomeric and dimeric forms would make the analysis difficult." - for completeness maybe expand on this with a sentence explaining how and/or why analysis would be difficult.

An explanation about how and why the analysis of an interaction A3/Rep17 in the presence of monomeric and dimeric forms of A3 has been included in the text. (now lines 328-332)

*Line 301 missing words- "such as 0.1 % Tween-20, to reduce surface tension (*in the* capillaries, chip, *and* biosensors)."*

Now line 347 missing word has been added.

Line 619 - "The MoSBio training school over a week with 20 students proved to be a very rich occasion for such discussions." - this sentence seems out of place. Perhaps it was intended to be added to the following section (Line 628)?

The sentence "The MosBio training school…" has been moved to the following paragraph as suggested (now line 683).

Line 636 - NMR shift mapping can also reveal residues involved in interaction surfaces.

Now line 692, NMR shift mapping has been added to the text.

Line 644 typo - feedbacks -> feedback

Now line 701 typo has been corrected.

Macromolecular interactions *in vitro*, comparing classical and novel approaches

Christophe Velours[1,2*], Magali Aumont-Nicaise[1*], Stephan Uebel[3], Patrick England[4], Adrian Velazquez-Campoy[5,6,7,8,9], David Stroebel[10], Guillaume Bec[11], Pierre Soule[12], Christophe Quétard[13], Christine Ebel[14], Alain Roussel[15], Jean-Baptiste Charbonnier[1], Paloma Fernández Varela[1#]

[1]Université Paris-Saclay, CEA, CNRS, Institute for Integrative Biology of the Cell (I2BC), 91198, Gif-sur-Yvette, France. [2]Microbiologie Fondamentale et Pathogénicité, MFP CNRS UMR 5234, University of Bordeaux, 146 rue Léo Saignat 33076 Bordeaux, France. [3]Bioorganic Chemistry & Biophysics Core Facility, Max-Planck-Institute of Biochemistry, Martinsried, Germany. [4]Molecular Biophysics platform, Institut Pasteur, Paris, France. [5]Institute of Biocomputation and Physics of Complex Systems (BIFI), Joint Units IQFR-CSIC-BIFI, and GBsC-CSIC-BIFI, Universidad de Zaragoza, Zaragoza, 50018, Spain. [6]Departamento de Bioquímica y Biología Molecular y Celular, Universidad de Zaragoza, 50009, Zaragoza, Spain. [7]Instituto de Investigación Sanitaria Aragón (IIS Aragón), 50009, Zaragoza, Spain. [8]Centro de Investigación Biomédica en Red en el Área Temática de Enfermedades Hepáticas y Digestivas (CIBERehd), 28029, Madrid, Spain. [9]Fundación ARAID, Gobierno de Aragón, 50009, Zaragoza, Spain. [10]Institut de biologie de l'Ecole normale supérieure (IBENS), Paris, France. [11]Institut de Biologie Moléculaire et Cellulaire (IBMC), Strasbourg, France. [12]NanoTemper Technologies GmbH, Munich, Germany. [13]ForteBio-Sartorius, Dourdan, France. [14]Univ. Grenoble Alpes, CNRS, CEA, IBS, Grenoble, France .[15]Architecture et Fonction des Macromolécules Biologiques (AFMB), Marseille, France.

**Contributed equally*

#Corresponding author: paloma.fernandez-varela@i2bc.paris-saclay.fr ORCID: 0000-0001-5078-7102

Abstract

Biophysical quantification of protein interactions is central to unveil molecular mechanisms of cellular processes. Researchers can choose from a wide panel of biophysical methods, including classical and more novel ones. A real-life proof-of-concept was carried out during an ARBRE-MOBIEU training school held in June 2019 in Gif-sur-Yvette, France. Twenty European students benefited from a one-week training with lessons and practical sessions on six complementary approaches: (i) Analytical UltraCentrifugation with or without a Fluorescence Detector System (AUC-FDS), (ii) Isothermal Titration Calorimetry (ITC), (iii) Size Exclusion Chromatography coupled to Multi-Angle Light Scattering (SEC-MALS), (iv) Bio-Layer Interferometry (BLI), (v) MicroScale Thermophoresis (MST) and, (vi) switchSENSE. They implemented all these methods on two examples of macromolecular interactions: firstly, a protein-protein interaction between an artificial alphaRep binder, and its target protein, also an alphaRep; secondly, a protein-DNA interaction between a DNA repair complex, Ku70/Ku80

(hereafter called Ku), and its cognate DNA ligand. The students acknowledged that the workshop provided them with a clearer understanding of the advantages and limitations of the different techniques and will help them in the future to choose the approaches that are most relevant or informative to their projects.

Keywords

Molecular scale biophysics, macromolecular interactions, artificial binders, double-stranded DNA breaks repair factors

Introduction

Macromolecular interactions play a central role in the activation/inactivation of most cellular mechanisms. These interactions can be measured *in cellulo*, or *in vitro,* and predicted *in silico*. The classical *in cellulo* methods (such as tap-tag or two-hybrid) allow large-scale studies, but in order to confirm that a direct interaction occurs between two macromolecules, quantitative *in vitro* measurements are needed. These measurements allow to characterize interactions not only in terms of affinity, but also to determine additional kinetic and thermodynamic parameters, as well as to define the hydrophobic or hydrophilic nature of the interface. They give access to the stoichiometry of the assembly and allow to map the regions involved by using different constructs or mutants. *In vitro* measurements can also be useful to evaluate the role of post-translational modifications or other regulatory events on the formation of complexes. By *in silico* docking analysis, we can predict the structure of macromolecular complexes or the impact of functional substitutions helping to optimize experimental design (Andreani and Guerois, 2014).

The original idea of the project presented here originated during the organization of a European Training School in Molecular Scale Biophysics (https://mosbio.sciencesconf.org/) within the MOBIEU COST Action. We proposed to the participants to compare different techniques allowing to measure macromolecular interactions *in vitro*. Nowadays, there is a large panel of possibilities, and it becomes difficult to choose which technology will be the best adapted when embarking into a new project. Each approach presents advantages and drawbacks, and it is therefore difficult for the user to choose from the beginning which one will be most adapted to the properties of the interaction partners. In the workshop, we

focused on six approaches (Fig. 1). Choosing between the different techniques can be considered in a progressive manner. If none of the interaction partners can be easily labeled or immobilized on a surface, approaches in which the macromolecules are in solution (AUC, ITC, and SEC-MALS) should be favored (Fig. 1, top). However, several of them require large quantities of biological material. When a partner can be immobilized easily on a bio-surface, without affecting its function, approaches like BLI, switchSENSE and Surface Plasmon Resonance (SPR) will be often tested, since they offer the possibility to use small amounts of the immobilized partner (called ligand) (Fig. 1, middle). Finally, when the partners can be labeled, again without affecting their function, fluorescent probes can be grafted allowing the use of reduced amounts of material and facilitated signal analysis (AUC FDS, MST, or Microfluidic diffusional sizing (MDS)) (Fig. 1, bottom).The choice of the optimal approach may further rely on additional criteria including the solubility of the partners, the instrument environment or non-specific interactions with instrument surfaces. Finally, it should be stressed that it is preferable to perform measurements using several orthogonal techniques to fully validate and characterize a biological interaction, and specify its features, such as stoichiometry, kinetics or thermodynamics.

Figure 1. Decisional tree to help choosing the biophysical approach that best suits the study of a specific molecular interaction.

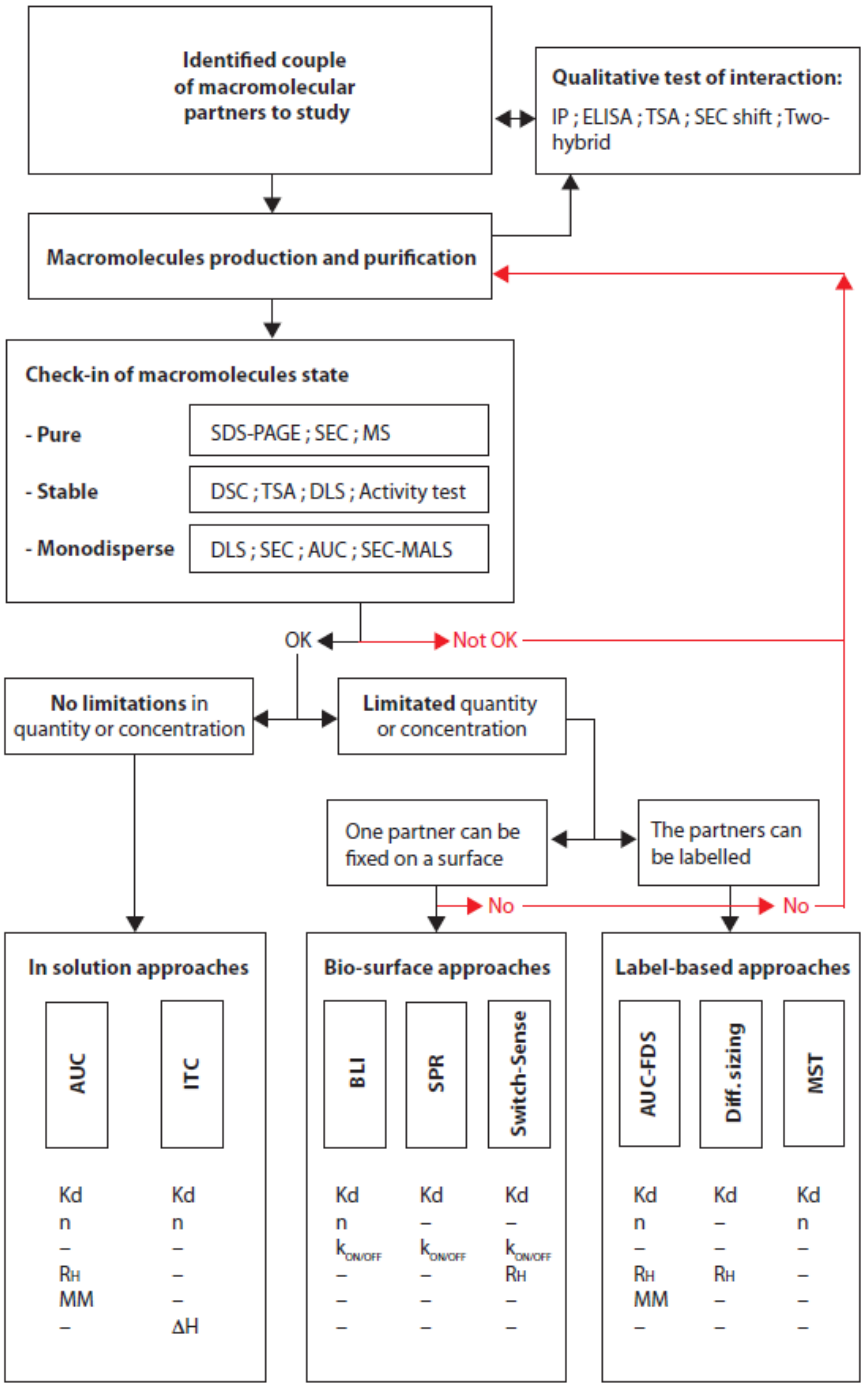

Six approaches were used in the training school. They can be classified in three main groups: measurements in solution and label free (bottom, left), on biosensor with a partner graft on a surface (bottom, middle), and methods with a partner labeled with a fluorescent probe (bottom, right). If a quality sample (pure, stable, monodisperse) is available in large quantity (up to mg amount) one may start with label-free and in solution approaches. Otherwise, if material is limited for one partner, surface approaches are a good alternative. Finally, when labeling is possible, MST and AUC-FDS are highly complementary approaches to cross-validate interactions measurements. The six approaches give access to different parameters of the interaction and present some specific limitations. AUC: Analytical Ultracentrifugation; ITC: Isothermal Titration Calorimetry, SEC-MALS: Size Exclusion Chromatography with Multi-Angle Light Scattering; BLI: Bio-Layer Interferometry; MST: MicroScale Thermophoresis; AUC-FDS: Analytical Ultracentrifugation with a Fluorescence Detector System; S: Sedimentation coefficient; KD, dissociation constant; n, stoichiometry; Dh, hydrodynamic diameter or Rh, hydrodynamic radius; kON, kOFF; association and dissociation rates; MT mass transport.

In this training school, we used as examples two different macromolecular interactions systems, that have been well characterized in our laboratories using several of the approaches discussed here. One is an interaction between two proteins, and the other a protein-DNA interaction, both with an affinity in the nanomolar range. Reference data were initially produced in our laboratories. A group of 20 participants reproduced our measurements during the five-day MoSBio Training School.

The first project comes from P. Minard's team, who uses an original family of artificial helicoidal repeat proteins, called alphaRep (Guellouz et al., 2013). AlphaRep libraries allow to select tight binders against a variety of targets by phage display. The alphaRep's are highly soluble proteins, easily expressed in *E. coli*, which display a very high thermal stability. These proteins are cysteine-free and, thus do not contain disulfide bonds. They are composed by repeated motifs made with two antiparallel alpha helices. Clusters of variable side chains, mainly in the second helix, are positioned on the same face of the motifs. The ensemble of all these variable motifs forms a library of surfaces from which tight binders can be extracted against a given target. The alphaRep's have been used for several applications, such as chaperones for crystallization and structural studies of difficult targets (Valerio-Lepiniec et al., 2015; Di Meo et al., 2017; Chevrel et al., 2018; Campanacci et al., 2019), as well as in biophysical and live cell applications (Léger et al., 2019; Prasad et al., 2019; Fernandez et al., 2020; Léger et al., 2020). New applications of these artificial binders are currently explored in relation to their ability to be expressed in eukaryotic cells. Here we analyzed the interactions between two alphaRep's (Rep2 and Rep17) selected against a protein target, (A3), which is itself an alphaRep. The interaction between the alphaReps has been extensively characterized before in the laboratory by ITC, SEC-MALS and AUC, but also by Circular Dichroism (CD), SPR and Fluorescence Resonance energy Transfer (FRET) (not used in this training school) (Guellouz et al.,2013; Di Meo et al., 2017; Léger et al., 2019). Both A3 / Rep2 and A3 / Rep17 interactions were tested previously to determine which one was the most appropriate for the training, and the former is weaker than the latter. During the training only A3 / Rep17 interaction was measured.

The second project comes from J.B. Charbonnier's team. It concerns proteins involved in DNA repair, and more precisely, in the classical Non-Homologous End Joining (c-NHEJ), the main Double-Strand Break (DSB) repair pathway in human. The Ku70/Ku80 (Ku) heterodimer plays

a central role in the recognition of DSB ends, as it is the first repair factor that interacts with them. Ku binds tightly to DNA ends in a sequence independent manner thanks to its ring-shaped structure (Walker et al., 2001). Ku then iteratively recruits different NHEJ partners (ligase 4, nucleases and polymerases) (Chang et al., 2017; Frit et al., 2019). Ku also contributes to the tethering (synapse) between the two DSB ends to avoid misrepair with other DSB ends. J.B. Charbonnier's team (Tadi et al., 2016; Nemoz et al., 2018) has recently described the recruitment mechanism of some NHEJ factors by Ku at the molecular level. DSBs, despite being deleterious DNA lesions, are generated on purpose during radiotherapy or in genome editing by CRISPR-Cas9. Understanding the molecular basis of the c-NHEJ is thus central to improve these major biotechnological applications. Here we analyzed the interaction between Ku and DNA substrates of different lengths, to determine the most appropriate to the training and to study the threading of Ku on DNA. The characterization of the interaction between Ku and DNA was extensively studied in the laboratory by ITC, MST (Tadi et al., 2016; Nemoz et al., 2018; Gontier, Chapter of MiMB, *in press*), switchSENSE, AUC, BLI (data not published) and, more recently by other techniques not used during the training school (SPR, MDS or FRET). One Ku occupies about 18 bp on DNA. Several Ku molecules can thread on DNA when the size of the DNA is longer than 18bp, and a long DNA can be covered by one Ku molecule every 18bp.

We present in this article the results obtained by 20 students during a European Training School in Molecular Scale Biophysics that took place from June 3rd to 7th, 2019 at I2BC at Gif-sur-Yvette, France. We report the protocols used to analyze the two systems under study (protein/protein and protein/DNA interactions) using the six biophysical methods mentioned above. The results obtained by the students during this week are shown and compared to our previous published data when available. Finally, we compare the advantages and drawbacks of the different approaches used during this training and present some feedbacks from the students, allowing to have a global overview of the pros and cons of these six complementary biophysical approaches.

Materials and Methods

Biophysical approaches in solution that do not require labeling of an interaction partner

Size Exclusion Chromatography with Multi-Angle Laser Light Scattering detection (SEC-MALS): SEC-MALS allows to determine the absolute molar mass of the components of a protein/multiprotein sample. It indicates if elution peaks are homogenous in term of protein composition or if they are composed of mixtures, either of different oligomers or of different conformers. SEC-MALS allows size determination if an online Dynamic Light Scattering (DLS) detector is included in the setup (Folta-Stogniew, 2006). We used an HPLC system from *Shimadzu* coupled to a MALS detector (miniDAWN TREOS) plus a DLS detector (QELS), and a refractometer (optilab T-rEX) from *Wyatt technologies* (Fig. S1). To run an experiment, one needs 1 L of running buffer to equilibrate the column and detectors, and 2 mg/mL of protein (for MW of 20 kDa), down to 0.5 mg/mL if the MW is higher than 150 kDa. Depending of the column used, the volume of the sample (30 µL for Bio-SEC-3 *Agilent*, 50 µL for KW-803/804 *Shodex*, and 100 µL for Superose 6, Superdex 75 or Superdex 200 increase 10/300 GL *Cytiva*) and the time of elution can differ. A run (including an equilibration step and a control BSA sample) takes typically a few hours and consumes about 40-200 µg of sample.

Isothermal Titration Calorimetry (ITC): ITC allows the direct, and thorough thermodynamic characterization of interactions between molecules in solution with no limitation of partner size (Holdgate, 2001; Krell, 2008; Velazquez-Campoy and Freire, 2006) and without labeling. ITC is an equilibrium solution technique to quantify dissociation constants (K_D) values, but also other interaction parameters (enthalpy, entropy, stoichiometry, and heat capacity). ITC is not affected by the optical properties of the samples, but may be very sensitive to the composition of the buffer (e.g. presence of DMSO or mismatches between solutions). For the ITC experiments, we used three instrument models: VP-ITC, ITC200 and PEAQ-ITC all from *Malvern Panalytical* (Fig. S1). One of the interacting partner is placed in a cell (1.4 mL for the VP-ITC, 200 µL for the ITC200 and PEAQ-ITC) and the other in a syringe (300 µL for the VP-ITC, 40 µL for the ITC200 and PEAQ-ITC). Sequential injections are made from a syringe (5-10 µL for the VP-ITC, 1-2 µL for the ITC200 and PEAQ-ITC). In the data described here, we used 80-990 µg of the molecule in the cell, and 130-320 µg of the molecule in the syringe. The transient heat effect due to complex formation (and other potential unspecific phenomena) upon partner injection is measured as the titration progresses, from which the binding isotherm is

constructed.

Biophysical approaches with a partner immobilized on a surface

Bio-Layer Interferometry (BLI): BLI is a fast, high throughput and label-free technology for measuring biomolecular interactions analyzing the interference pattern of white light reflected from a layer of immobilized macromolecules on a biosensor tip and an internal reference (Abdiche et al., 2018). It enables real-time analysis for determination of affinity, kinetics and concentration, with one of the binding partners immobilized onto the biosensor surface (ligand) and the other in solution (analyte). This microfluidic-free technology is particularly adapted for performing binding assays in crude lysates or cell culture media. We used an Octet RED96e during the training, and previously a RED384, both from *FortéBio* (Fig. S1). We used 1-5 µg/mL of ligand to load NTA sensors for 20-120 s for low density or 120-600 s for high density, and a range of at least 7 (2-fold dilutions starting at 100-200 nM) of the analyte with an association time of 600-900 s. We consumed per run about 8 µg of protein A3, and 400 ng of 42 bp biotinylated DNA for the immobilization, and about 2-14 µg of respective analytes. The concentration of ligand could be reduced (at least by 2) in favor of a longer incubation. The consumption of the analyte, depends on the affinity of the interaction, as the concentrations used should range from K_D /20 to 10 x K_D.

switchSENSE: switchSENSE technology is based on short DNA nanolevers (48 bp in our case), which are immobilized on gold electrodes in a microfluidic channel. The intrinsically negatively charged DNA nanolevers can be electrically actuated ("switched") on the gold surface to oscillate at high frequencies (Knezevic et al., 2012). A switchSENSE microfluidic biochip contains four flow channels, each containing six gold electrodes. Switching of the DNA is mediated by alternating the voltage across the gold surface. The motion of the levers is tracked in real time (µs scale) via time-resolved single photon counting detecting a fluorescent probe present on the immobilized DNA strands. The complementary DNA strands can be cross-linked to a ligand via amine or thiol coupling or click-chemistry. By hybridization of this conjugated complementary strand to the surface-tethered DNA nanolever, the surface is functionalized with the ligand of interest. Upon binding of an analyte, the hydrodynamic friction of the levers is affected and subsequently the movement of the levers is slowed down. This change in switching speed is used by the system to determine the size (D_h) or conformational changes of ligands and complexes. The kinetics of molecular interactions (k_{ON},

k_{OFF}, K_D) can be followed using two measurement modes: dynamic or static. In the first case, analyte binding is measured through the change of the oscillation rate of the electrically actuated DNA nanolevers (changes in dynamic response). In the second case, the DNA nanolevers are kept at an upright position, in a constant electric field, and analyte in close proximity to a dye can alter the local chemical environment resulting in a fluorescence change (also called Fluorescence Proximity Sensing). Binding is then measured thanks to the fluorescence intensity variation of the functionalized nanolever. For the switchSENSE experiments, we used a DRX^2 device from *Dynamic Biosensors* with two LED light sources (for the excitation of red and green fluorophores) (Fig. S1). In all cases, a hundred µg of protein where enough to generate cross-linked complementary strands (cNL-DNA) for several round of experiments, since one measurement needs only 40 µL of 100 nM DNA-protein conjugate. A sizing measurement classically takes less than an hour. The amount of analyte needed for a kinetic experiment depends on the overall affinity, which delimits flow rates, and association/dissociation times to be used. During association, a too slow flow rate can be the cause for mass transport limitation effect and during dissociation an inadequate flow rate can result in re-binding effects. Here we used flow rates of 100-500 µL/min, association times of 80-300 s, and 1500 s of dissociation time. In sample quantities, we used 150 ng of the cross-linked ligands, and 2-20 µg of its partner for a series of 3 concentrations.

Biophysical approaches with a labeled partner

Analytical UltraCentrifugation with Fluorescence Detection (AUC-FDS): AUC is a powerful technique for the characterization of macromolecules and macromolecular self- and hetero-association processes in solution. It was used here with labeled protein or DNA, but it can be used with non-labeled material like SEC-MALS and ITC. An analytical ultracentrifuge is a high-speed centrifuge equipped with one or more detectors (absorbance/interference, fluorescence) allowing to monitor sedimentation in real time. Two types of complementary experiments can be performed, sedimentation velocity and sedimentation equilibrium (Zhao et al., 2013). Sedimentation velocity experiments allow to determine the size distribution of species, their aggregation and oligomerization, sedimentation coefficients, hydrodynamic radius, shape and molar masses, their stoichiometry and K_D (by isotherm fitting sedimentation coefficients measured at various concentrations). Sedimentation equilibrium is suited for well-defined samples, and gives molar mass and K_D information. The centrifugation speed can be

set between 600 and 260 000 g allowing to study all sizes of macromolecules. The duration of sedimentation experiments ranges from 2 h to several days (Fig. S1). For the AUC-FDS experiments we used a ProteomeLab XL-I ultracentrifuge from *Beckman Coulter* equipped with a Fluorescence Detection System (FDS) from *AVIV Instruments* (Fig. S1). A sedimentation velocity experiment requires 100-450 µL of sample at 0.3 to 1.5 OD, for absorbance/interference detection, and 5-60 nM concentration, for fluorescence detection, whereas sedimentation equilibrium requires 130 µL at 0.2 to 0.5 OD. In interference, the limit of detection is 0.1 mg/mL, but in absorbance it depends on sample extinction coefficients. To produce the data described here, we used about 1-3.5 µg of the fluorescent molecule and 8-80 µg of the non-fluorescent molecule.

Microscale Thermophoresis (MST): MST is a novel technology for the analysis of biomolecules based on the modification of fluorescence intensity induced by the temperature, due to Temperature Related Intensity Changes (TRIC) and the directed movement of particles in a microscopic temperature gradient (thermophoresis) (Asmari et al., 2018; Jerabek-Willemsen et al., 2011). Thermophoresis is influenced by a combination of changes at the level of the hydration shell, shape, charge…, (all the parameters that influence the Soret coefficient) of biomolecules, which result in differences of movement along the temperature gradient as well as the brightness of the fluorescent tag. MST provides information on the binding affinities with good accuracy and sensitivity in the pM to mM range. This technology allows immobilization-free measurement of interactions in any buffer and complex biological liquid, but requires one of the two partners to be labeled with a fluorescent dye to measure protein-protein interactions (there is also a label free instrument that detects the intrinsic fluorescence of proteins). Any size of unlabeled molecules can be used (from ions, to large proteins). We used a Monolith NT.115 blue/green and red/blue from *NanoTemper Technologies* (Fig. S1). MST experiments, performed in capillaries, require a low sample consumption (200 µL at 20 nM of the fluorescent molecule, and 20 µL of the non-fluorescent molecule at the highest concentration needed, depending on the expected K_D). To produce the data described here, we used about 50-350 ng of the fluorescent molecule and 6-12 µg of the non-fluorescent molecule.

Sample preparation

AlphaReps are recombinant proteins produced by standard overexpression procedures in

E.coli (Guellouz et al., 2013). For our experiments, we used the following alphaRep proteins: A3, which is the target and Rep17 and Rep2, which are the binders. Because A3 forms homodimers at high concentration, it was used as ligand for real-time biosensors approaches (BLI, switchSENSE) and was the labeled partner in AUC-FDS and MST experiments. In the conditions used, we assumed A3 is a monomer, as the simultaneous presence of the monomeric and dimeric forms would make the analysis difficult.

Ku is a recombinant protein produced by standard overexpression procedures in insect cells (Nemoz et al., 2018). For our experiments, we used different lengths of dsDNA depending on the assay format. Shorter DNA are not adapted for biosensor approaches, since a DNA too close to the surfaces will hinder its interaction with Ku. DNA is practical to work with, because it is easy to modify and is commercially available. For immobilized on BLI biosensors and for detection in AUC-FDS and MST, we ordered biotinylated and 5-Carbofluorescein (5-FAM)-labeled DNA oligonucleotides, respectively.

To perform biophysical characterization measurements, samples of high purity, stability and monodispersity are needed (Fig. S2). All proteins were dialyzed to eliminate glycerol from the storage buffer, which can interfere with the measurements. We chose the pH and ionic strength of the buffer for the best solubility of the samples. To simplify as much as possible, we used the dialysis buffer (20 mM Tris-HCl pH 8, 150 mM NaCl, 5 mM β-mercaptoethanol) as running buffer in most experiments. Due to the particularities of each approach and measurement devices, there are some limitation in the buffer choice. In some cases, blocking agents were required, such as 1mg/mL BSA, especially for low protein concentrations (in the nM range), to prevent surface adsorption, as well as detergents, such as 0.1 % Tween-20, to reduce surface tension (capillaries, chip, biosensors). For AUC-FDS, we had to avoid Tris-HCl or HEPES above 20 mM, which can cause problems at 230 nm wavelength, and be aware of other absorbent molecules (nucleotides, old DTT or β-mercaptoethanol). For MST experiment, we used the commercial MST buffers (50 mM Tris-HCl pH 7.4, 150 mM NaCl, 10 mM $MgCl_2$, 0.05 % Tween-20) for Ku-DNA and, Roti®-Stock 1x PBS (10 mM Na_2HPO_4, 2 mM KH_2PO_4 pH 7.6137 mM NaCl, 2.7 mM KCl, 0.005% Tween 20) for A3-Rep17. For switchSENSE sizing experiments D_h estimation, a low salt buffer is required (10 mM Tris-HCl, 40 mM NaCl, 0.05 % Tween-20, 50 µM EGTA, 50 µM EDTA).

Results

Biophysical measurements of alphaRep interactions

We characterized the interaction of A3 with its binders Rep2 and Rep17 using the following techniques presented in the Fig. 1: in solution approaches, which do not require labeling (SEC-MALS and ITC), in solution approaches that require labeled protein or DNA (MST and AUC-FDS), and surface approaches (BLI and switchSENSE). The students performed the measurements presented here during the training (Fig. 2, Fig. S3 and Table S1). The studied interactions data represent limited value due to students measuring and protein concentration as common denominators, but added benefits of putting the techniques in context. For most of them, additional measurements and controls are needed. When available, we mention the values that have been reported for some approaches in previous articles.

AlphaRep interactions measured by label free in solution approaches

Due to time limitations, the SEC-MALS experiments were performed in our platform prior to the training. We used a Superdex 200 increase 10/300 GL column (*Cytiva*), and compared three different runs with A3 alone, Rep2 alone and A3-Rep2 complex at 2 mg/mL concentration each. A3 eluted as a dimer with a molar mass of 44.8 ± 0.4 kDa and, a hydrodynamic radius of 3.0 ± 0.2 nm. Rep2 eluted as a monomer with a molar mass of 11.6 ± 0.9 kDa. The Rep2 concentration was insufficient, in view of the small molar mass, to make accurate sizing measurement by DLS. Finally, the A3-Rep2 complex eluted before the free proteins, with a molar mass of 65.5 ± 0.4 kDa and hydrodynamic radius of 4.0 ± 0.2 nm (Fig. 2b). The stoichiometry was determined by using the protein conjugate method (Loiseau et al., 2017). Accurate mass can be calculated from MALS data with this method, which uses two concentration detectors simultaneously (a refractometer and UV spectrophotometer), and information about refractive index increment (dn/dc) and UV extinction coefficient of each component. In our case, the complex corresponds to one dimer of A3 and two Rep2 molecules.

Preparatory ITC experiments were performed in our platform on a PEAQ-ITC instrument with A3 in the cell at 18 µM and Rep17 in the syringe at 187 µM (Fig. S3a). Three different groups of students did a triplicate measurement (Fig. 2c) during the training using the same

instrument. We observed bi-phasic thermograms, and isotherms were fitted using a model of two identical binding sites with cooperativity. This cooperativity could stem from the propensity of A3 to form homodimers at µM concentration as shown by SEC-MALS (Freire et al., 2009; Vega et al., 2015). We could estimate two K_D values, the first K_D corresponds to an interaction with a tight affinity (K_{D1} 0.5 - 0.7 nM) and the second one to a weaker affinity (K_{D2} 16 – 32 nM). With the obtained parameters for each site, described in the table at the bottom of thermograms, an average global affinity (Wyman and Gill, 1990) could be calculated (geometric mean of both dissociation constants: $K_{D,av} = \sqrt{K_{D1} \times K_{D2}}$), which for each assay was 3.9 nM, 3.1 nM, and 3.2 nM, close to that obtained with other techniques. Data were analyzed during the training using the Origin software and the new PEAQ ITC software for comparison.

AlphaRep interactions measured by biophysical approaches with a partner immobilized on a surface

Preliminary BLI experiments were performed before the training on an Octet RED384 instrument where His-tagged A3 protein was captured on Ni-NTA sensors at 5 µg/mL for 20 s and Rep17 concentration ranges from 200 nM to 1.56 nM. In these conditions, in which A3 is most probably in a monomeric form, the calculated kinetic rates were k_{ON} of 1.3 10^{+5} $M^{-1}s^{-1}$, k_{OFF} of 5.9 10^{-3} s^{-1} and K_D of 22.4 nM (data not shown). We observed that the fit was not correct with a single site model and that residuals showed systematic errors. During the training, a duplicate experiment was performed on an Octet RED96e in a buffer containing 1 mg/mL BSA and 0.1 % Tween-20 to limit the non-specific binding. In this case, the fitting was improved (Fig. 2d). We obtained the following preliminary values: k_{ON} of 2.6 ± 0.7 10^{+5} $M^{-1}s^{-1}$, k_{OFF} of 7.6 ± 0.7 10^{-4} s^{-1}, K_D of 3.2 ± 1.1 nM. The K_D measured from the plateau of the curve (steady state) was of 3.3 ± 0.8 nM, close to the one obtained from kinetics (Fig. S3c).

For the switchSENSE experiments, we first coupled A3 with the DNA strand (cNL-B48), which was complementary to the surface-tethered DNA strand on the chip. In this case, the surface-tethered DNA strand was labeled with a red fluorescent probe (NLB48-red dye). The DNA-protein conjugate was purified using an anion-exchange-chromatography (Fig. S3d, top left). We then hybridized the A3-cNLB48 with the NLB48 on the sensor surface at a concentration of 100 nM. The hybridization step could be monitored in real-time by measuring the

fluorescence increase (Fig. S3d, top right). Preliminary kinetic experiments were done using the dynamic mode (switching of the nanolevers) in our platform. Rep2 alphaRep was used as analyte at three different concentrations ranging from 100 nM to 11.1 nM. Preliminary kinetic rates were calculated from a global fit for the three concentrations: k_{ON} of 2.40 ± 0.05 10^{+6} $M^{-1}s^{-1}$, k_{OFF} of 6.86 ± 0.23 10^{-4} s^{-1} and K_D of 0.29 ± 0.01 nM (Fig. S3d, bottom, left). For each analyte concentration, it was possible to perform a sizing experiment to measure the hydrodynamic diameter of the ligand A3, before or after association with Rep2. The D_h of the dimeric form of A3 calculated from the crystal structure (PDB 6FT) is found to be equal to 4.8 nm. Due to protein dilution, we expect A3 to be present as a monomer on the DNA conjugated strand. Indeed, the D_h of 3.0 ± 0.1 nm measured in our switchSENSE experiments is compatible with a monomeric form of A3 (Fig. S3d, bottom, right). The D_h = 3.8 ± 0.1 nm measured for the complex A3-Rep2 corresponds to an increase of 0.8 nm when compared to the hydrodynamic diameter of the monomeric form of A3 (Fig. S3d, bottom, left). During the training, kinetic experiments in static mode (nanolevers in up position) were performed, in the same conditions as before for Rep2, but with Rep17 alphaRep as ligand. The calculated kinetic values measured in this case were in the same range than the ones obtained previously: k_{ON} of 2.35 ± 0.17 10^{+6} $M^{-1}s^{-1}$, k_{OFF} of 2.30 ± 0.34 10^{-3} s^{-1} and K_D of 0.98 ± 0.16 nM (Fig. 2e). During the training, students did not have time to run a sizing experiment.

Comparable analysis using SPR classical technology, were carried out in our platform using a ProteON XPR36 instrument from *Biorad* (data not published, Fig. S3b).

AlphaRep interactions measured by biophysical approaches with a labeled partner

Because AUC-FDS experiment were time consuming, data were collected before the training in our platform. We first labeled A3 with the dye NT495 using the commercial *NanoTemper* Monolith Protein Labeling Kit BLUE-NHS (Amine Reactive). In these conditions, we were able to use a low concentration of A3 (5 nM). At this nanomolar concentration, A3 is a monomer as observed before by switchSENSE. We used variable concentrations of Rep17 from 0.5 nM to 0.5 µM, and an An-50 Ti rotor at 42 000 rpm (130 000 g) speed. The sedimentation coefficients for A3 and A3-Rep17 complex were 2.16 ± 0.08 S and 2.96 ± 0.05 S, respectively and the calculated K_D at equilibrium was 13.4 ± 1.8 nM (Fig. 2e).

Finally, for the MST experiment, we decided to use another dye *from NanoTemper* Monolith His-Tag Labeling Kit Red-tris-NTA 2nd Generation, this site-specific non covalent labeling substantially improved the signal and respected better the integrity of protein. In this MST experiment, labeled A3 was at 70 nM, and the highest concentration of Rep17 was 8 µM. The titration curves we obtained allowed us to measure a K_D of 8.0 ± 4.3 nM (Fig. 2g). Using the labeled A3 produced for the AUC-FDS at 20 nM did not provide us with substantial results due to high inhomogeneity in the sample preparation (Fig S3e), thus leading to a strong noise and suggesting that this labeling of A3 influences the interaction on the time scale of the MST measurement. Interestingly, we observed a titration curve with a K_D at 10.5 ± 2.4 µM, which could be linked to an additional interaction between A3-Rep17 complexes at the highest Rep17 concentration of 288 µM or some steric hindrance of the fluorescent probe. Orthogonal confirmation would help to better understand the origin of this K_D difference, unfortunately none of the other approaches were performed at such high concentration.

Figure 2. Biophysical measurements of alphaRep interactions.

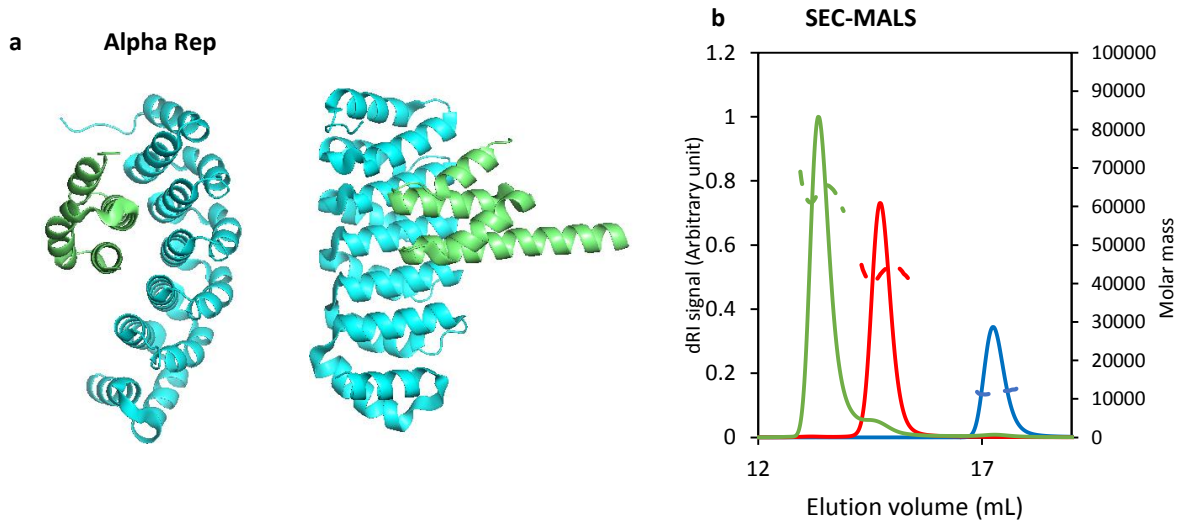

c ITC

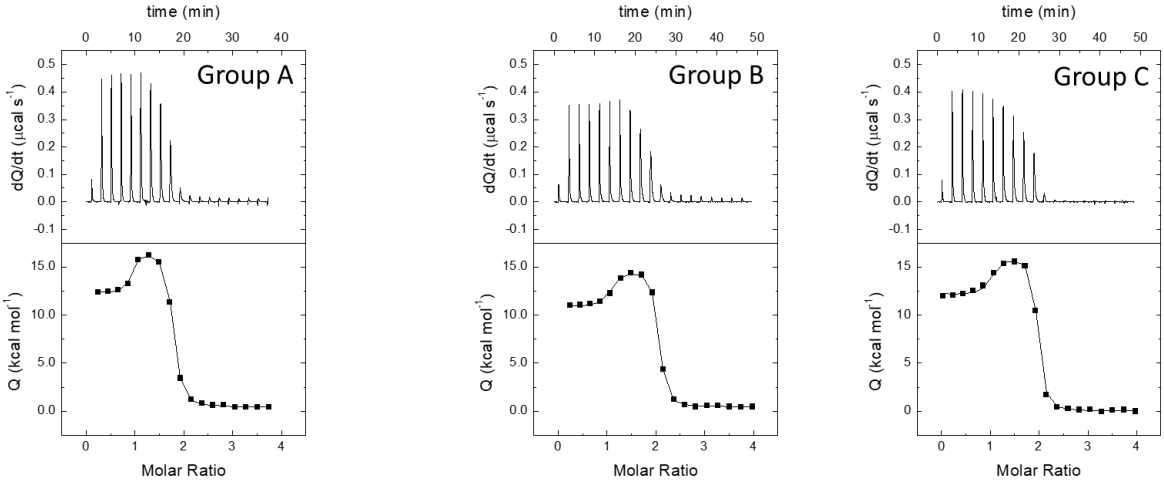

	K (M^{-1})	K_D (nM)	ΔH (kcal/mol)	α	Δh (kcal/mol)	n
Group A	$2.1 \cdot 10^9$	0.48	12.0	0.015	4.3	0.84
Group B	$1.7 \cdot 10^9$	0.59	10.5	0.036	3.6	0.98
Group C	$1.5 \cdot 10^9$	0.66	12.2	0.041	3.8	0.94

	K_{D1} (nM)	ΔH_1 (kcal/mol)	K_{D2} (nM)	ΔH_2 (kcal/mol)
Group A	0.48	12.0	32	16.3
Group B	0.59	10.5	16	14.1
Group C	0.66	12.2	16	16.0

d BLI

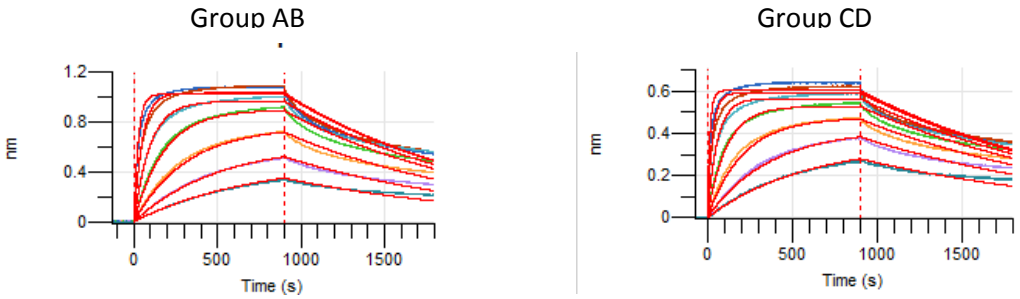

e switchSENSE

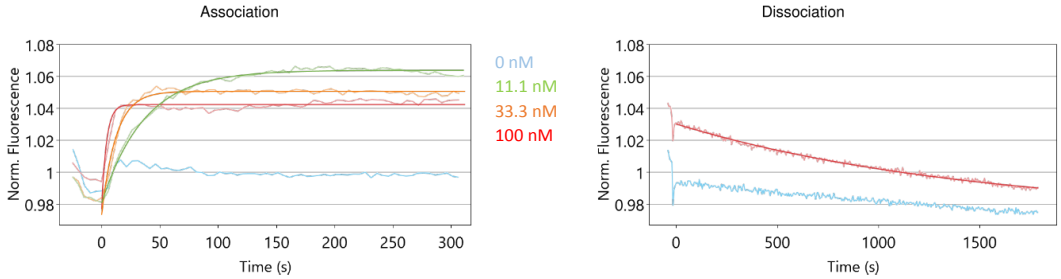

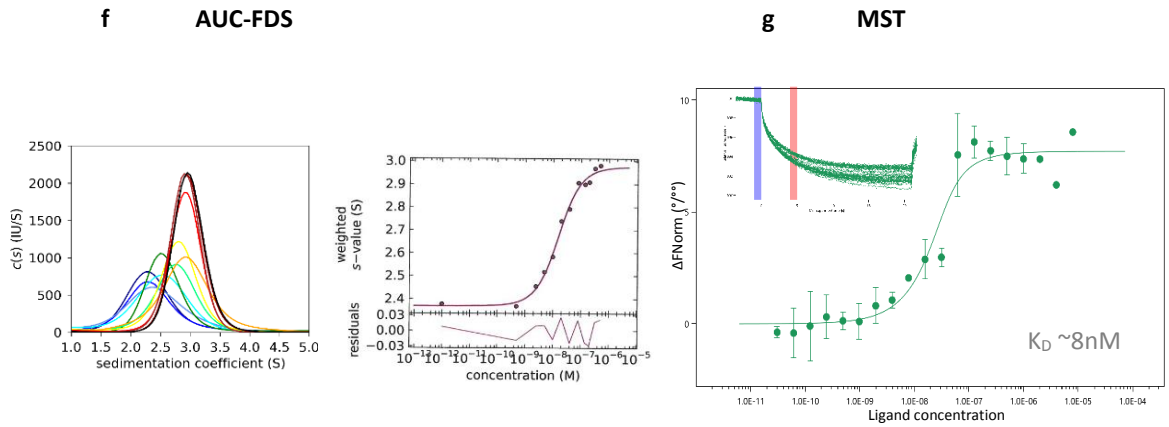

a) Crystal structure of A3 alphaRep (a-A3, blue) in complex with Rep2 (bA3-2, green) (PDB: 4JW2) at 90° view (left). b) SEC-MALS analysis. Elution profiles and molar masses of Rep2 in blue, A3 in red, and the complex of A3-dimer and two molecules of Rep2 in green. c) PEAQ-ITC data of A3-Rep17 interaction obtained during the training for three groups (A, B and C). K, K_D, and ΔH were the association constant, the dissociation constant, and the interaction enthalpy of either of the two binding sites when the A3 dimer was unoccupied. α and Δh were the cooperative interaction constant and the cooperative interaction enthalpy, which reflect the binding cooperative phenomenon (a factor that modulates the binding affinity and a term that modulates the binding enthalpy to the second site when there was a site already occupied, respectively). n was the active (or binding-competent) fraction of protein, since the stoichiometry was already included in the model. K_{D1} and ΔH_1 were the intrinsic site-specific dissociation constant and binding enthalpy for the first binding site ($K_{D1} = K_D$, $\Delta H_1 = \Delta H$). K_{D2} and ΔH_2 were the intrinsic site-specific dissociation constant and binding enthalpy for the second binding site ($K_{D2} = K_{D1} / \alpha$, $\Delta H_2 = \Delta H_1 + \Delta h$). d) Octet RED96e BLI kinetic analysis of A3-Rep17 interaction in duplicate. Colors code of Rep17 concentration: 3.13 nM (teal), 6.25 nM (purple), 12.5 nM (orange), 25 nM (green), 50 nM (cyan), 100 nM (red), 200 nM (blue). e) switchSENSE kinetics analysis of A3-Rep17 interaction on dynamic mode, at three Rep17 concentrations. Normalized association (left) and dissociation (right) data were represented in function of time. f) AUC-FDS distribution of sedimentation coefficients (left) with labeled A3 at 5 nM and increasing concentrations of Rep17 from 0.5 nM to 0.5 µM, obtained with the program SEDFIT (Schuck, 2000) and GUSSI (Brautigam, 2015). Colors code of Rep17 concentrations: 0 µM (navy blue), 0.5 nM (blue), 1 nM (cornflower blue), 2 nM (cyan), 4 nM (green), 8 nM (springgreen), 16 nM (yellow), 32 nM (orange), 64 nM (red), 128 nM (maroon), 256 nM (brown) and 0.5 µM (black). AUC-FDS K_D calculation (right), by fitting with isotherm tool in the program SEDPHAT. g) MST analysis with red fluorophore. Inset, MST traces, MST on used was 10 s (red band).

In summary, the students obtained preliminary results in one week with the six approaches that were consistent in stoichiometry, and to a lesser extent, in kinetic rates or affinity (Table S1). They could observe that the required amount of material, ligand or analyte, for each approach differs significantly. They also observed that some approaches gave highly complementary information on the system studied (Fig. S3). For example, ITC shows that the interaction is cooperative when A3 alphaRep is used at high concentration needed for ITC (18µM). This cooperativity, linked to the dimeric state of A3, was not observed with monomeric ligand immobilized on BLI or switchSENSE. They observed higher K_D values with AUC-FDS and MST, where one of the partner is labeled, reflecting possible steric hindrance between the fluorophore and the interaction site. This was particularly true with the covalent amine labeling strategy where the K_D measured by MST was three order of magnitude higher.

Biophysical measurements of Ku-DNA interactions

We determined the interaction of the heterodimeric full-length protein Ku with four double-strand DNAs (dsDNAs) of different lengths: 18 bp, 42 bp, 48 bp, and 200 bp (Fig. 3, Fig. S4). Ku binds DNA through its ring-shaped structure (Fig. 3a). The main observations made during the training for the Ku-DNA interactions, using the same six approaches, as for the alphaRep interactions, are shown in Fig. 3 and Table S2.

Ku-DNA interactions measured by label-free in solution biophysical approaches

For SEC-MALS, we used the same column as above and ran first a quadruplicate experiment with Ku alone, resulting in an average molar mass of 144.4 kDa (Fig. S4a). We then ran a duplicate experiment with Ku and a 1.2 excess of 42 bp DNA. We obtained three peaks: the first corresponded to 2 Ku : 1 DNA complex (average Mw of 306.2 kDa), the second corresponded to 1 Ku : 1 DNA (average Mw of 171.0 kDa), and the last corresponded to the excess of dsDNA alone (average Mw of 26.1 kDa). This suggests that there is an equilibrium between 2:1 and 1:1 Ku-DNA complexes (Fig. 3b) with stoichiometries determined by using the protein conjugated method (Loiseau et al.; 2017).

For ITC experiments, we used in our laboratory two different sizes of dsDNA, 18 bp and 42 bp (Gontier, Chapter of MiMB, *in press*). Due to time limitations students repeated the measurement only with the 42 bp. We used a VP-ITC instrument which consumes more sample, but was more sensitive to study these protein-DNA interactions. The heat effects were positive (endothermic interaction) and small (0.2 µcal.sec^{-1}) (Fig. 3c). Students did two runs, the first at 20 µM and the second at 40 µM concentration of DNA in the syringe, and in both cases Ku at 4 µM in the cell. We obtained a mean K_D at equilibrium of 3.7 ± 0.7 nM with a molar ratio of 0.34 ± 0.02 and a ΔH of 24.4 ± 2.7 kcal/mol. The molar ratio was in good agreement with a ratio of 0.5 expected for the interaction of two Ku molecules with a DNA of 42 bp. No evidence for cooperativity was observed. All the data were analyzed using the Origin software and the new PEAQ ITC software for comparison.

Ku-DNA interactions measured by biophysical approaches with a partner immobilized on a surface

Preparatory BLI experiments were performed on an Octet RED384 instrument. Firstly, we tried the same strategy that was used for the A3 alphaRep protein, i.e. captured Ku heterodimer on

Ni-NTA sensors. We did not observe any binding with an 18 bp DNA as analyte (data not shown). We hypothesized that the DNA binding site may not be accessible when Ku is immobilized through its His-tag. We therefore tested another strategy, which relied on the capture of a biotinylated 42 bp DNA on Streptavidin sensors (at 10 nM for 120 s), which were then incubated with Ku protein as analyte (at concentrations in 200 nM to 1.56 nM range). In these conditions, we observed an interaction, with an estimated K_D around 40 nM (data not shown). We repeated the experiment in duplicate during the training on an Octet RED96e using an optimized buffer with 1mg/mL BSA and 0.1 % Tween-20, and Ku protein concentrations ranging from 200 nM to 3 nM. The results of the two runs were consistent, with apparent kinetic rates, k_{ON} of 1.91 ± 0.02 10^{+6} $M^{-1}s^{-1}$, k_{OFF} of 7.17 ± 0.33 10^{-4} s^{-1}, and a K_D of 0.37 ± 0.01 nM (Fig. 3d). However, the deviation between the fitted curves and the experimental data was high, indicating that the interaction mechanism was more complex than a simple 1:1 binding. For instance, the association and the dissociation processes could be limited by the diffusion of Ku towards and from the biosensor surface (mass transport limitation). We therefore analyzed the concentration-dependence of the steady state responses and measured a K_D of 5.2 ± 0.2 nM (Fig. S4b). As several curves did not reached a steady state, this K_D value could however be overestimated and experiments should be reproduced with longer association times.

Preliminary switchSENSE experiments were done before the training by forming an 80 bp dsDNA on the sensor. For that, we hybridized an 80-mer DNA with a 32-mer DNA. This DNA was complementary to the NL48 ssDNA on the chip (Fig. S4c, top, left). We performed kinetic analyses in duplicate using static mode and Ku protein at 500 nM concentration. We obtained the following kinetic rates: k_{ON} of 9.3 ± 0.1 10^{+4} $M^{-1}s^{-1}$, k_{OFF} of 2.8 ± 0.1 10^{-4} s^{-1}, and K_D of 3.1 ± 0.1 nM (Fig. S4c, bottom). We monitored the dissociation over a long time (5000 s) to measure a significant proportion of dissociated Ku molecules. In between, we performed a sizing measurement. The calculated value (D_h = 8.9 ± 0.3 nm) was in good agreement with the one obtained from the crystal structure of the Ku-DNA complex (PDB: 1JEQ; D_h = 8.9 nm) (Fig. S4c, top, right). During the training, we performed experiments in dynamic mode using a 48 bp DNA (without overhang). We used Ku concentration range from 200 nM to 22.2 nM with 1/3 serial dilution this time. In these conditions, the protein was closer to the fluorophore at the tip of the 48 bp DNA on the chip. We measured in these conditions a k_{ON} of 2.6 ± 0.2 10^{+6} M^{-}

$^{1}s^{-1}$, a k_{OFF} of 2.3 ± 0.3 10^{-3} s^{-1}, and a K_D of 1.0 ± 0.2 nM (Fig. 3e). During the training, students did not have time to run a sizing experiment.

Comparable preliminary data were obtained by SPR in our platform using a ProteON XPR36 instrument from *Biorad* (Fig. S4d, left), and in Institut Pasteur platform using a Biacore T200 instrument from *Cytiva* (Fig. S4d, right).

Ku-DNA interactions measured by biophysical approaches with a labeled partner

For AUC-FDS, we used an 18 bp DNA labeled with fluorescein (FAM) in 5'. We titrated Ku protein from 0.5 nM to 0.5 µM concentrations with 60nM of DNA. The sedimentation profile showed two species, corresponding to the DNA alone (2.15 ± 0.05 S) and to the 1:1 protein-DNA complex (7.25 ± 0.15 S), and we were able to determine the K_D at equilibrium (12.9 ± 3.2 nM) (Fig. 3f).

For MST, we used the same labeled 18 bp DNA as for AUC-FDS, but at 10 nM concentration; and titrated Ku from 2 µM concentration. Training participants performed four runs in total, in duplicates or triplicate measurements (Fig. 3g). We could see some variability in the curves that might originate from the pipetting of the different students. All curves were fitted globally resulting in a K_D of 2.8 nM.

Comparable data were obtained with a novel technology, microfluidic diffusional sizing (MDS) in collaboration with Fluidic Analytics (Fig. S4e). The Fluidity One-W instrument measures the rate of diffusion of macromolecules under steady state laminar flow in a microfluidic chip. In a diffusion chamber with two parallel streams, the migration of a labeled partner depends on its size. At the end, the streams are re-split and from the ratio of the fluorescence between them, R_h is calculated. Then, changes in average size after titration of an unlabeled binding partner against the labeled partner, give a binding curve to calculate a K_D value.

Figure 3. Biophysical measurements of Ku-DNA interactions.

a **Ku-DNA**

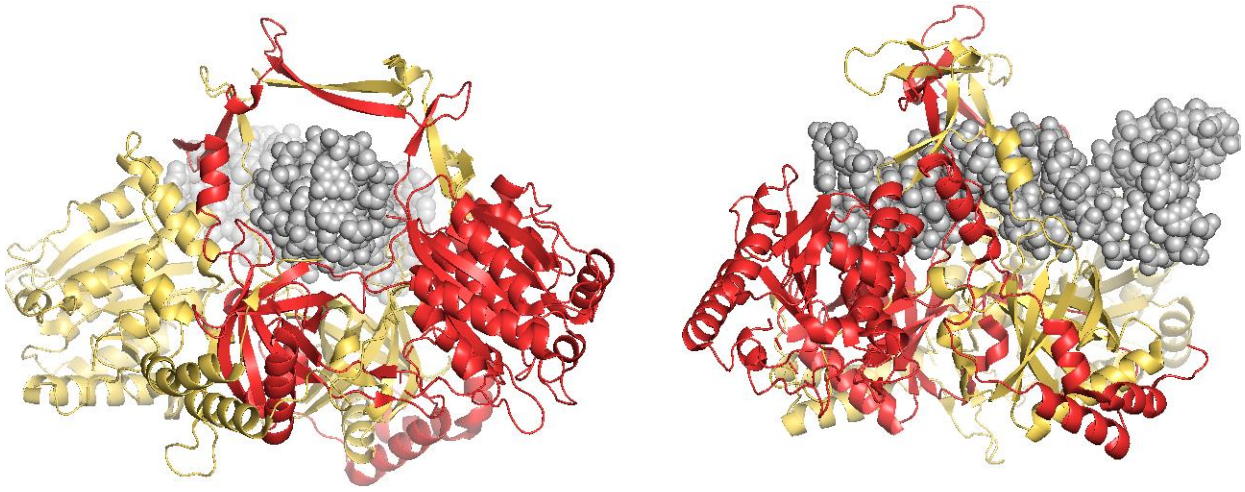

b SEC-MALS

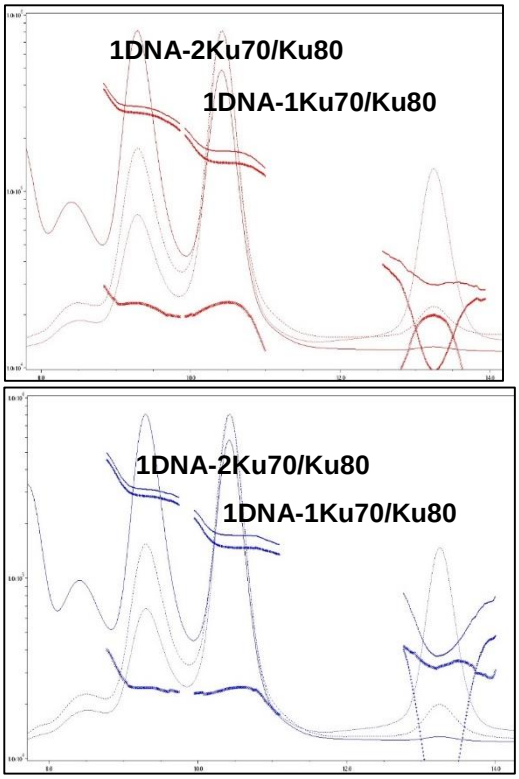

		Peak 1	Peak 2	Peak 3
Group C	**Protein molar mass**	279.1	145.7	9.6
	DNA molar mass	23.3	23.3	19.9
	Total molar mass	302.3	169.0	29.6
Group D	**Protein molar mass**	285.3	148.4	4.8
	DNA molar mass	24.7	24.6	32.3
	Total molar mass	310.1	172.9	37.1

c ITC

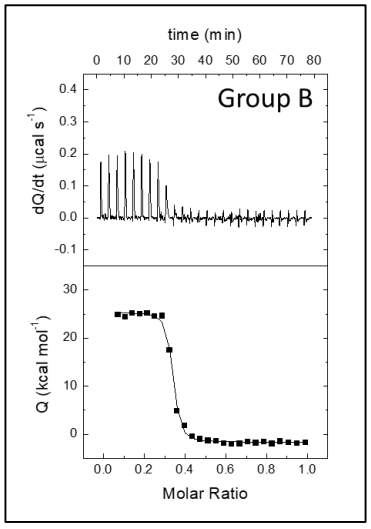

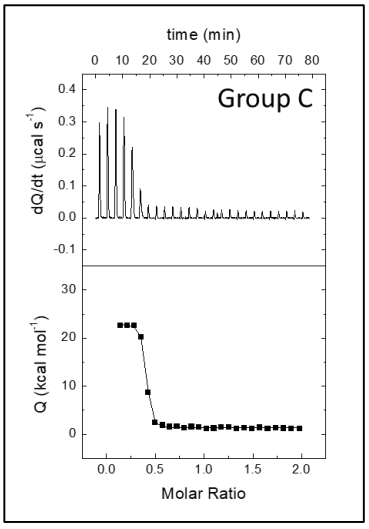

	K (M^{-1})	K_D (nM)	ΔH (kcal/mol)	n
Group B	$3.4\ 10^8$	3.0	27.1	0.32
Group C	$2.3\ 10^9$	4.3	21.7	0.37

d BLI: Group AB and Group CD

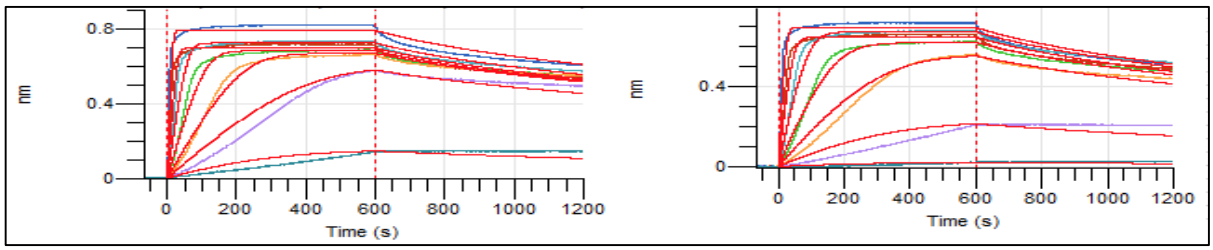

e switchSENSE

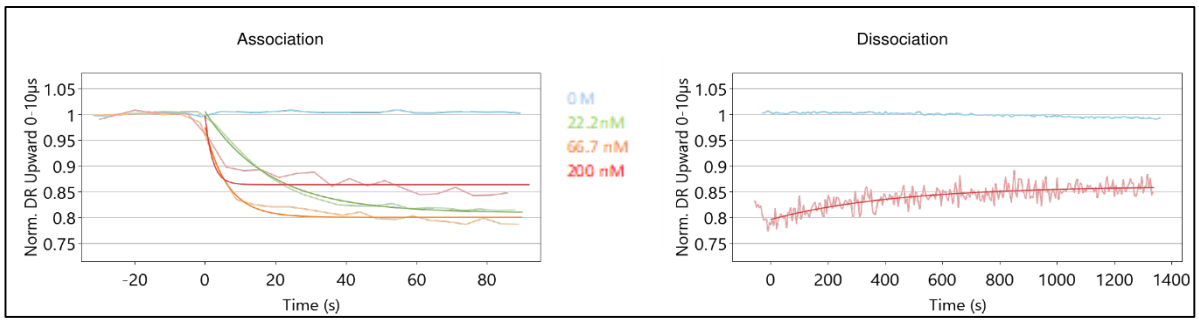

f AUC-FDS

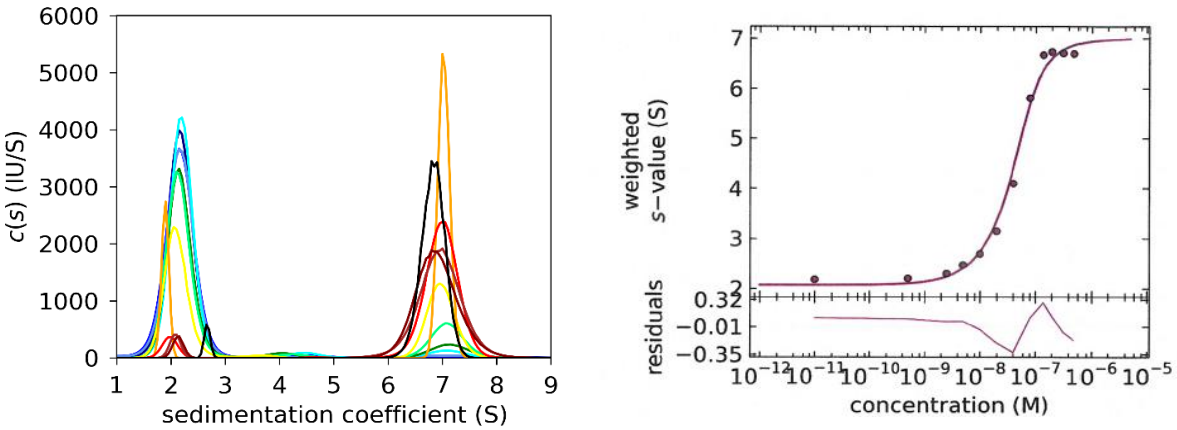

g MST

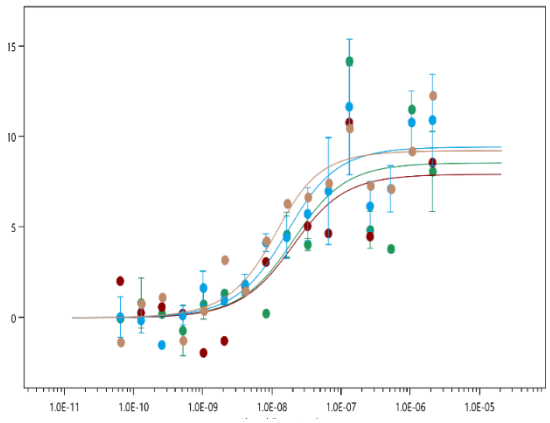

GROUPS	Excitation Power	K_D	K_D Confidence	Std. Error of Regression	Signal to Noise
A1-B1	60	$1.53\ 10^{-08}$	$1.86\ 10^{-08}$	2.77	3.33
A2	40	$1.49\ 10^{-08}$	$1.73\ 10^{-08}$	2.01	4.33
B2-C2-D2	100	$1.14\ 10^{-08}$	$7.26\ 10^{-09}$	1.61	6.31
D1	100	$6.15\ 10^{-09}$	$4.3\ 10^{-09}$	1.56	6.37

530 a) Crystal structure of the Ku- DNA complex (PDB: 1JEQ). View down the DNA helix (left) and side view (right),
531 with Ku70 colored in red, Ku80 in yellow cartoons and DNA in grey spheres. b) SEC-MALS elution profiles and

molar masses of Ku-DNA complex in duplicate. Representation of elution volumes in mL and molar mass in g/mol. c) VP-ITC data in duplicate. d) Octet RED96e BLI kinetics data in duplicate. Colors code of Ku concentration: 3.13 nM (teal), 6.25 nM (purple), 12.5 nM (orange), 25 nM (green), 50 nM (cyan), 100 nM (red), 200 nM (blue). e) switchSENSE dynamic mode data for three Ku concentrations. F) AUC-FDS measurement of Ku-DNA interaction. AUC-FDS distribution of sedimentation coefficients (left) with labeled DNA at 60 nM and increasing concentrations of Ku from 0.5 nM to 0.5 µM, obtained with the program SEDFIT (Schuck, 2000) and GUSSI (Brautigam, 2015). Colors code of Ku concentration: 0 µM (navy blue), 0.5 nM (blue), 1 nM (cornflower blue), 2 nM (cyan), 4 nM (green), 8 nM (springgreen) , 16 nM (yellow), 32 nM (orange), 64 nM (red), 128 nM (maroon), 256 nM (brown) and 0.5 µM (black). AUC-FDS K_D calculation by fitting with isotherm tool in the program SEDPHAT (right). g) MST analysis. Representation of ligand concentration against ΔFNorm °/°° (left). Superposition of several run in the similar conditions, but different excitation power and students. Summary of MST data (right).

In summary, the students obtained also for the Ku-DNA project results consistent in stoichiometry, and in the same range for kinetic rates or affinity (Fig. 3, Table S2). As for the alphaRep project, they observed that the amount of material varies between the different approaches. ITC, SEC-MALS and AUC-FDS were very efficient for measuring the stoichiometry of Ku on DNA with one Ku molecule bound every 18-21bp DNA. They observed that measurements on surfaces, either by BLI or switchSENSE, were successful only when the DNA was immobilized. They could observe that switchSENSE allows a quite accurate estimation of the Ku size (Fig. S4d, bottom). Oligonucleotides with a fluorescent probe in 5' or 3' are inexpensive and allow to follow the interaction between a fluorescent DNA and a protein quite easily by MST or AUC-FDS, without major steric hindrance between the fluorescent probe and the interaction sites.

Discussion

The study presented here compares six different *in vitro* biophysical approaches to characterize the architecture and binding parameters of two different types of complexes (protein-protein and protein-DNA). It was designed to provide a rather complete overview of six different techniques in a short period. During a week, 20 participants performed this study in the context of a MoSBio Training School (ARBRE-MOBIEU COST Action). During the first day of the training school, experts of each field presented the projects, the theory and examples of applications for the three classical techniques (AUC, SEC-MALS, ITC), and the three more recent ones (MST, BLI, switchSENSE). An additional presentation about, sample quality control, a relevant subject regarding reproducibility of experimental measurements, completed the first day training (Raynal et al., 2014). The remainder of the week was dedicated fulltime to practical sessions where the participants could perform experiments on instruments, analyze results and discuss with experts. All six approaches, except AUC, and SEC-MALS for the alphaRep interaction, were successfully used during the training school to study

two important types of macromolecular interactions (protein-protein and protein-DNA). The training allowed the students, first, to compare the quantity of material consumed for each technique, and, second, to understand the parameters that can be measured by each of them (Fig. 4). This first edition of the MoSBio Training School was positively assessed by both experts and participants. It was a unique opportunity to compare advantages and limitations of this large ensemble of techniques. A new edition will be scheduled soon. The participants were able to use all instruments quite easily by themselves, with the exception of AUC, which requires a little more expertise and longer run times. Finally, this study showed that a nanomolar range affinity is easy to be assessed with all tested techniques. Nevertheless, this is not the case when we want to measure lower K_D (pM) or higher K_D (µM) values.

The results presented here for the alphaRep-proteins and Ku-DNA complexes highlight the advantages and drawbacks of each approach. The amount of required material was not limited in our case, but the participants clearly observed that the amounts of protein and DNA used for each approach are very different (Fig. 4). AUC, SEC-MALS and ITC are the most sample-consuming techniques. ITC200 and PEAQ-ITC were an important progress for ITC in this regard, but we observed that for interactions with very weak heat exchange like Ku-DNA, the more sensitive, but more sample-consuming VP-ITC was still needed to obtain good results. Surface methods like BLI and switchSENSE require only small amounts of the immobilized protein. For the study of high affinity systems (in the nM range) like those characterized here, the consumption of analyte is small too. For weaker affinities (higher K_D in the µM range) the amount of analyte will however rise significantly to cover concentrations from 1/10 of the K_D to 10 times the K_D. The MST technique consumes very small volumes of material once the labeling step is successfully achieved. Anyway, the time and sample consumption for a given technique must be evaluated not just for a single successful experiment, but also considering the experimental design and optimization stage.

Figure 4. Comparison of results obtained for the alphaReps and the Ku-DNA interaction with the six approaches.

SEC-MALS	**AlphaReps** ✓ 200 µg A3, 200 µg Rep2 ➢ Molar mass ➢ Stoichiometry: (A3-dimer): 2 Rep2	**ITC**	**AlphaReps** ✓ 80 µg A3, 130 µg Rep17 ✓ Biphasic curve ➢ Cooperativity (A3 dimer) ➢ K_{D1}, K_{D2}, ΔH, -TΔs
	Ku-DNA ✓ 40µg of DNA, 200 µg Ku ➢ Molar mass ➢ Stoichiometry: 1 Ku /18-21 bp		**Ku-DNA** ✓ 990 µg Ku, 320 µg DNA ✓ Biphasic curve ➢ Stoichiometry: 1 Ku /18-21bp ➢ K_D, ΔH,-TΔS
BLI	**AlphaReps** ✓ 8 µg A3, 2 µg Rep17 ✓ A3-monomer ➢ K_D, k_{ON}, k_{OFF}	**switchSENSE**	**AlphaReps** ✓ 150 ng A3, 2-20 µg Rep17 ✓ A3-monomer ✓ Size (D_h) ✓ K_D, k_{ON}, k_{OFF}
	Ku-DNA ✓ 400 ng DNA, 14 µg Ku ✓ Failed with Ku immobilized ➢ K_D, k_{ON}, k_{OFF}		**Ku-DNA** ✓ 150 ng DNA, 2-20 µg Ku ✓ Ligand is the nanolever ✓ Size (D_h) ➢ K_D, k_{ON}, k_{OFF}
AUC-FDS	**AlphaReps** ✓ 1 µg A3, 8 µg Rep17 ➢ Sedimentation coefficient ➢ Stoichiometry ➢ K_D	**MST**	**AlphaReps** ✓ 620 ng A3, 6 µg Rep17 ✓ One labeling failed ➢ K_D
	Ku-DNA ✓ 3.5 µg DNA, 80 µg Ku ✓ DNA easily labeled ➢ Sedimentation coefficient ➢ Stoichiometry ➢ K_D		**Ku-DNA** ✓ 50 µg DNA, 12 µg Ku ✓ DNA easily labeled ➢ K_D

The experiments performed by the students on the two systems of study with the six approaches were successful. Quantity of materials used for the different approaches are very different. Here are the amount needed per run. The training highlighted the parameters that can be deduced from the different approaches.

All experimental approaches used in this study can provide K_D values of the interaction. Interestingly, they provide additional information that may orient the users to one or the other according to the main questions raised in their specific project. In the two examples we studied, the stoichiometry issue is an important point, since the A3 alphaRep is a dimer when its concentration is in the µM range, while it is a monomer in the nM range. According to this oligomeric state, we can observe some cooperative binding of its partner or not, or some influence on the binding parameters. In this regards, ITC, SEC-MALS and AUC allow characterizing the ratio between the dimeric alphaRep target and its binders or between Ku and DNA of increasing lengths, and confirm the information provided by their crystal

structures. The sizing measurement in switchSENSE can also provide some information regarding the stoichiometry/conformation.

Kinetic parameters are important data to estimate the half-time of a complex, which is an interaction parameter gaining attention recently. BLI and switchSENSE (as well as SPR) proved to be efficient in this study to determine k_{ON} and k_{OFF}. We observed that the switchSENSE allows to characterize very tight interactions with small k_{OFF} values (k_{OFF} about 10^{-4} s) by monitoring the dissociation over a long time period (5000 s). Thermodynamic parameters (enthalpy, entropy and Gibbs free energy) also provide key information about macromolecular interactions, notably about the polar/apolar nature of the interface between a protein and its ligand. The Ku-DNA thermograms for example indicate that the interaction is entropically driven with a positive and unfavorable enthalpy probably linked to desolvation of the DNA and Ku surface upon binding. The MoSBio training school over a week with 20 students proved to be a very rich occasion for such discussions.

The choice of one technique over another depends mainly on the questions one wants to answer. Some practical issues can also guide the choice of the method, such as the quantity and solubility of protein and ligands available, the possibility to immobilize or to label one of the interaction partners, and the time available. The presence of an instrument and experts in or nearby the user is another criterion. Noteworthy, all these approaches are available in many research institutions in Europe, especially in those engage in Structural Biology studies. If needed, these approaches are also available through network infrastructures, like Instruct in Europe or FRISBI in France. Finally, there are research networks, like ARBRE-MOBIEU, allowing and fostering fruitful exchanges with experts in the different fields.

Studying macromolecular interactions *in vitro* are extremely complementary to *in cellulo* analyses. Interactions observed in cells or in cellular extracts need often need *in vitro* validation and target engagement to confirm the specificity of the proposed interaction. Training school as the one described in this article are central to further disseminate the importance of biophysical studies in cellular biology laboratories. This training school contribute to initiate students from various fields on biophysical approaches and show in a short period the added-value of quantitative measurements of protein interactions.

By mutagenesis or HDX-MS, one can determine the residues involved in the interaction, and structural analysis can yield information about their topology. One can play with the

experimental conditions (pH, ionic strength, temperature) to expand the knowledge about the nature of the interaction under study (electrostatic and/or hydrophobic, exo- or endothermic, presence/absence of conformational changes, coupling with additional binding equilibria). Furthermore, pharmacological studies require this kind of biophysical approaches. Finally, molecular scale biophysics data can be also used to implement *in silico* simulations to predict other interactions in basic research. A second edition of this Training School will be held as soon as possible. The extremely positive feedbacks from the students, and from the academic experts and industrials participating in this school highlights the need for a better understanding of the theoretical bases and hands-on experimental practical of such a panel of biophysical methods.

References

Abdiche Y, Malashock D, Pinkerton A, Pons J.(2018) Determining kinetics and affinities of protein interactions using a parallel real-time label-free biosensor, the Octet. *Anal Biochem*. 377(2):209-17

Andreani J, Guerois R. (2014) Evolution of protein interactions: from interactomes to interfaces. *Arch Biochem Biophys*. 554:65-75

Asmari M, Ratih R, Alhazmi HA, El Deeb S. (2018) Thermophoresis for characterizing biomolecular interaction. *Methods* 146:107-119

Brautigam, CA. (2015) Chapter Five - Calculations and Publication-Quality Illustrations for Analytical Ultracentrifugation Data. In *Methods in Enzymology*, Cole, J. L., Ed. Academic Press: Vol. 562, pp 109-133

Campanacci V, Urvoas A, Consolati T, Cantos-Fernandes S, Aumont-Nicaise M, Valerio-Lepiniec M, Surrey T, Minard P, Gigant B. (2019) Selection and Characterization of Artificial Proteins Targeting the Tubulin α Subunit. *Structure*. 27(3):497-506

Chang HHY, Pannunzio NR, Adachi N, Lieber MR. (2017) Non-homologous DNA end joining and alternative pathways to double-strand break repair. *Nat Rev Mol Cell Biol* 18(8):495-506

Chevrel A, Mesneau A, Sanchez D, Celma L, Quevillon-Cheruel S, Cavagnino A, Nessler S, Li de la Sierra-Gallay I, van Tilbeurgh H, Minard P, Valerio-Lepiniec M, Urvoas A. (2018) Alpha repeat proteins (αRep) as expression and crystallization helpers. *J Struct Biol*. 201(2):88-99

Di Meo T, Ghattas W, Herrero C, Velours C, Minard P, Mahy JP, Ricoux R, Urvoas A. (2017) αRep A3: A Versatile Artificial Scaffold for Metalloenzyme Design. *Chemistry*. 23(42):10156-10166

Fernandez M, Urvoas A, Even-Hernandez P, Burel A, Mériadec C, Artzner F, Bouceba T, Minard P, Dujardin E, Marchi V. (2020) Hybrid gold nanoparticle-quantum dot self-assembled nanostructures driven by complementary artificial proteins. *Nanoscale*. 12(7):4612-4621

Folta-Stogniew E. (2006) Oligomeric states of proteins determined by size-exclusion chromatography coupled with light scattering, absorbance, and refractive index detectors. *Methods Mol. Biol. 328*, 97-112

Freire E, Schön A, Velazquez-Campoy A. (2009) Isothermal titration calorimetry: general formalism using binding polynomials. *Methods Enzymol*. 455:127-55

Frit P, Ropars V, Modesti M, Charbonnier JB, Calsou P. (2019) Plugged into the Ku-DNA hub: The NHEJ network. *Prog Biophys Mol Biol*. 147:62-76

Guellouz A, Valerio-Lepiniec M, Urvoas A, Chevrel A, Graille M, Fourati-Kammoun Z, Desmadril M, van Tilbeurgh, Minard P. (2013) Selection of Specific Protein Binders for Pre-Defined Targets from an Optimized Library of Artificial Helicoidal Repeat Proteins (alphaRep). *PLoS One*. 8(8):e71512

Holdgate GA. (2001) Making cool drugs hot: isothermal titration calorimetry as a tool to study binding energetics. *Biotechniques* 31(1):164-170

Jerabek-Willemsen M, Wienken CJ, Braun D, D, Baaske P, Duhr S. (2011) Molecular interaction studies using microscale thermophoresis. *Assay Drug Dev Technol* 9(4):342-353

Knezevic J, Langer A, Hampel PA, Kaiser W, Strasser R, Rant U. (2012) Quantitation of Affinity, Avidity, and Binding Kinetics of Protein Analytes with a Dynamically Switchable Biosurface *J. Am. Chem. Soc.* 134 (37), 15225–15228

Krell T. (2008) Microcalorimetry: a response to challenges in modern biotechnology. *Microb Biotechnol* 1(2):126-136

Léger C, Di Meo T, Aumont-Nicaise M, Velours C, Durand D, Li de la Sierra-Gallay I, van Tilbeurgh H, Hildebrandt N, Desmadril M, Urvoas A, Valerio-Lepiniec M, Minard P. (2019)

Ligand-induced conformational switch in an artificial bidomain protein scaffold. *Sci Rep*. 9(1):1178

Léger C, Yahia-Ammar A, Susumu K, Medintz IL, Urvoas A, Valerio-Lepiniec M, Minard P, Hildebrandt N. (2020) Picomolar Biosensing and Conformational Analysis Using Artificial Bidomain Proteins and Terbium-to-Quantum Dot Förster Resonance Energy Transfer. *ACS Nano*. 14(5):5956-5967

Loiseau L, Fyfe C, Aussel L, Hajj Chehade M, Hernández SB, Faivre B, Hamdane D, Mellot-Draznieks C, Rascalou B, Pelosi L, Velours C, Cornu D, Lombard M, Casadesús J, Pierrel F, Fontecave M, Barras F. (2017) The UbiK protein is an accessory factor necessary for bacterial ubiquinone (UQ) biosynthesis and forms a complex with the UQ biogenesis factor UbiJ. *J Biol Chem.* 292(28):11937-11950

Nemoz C, Ropars V, Frit P, Gontier A, Drevet P, Yu J, Guerois R, Pitois A, Comte A, Delteil C, Barboule N, Legrand P, Baconnais S, Yin Y, Tadi S, Barbet-Massin E, Berger I, Le Cam E, Modesti M, Rothenberg E, Calsou P, Charbonnier JB. (2018). XLF and APLF bind Ku at two remote sites to ensure DNA repair by non-homologous end joining. *Nat Struct Mol Biol.* 25(10):971-980

Prasad J, Viollet S, Gurunatha KL, Urvoas A, Fournier AC, Valerio-Lepiniec M, Marcelot C, Baris B, Minard P, Dujardin E. (2019) Directed evolution of artificial repeat proteins as habit modifiers for the morphosynthesis of (111)-terminated gold nanocrystals. *Nanoscale*. 11(37):17485-17497

Raynal B, Lenormand P, Baron B, Hoos S, England P. (2014) Quality assessment and optimization of purified protein samples: why and how? Microb Cell Fact. 13:180

Schuck, P. (2000) Size-distribution analysis of macromolecules by sedimentation velocity ultracentrifugation and lamm equation modeling. *Biophys. J.* 78, 1606-1619

Tadi SK, Tellier-Lebegue C, Nemoz C, Drevet P, Audebert S, Roy S, Meek K, Charbonnier JB, Modesti M. (2016) PAXX Is an Accessory c-NHEJ Factor that Associates with Ku70 and Has Overlapping Functions with XLF. *Cell Rep* 17(2):541-555

Valerio-Lepiniec M, Urvoas A, Chevrel A, Guellouz A, Ferrandez Y, Mesneau A, de la Sierra-Gallay IL, Aumont-Nicaise M, Desmadril M, van Tilbeurgh H, Minard P. (2015) The αRep artificial repeat protein scaffold: a new tool for crystallization and live cell applications. *Biochem Soc Trans*. 43(5):819-24

Vega S, Abian O, Velazquez-Campoy A. (2015) A unified framework based on the binding polynomial for characterizing biological systems by isothermal titration calorimetry. *Methods. Apr.* 76:99-115

Velazquez-Campoy A, Freire E. (2006) Isothermal titration calorimetry to determine association constants for high-affinity ligands. *Nat Protoc* 1(1):186-191

Walker JR, Corpina RA, Goldberg J. (2001) Structure of the Ku heterodimer bound to DNA and its implications for double-strand break repair. *Nature* 412(6847):607-614

Wyman J, Gill SJ. (1990) Binding and linkage: Functional chemistry of biological macromolecules. *Mill Valley, CA: University Science Books*

Zhao H, Brautigam CA, Ghirlando R, Schuck P. (2013) Overview of current methods in sedimentation velocity and sedimentation equilibrium analytical ultracentrifugation. *Curr Protoc Protein Sci*. Chapter 20

Declarations

Funding JBC is supported by ARC program (SLS220120605310), ANR (ANR-12-SVSE8-012), INCA DomRep (PLBIO 2012-280), and by the French Infrastructure for Integrated Structural Biology (FRISBI) ANR-10-INBS-05.

Conflicts of interest/Competing interests The authors declare no competing interest. Pierre Soule (NanoTemper) and Christophe Quétard (FortéBio) help during the training without commercial interest

Ethics approval Not applicable.

Consent to participate The authors consent to participate to this project.

Consent for publication The authors consent to publish the work reported in this paper.

Availability of data and material Data can be obtained by requesting the corresponding author.

Code availability Not applicable.

Authors' contributions PFV, PE, SU, CE, AVC, AR, JBC authors contributed to the study conception and design. Material preparation, data collection and analysis were performed by CV, MAN, SU, PE, AVC, DS, GB, PS, CQ, CE, AR. The first draft of the manuscript was written by PFV and all authors commented on previous versions of the manuscript. All authors read and approved the final manuscript.

Acknowledgments

We thank: members of Philippe Minard's and Jean-Baptiste Charbonnier's teams at I2BC for the sample preparation, Bruno Baron and Bertrand Raynal from *Institut Pasteur, Paris* for all their expert advices in molecular scale biophysics, and Eric Ennifar from *Institut de Biologie Moléculaire et Cellulaire, Strasbourg* for sharing its expertise in the study of biomolecular machineries using biophysical approaches. Friederike Möller and Hanna Müller-Landau from *Dynamic Biosensors*, Aymeric Audfray from Malvern Panalytical, Mathilde Belnou from *NanoTemper technologies*, and Stephanie Bourgeois and coworkers from *Fluidic Analytics* for their availability and all the fruitful discussion. We kindly thank all the participants to the MoSBio Training School, all the sponsors without whom this successful event had not been possible, and finally the keynote speakers, Julie Ménétrey and Terence Strick who shared their projects with us. Most of preparatory experiments were performed in the I2BC, PIM platform (https://www.pluginlabs-universiteparissaclay.fr/fr/results/keywords/PIM), while some others were performed in Institut Pasteur, PFBMI platform.

Supplementary material

Figures

Figure S1. Flyer of the Molecular Scale Biophysics (MoSBio):

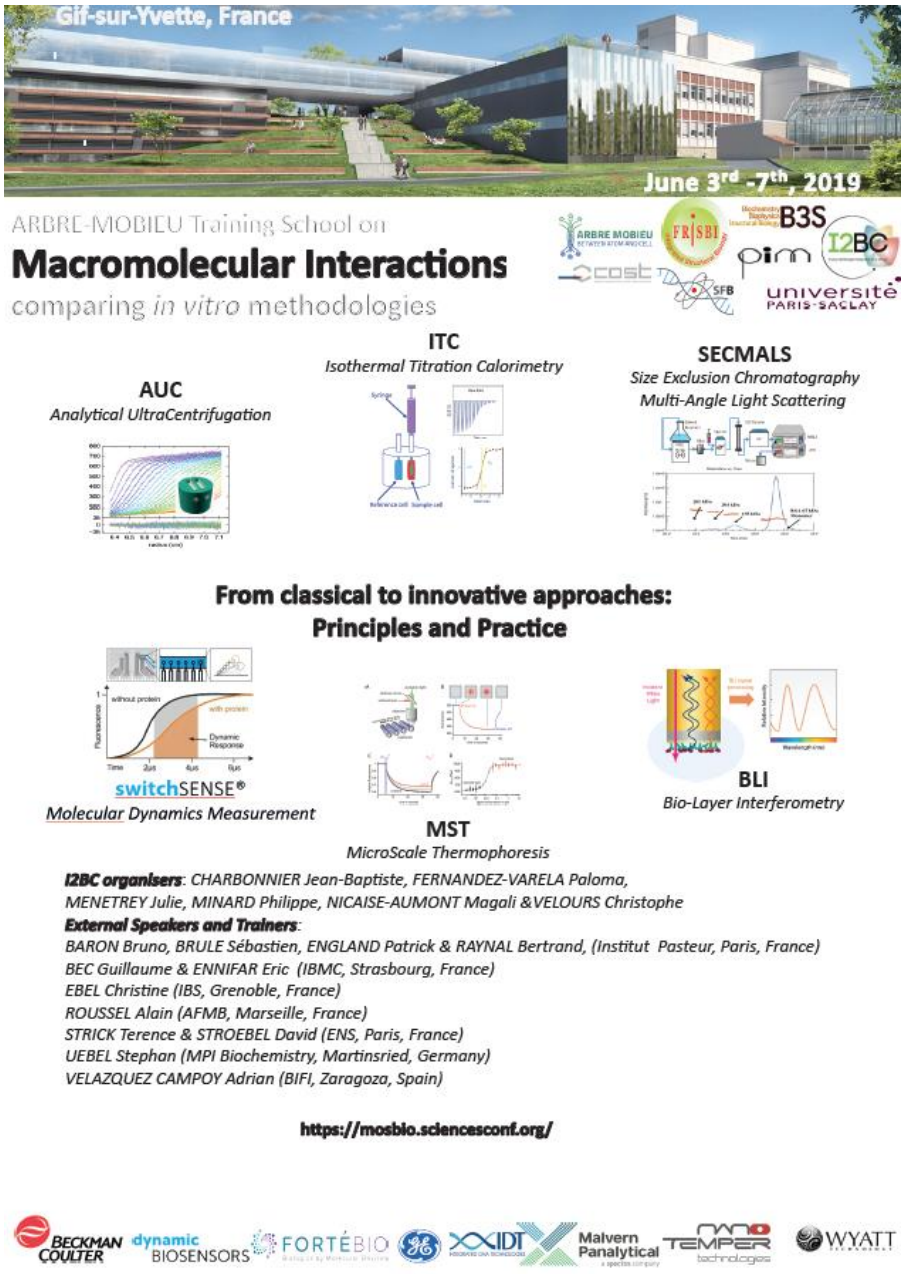

Macromolecular interactions *in vitro*, comparing classical and innovative approaches **training school.** Students during this training were able to use different approaches: Hydrodynamic (AUC-FDS, MST, SEC-MALS); Real time biosensor (BLI, switchSENSE) and Thermodynamic (ITC) to measure *in vitro* macromolecular interactions (protein-protein and protein-DNA). Experts on these approaches came from France and Europe as speakers and trainers. This event was made possible thanks to several networks and sponsors.

Figure S2. Unfolding profile plot of Ku70/Ku80.

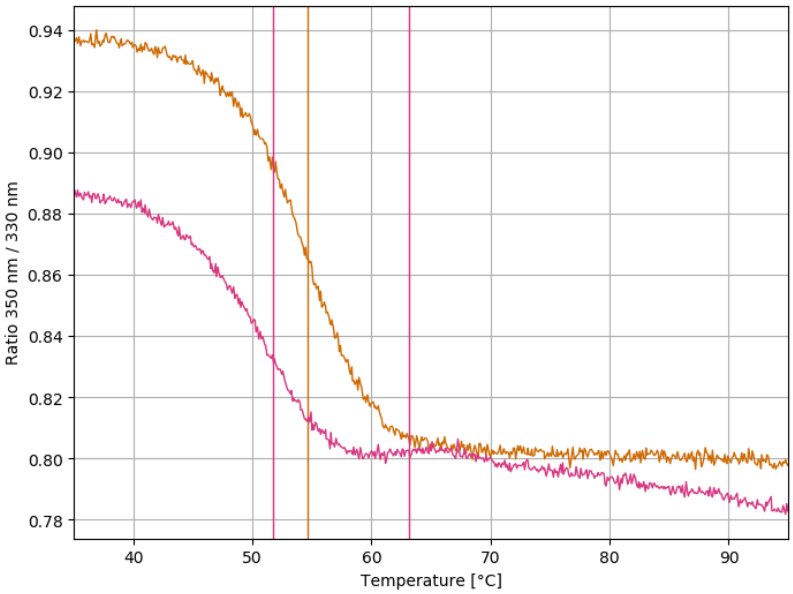

Quality and stability of samples are crucial to obtain accurate biophysical data. For all the biophysical studies shown in this manuscript, we used a full-length version of Ku (called KuFL), but for structural studies we used a shorter version where the C-terminus of each monomer is deleted (called KuCC). We took advantage of the new technology of *NanoTemper*, the Tycho NT.6 instrument, present during the training, to compare the thermal stability of these two versions of Ku protein by a fast measurement. Fluorescence intensity is recorded at 330 nm and 350 nm (emission profile of the Tryptophan residues). The brightness ratio 350 nm / 330 nm plotted against the temperature is called the unfolding profile plot and inflexion temperatures can be derived representing unfolding events. Tryptophan fluorescence of KuFL (orange) and KuCC (pink) were follow during a ramp of temperature of 35-95°C. KuFL showed a higher temperature of unfolding than KuCC (vertical bars). Thus, KuFL appears to be more stable than KuCC by a few degrees.

Figure S3. Additional biophysical measurements of alphaRep interactions.

a **ITC**

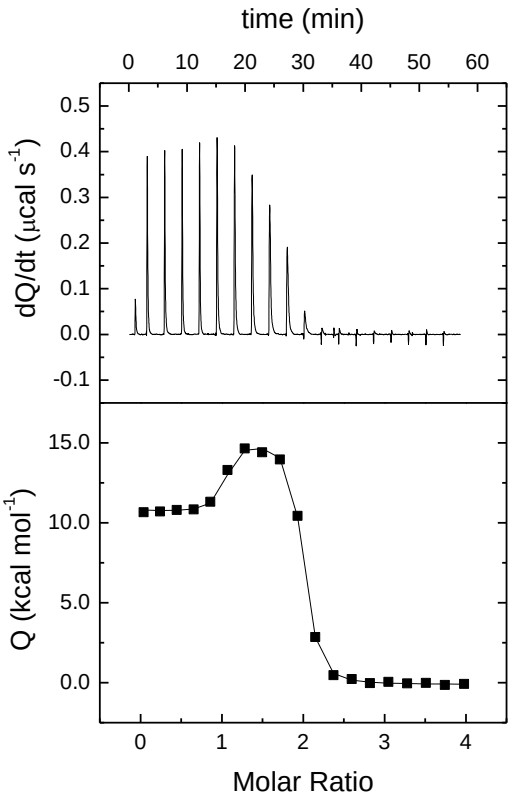

K (M^{-1})	K_D (nM)	ΔH (kcal/mol)	α	Δh (kcal/mol)	n
$1.4 \cdot 10^9$	0.71	10.9	0.024	4.4	0.95

K (M^{-1})	K_D (nM)	ΔH (kcal/mol)	α	Δh (kcal/mol)	n
$1.4 \cdot 10^9$	0.71	10.9	0.024	4.4	0.95

b **SPR**

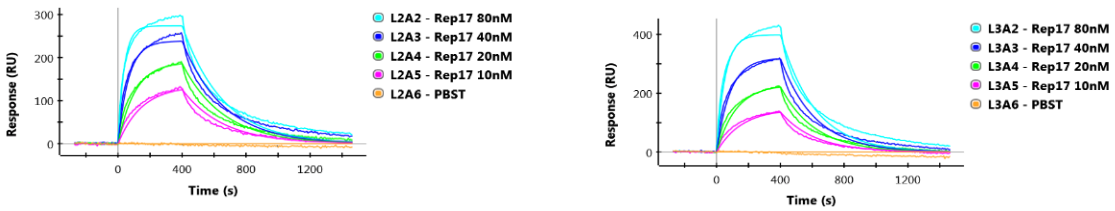

c **BLI**

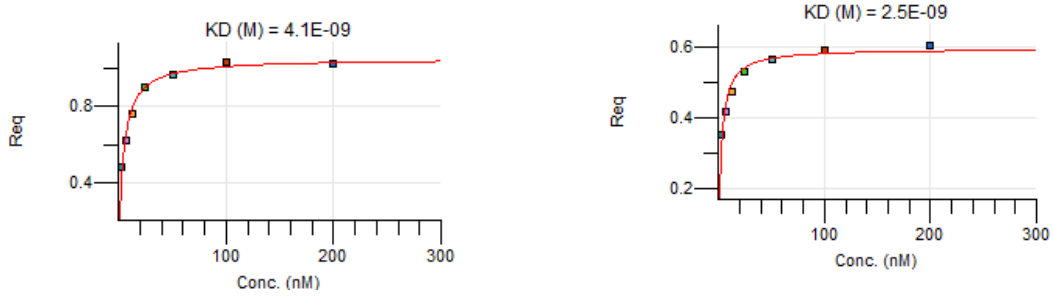

d **switchSENSE**

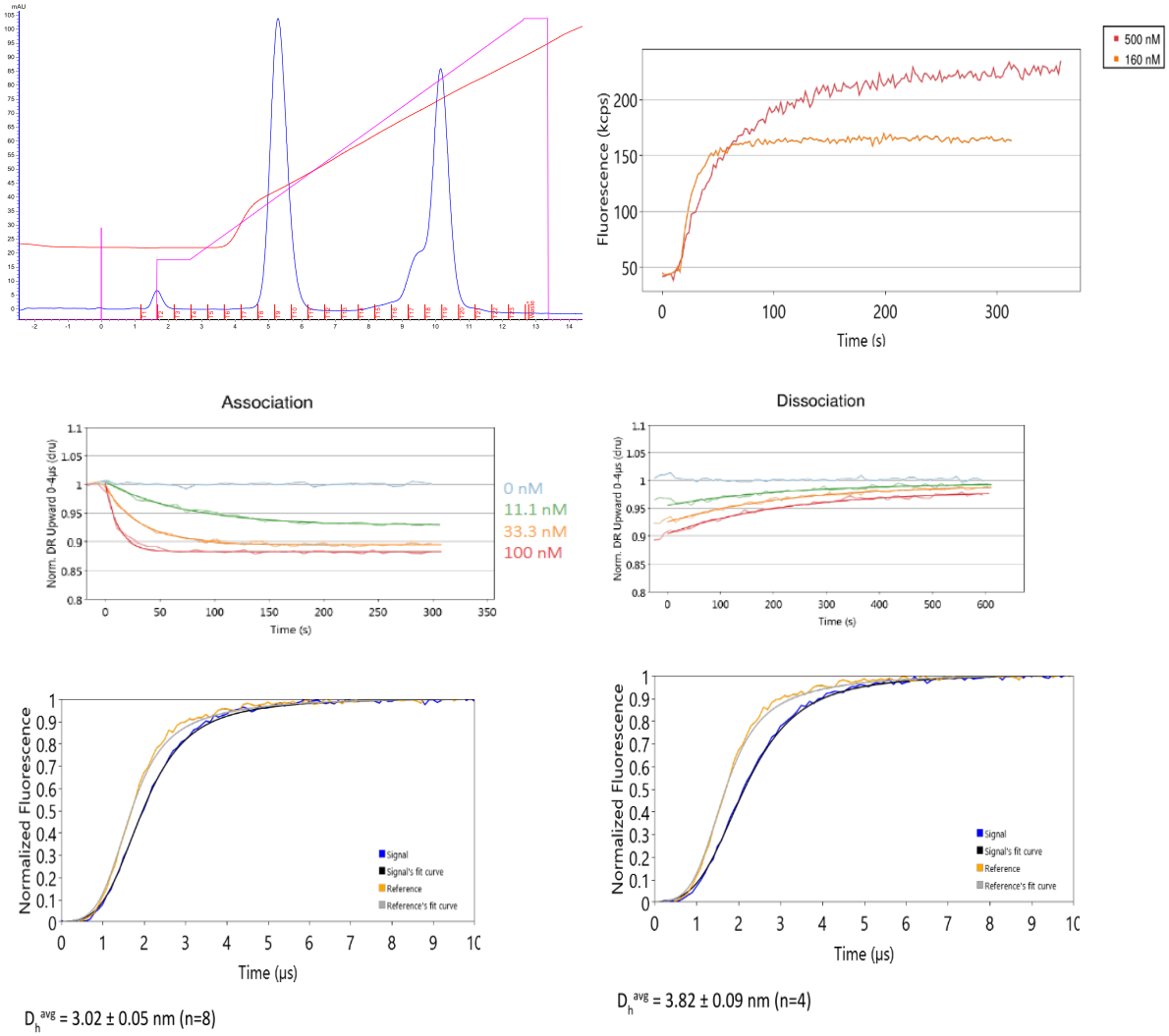

D_h^{avg} = 3.02 ± 0.05 nm (n=8)

D_h^{avg} = 3.82 ± 0.09 nm (n=4)

e **MST**

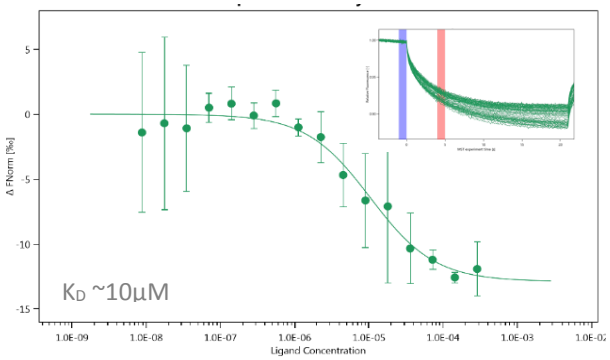

a) PEAQ-ITC data obtained before the training in our laboratory. K, K_D, and ΔH were the association constant, the dissociation constant, and the interaction enthalpy of either of the two binding sites when the dimer was unoccupied. α and Δh were the cooperative interaction constant and the cooperative interaction enthalpy, which modulate the binding cooperative phenomenon (a factor that modulates the binding affinity and a term that modulates the binding enthalpy to the second site when there was a site already occupied, respectively). n was the active (or binding-competent) fraction of protein, since the stoichiometry was already included in the model. K_{D1} and ΔH_1 were the intrinsic site-specific dissociation constant and binding enthalpy for the first binding site ($K_{D1} = K_D$, $\Delta H_1 = \Delta H$). K_{D2} and ΔH_2 were the intrinsic site-specific dissociation constant and binding enthalpy for the second binding site ($K_{D2} = K_{D1} / \alpha$, $\Delta H_2 = \Delta H_1 + \Delta h$). b) Sensograms of alphaRep A3-Rep17 interaction measured in duplicate on a ProteON XPR36 instrument from *Biorad*. For this experiment, association and dissociation times were 400 s and 1000 s, respectively with a flow rate of 50 µL/min in phosphate buffered saline with 0.1 % Tween-20 (PBST) using His-Tag capturing (HTG) chip to immobilized A3 at 6.25 or 12.5 µg/mL during 80 s (inducing 60 RU and 95 RU, respectively). Rep17 ranges from 10 to 80 nM concentration. A k_{ON} of 2.8 10^{+5} $M^{-1}s^{-1}$, a k_{OFF} of 3.9 10^{-3} s^{-1} and a K_D of 13.8 nM were measured in the first run, and a k_{ON} of 1.8 10^{+5} $M^{-1}s^{-1}$, a k_{OFF} of 4.6 10^{-3} s^{-1} and a K_D of 25.9 nM in the second one. c) Octet RED96e BLI steady-state analysis in duplicate. Colors code of Rep17 concentrations: 3.13 nM (teal), 6.25 nM (purple), 12.5 nM (orange), 25 nM (green), 50 nM (cyan), 100 nM (red), 200 nM (blue). D) Sample preparation for switchSENSE experiments. Anion-exchange chromatogram of the A3 cross-linked protein (up, left). The cross-linked protein was the shoulder of the final peak that correspond to the free DNA. Hybridization of the cross-linked ssDNA-A3 on the chip, which carries a red fluorescent probe (up, right). Red profile corresponds to the control (free cNLB48 without protein) and the orange one to the cross-linked cNLB48-A3 conjugate. switchSENSE dynamic mode data of A3-Rep2 at three concentrations (middle, left). Normalized association (left) and dissociation (right) data were represented in function of time. switchSENSE sizing measurement of A3 hydrodynamic diameter (D_h) (bottom, left), and of the A3-Rep17 complex (bottom, right). Measured signal curve is in blue (conjugated DNA), the associated fitted curve in blank, reference signal (cNLB48) is in orange, and the associated fitted curve in grey. d) MST analysis with blue fluorophore. Inset, MST traces, MST on used was 10 s (red band).

Figure S4. Additional biophysical measurements of Ku-DNA interactions.

a **SEC-MALS**

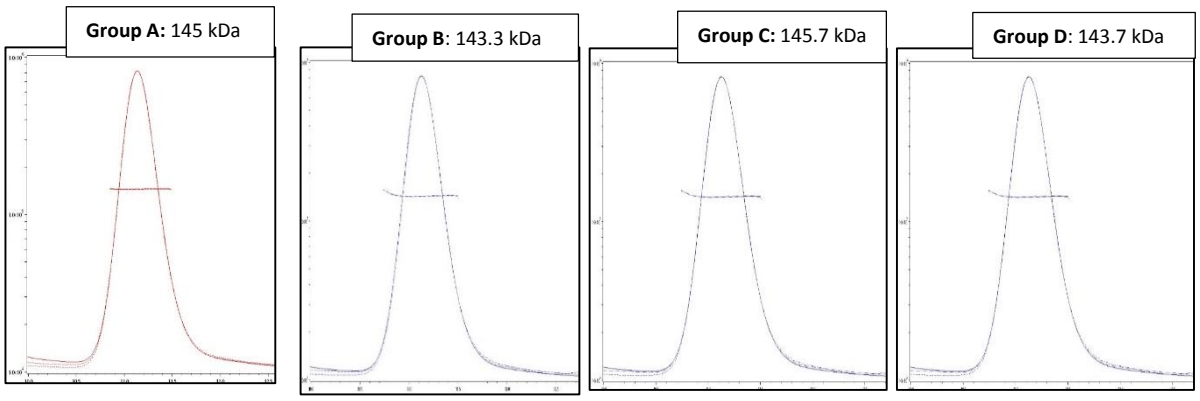

b **BLI**

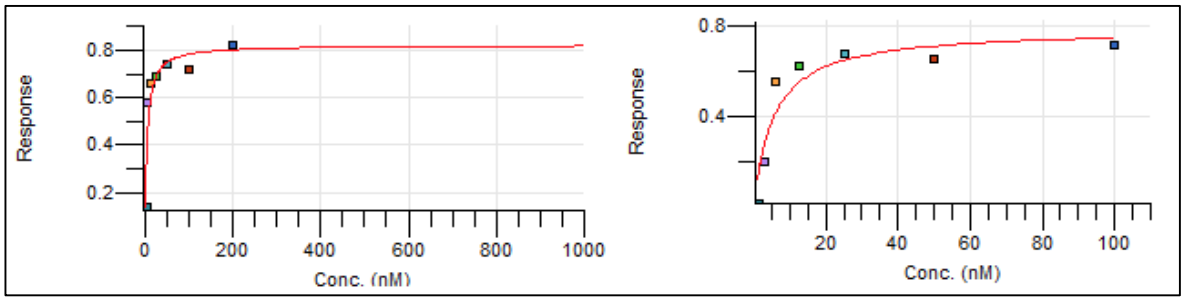

c **switchSENSE**

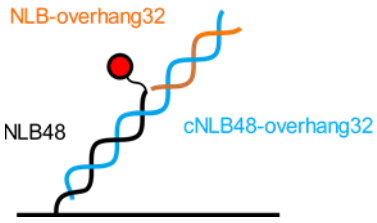

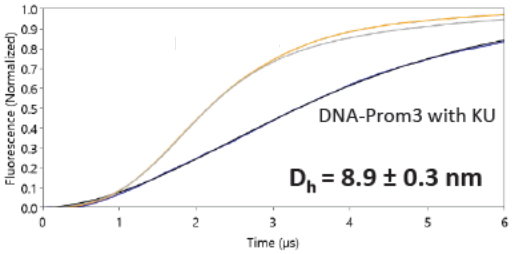

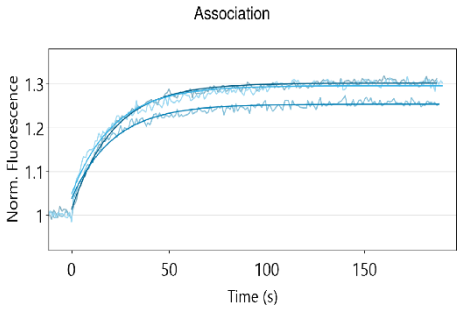

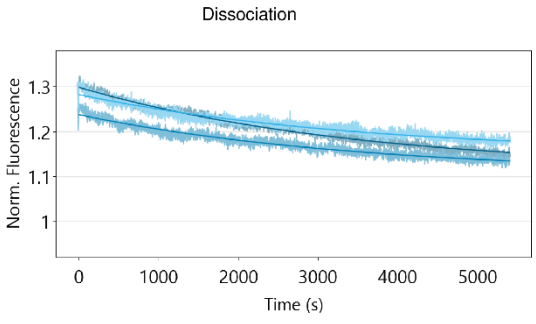

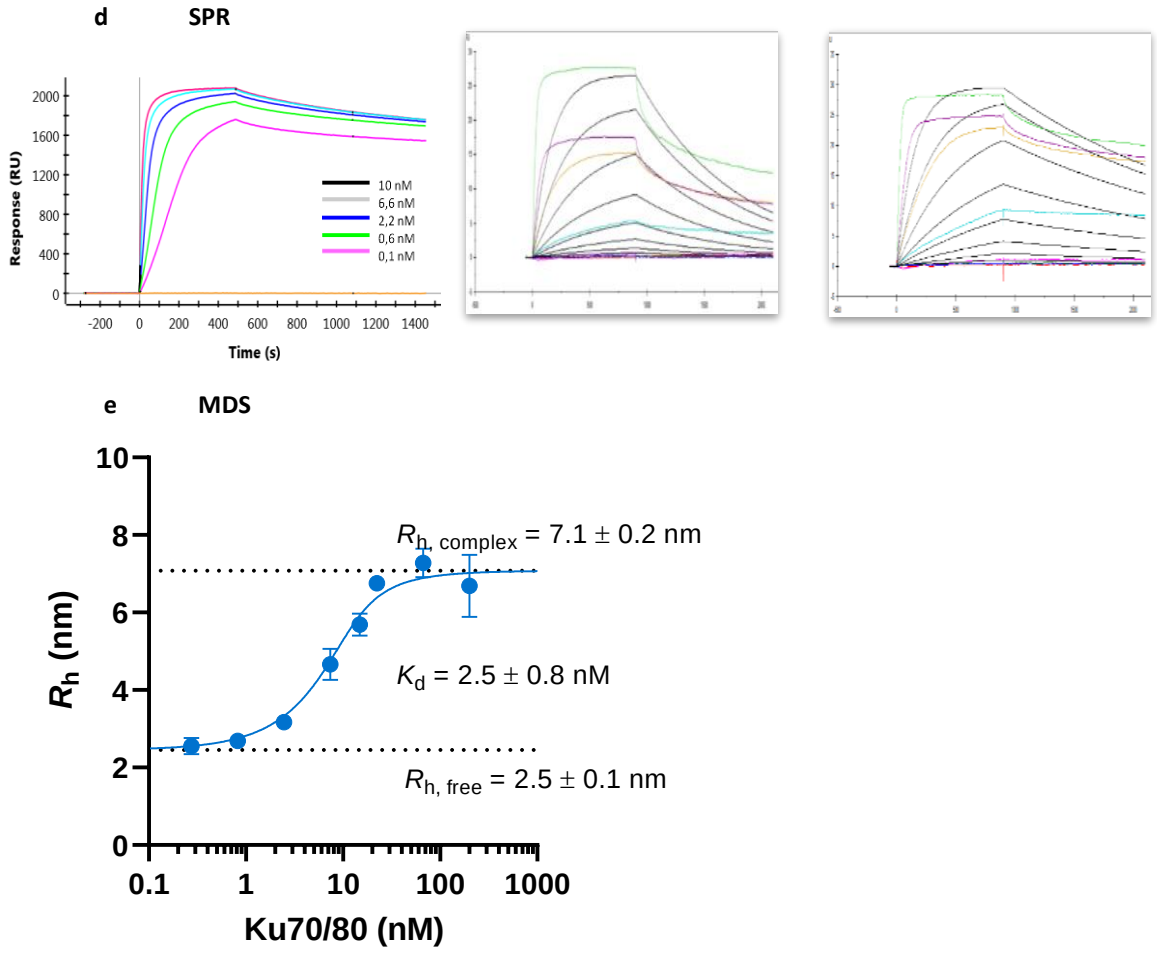

a) SEC-MALS elution profiles and molar masses of Ku alone in quadruple. b) Octet RED96e BLI steady-state data in duplicate. Colors code of Ku concentration: 3.13 nM (teal), 6.25 nM (purple), 12.5 nM (orange), 25 nM (green), 50 nM (cyan), 100 nM (red), 200 nM (blue). c) switchSENSE measurement set up (top, left). By hybridization of complementary DNA carrying the target sequence as overhang, the surface is functionalized with the sequence of interest. switchSENSE static mode data of 1 Ku concentration in duplicate (bottom). switchSENSE sizing data (top, right). Reference (bare DNA) is depicted in yellow. DNA-protein-complex is depicted in blue. d) SPR sensograms by ProteON XPR36 of Ku-200 bp dsDNA interaction measured (right). A 200 bp biotinylated DNA was immobilized on a Streptavidin (NLC) chip. Ku70/Ku80 ranged from 0.1 to 10 nM concentrations, one heterodimer may induce 200 RU. A k_{ON} of 7.8 ± 4 10^{+6} $M^{-1}s^{-1}$, a k_{OFF} of 1.5 10^{-4} s^{-1} and a K_D of 7.3 ± 3 nM were measured. This experiment showed the threading of Ku on DNA, approximately 10 heterodimers bound to this 200 bp DNA. SPR sensograms by BIAcore T200 of Ku-42 bp dsDNA (middle) and, Ku-60 bp dsDNA (left) interaction measured by biotinylated DNA immobilized in a serie S sensor chip SA at 10 nM concentration. Same buffer as in switchSENSE experiment adding 0.2 mg/mL of BSA, flow rates of 20 to 100 µL/min, and Ku at 5 nM as higher concentration for 900 s of association and dissociation. A k_{ON} of 1.0 10^{+6} $M^{-1}s^{-1}$, a k_{OFF} of 11.7 10^{-4} s^{-1} and a K_D of 1.2 nM (R_{max} of 32.9 RU) were measured for the 42 bp DNA and, a k_{ON} of 1.4 10^{+6} $M^{-1}s^{-1}$, a k_{OFF} of 5.0 10^{-4} s^{-1} and a K_D of 35.4 nM (R_{max} of 31.6 RU) for the 60 bp DNA. Colors code of Ku concentrations: 5 nM (light green), 2.5 nM (purple), 1.25 nM (orange), 0.625 nM (cyan), 0.3125 (pink), 0.156 (dark green), 0.078 (blue), 0.039 (red). The differences observed in the results depend mainly on the setup strategy of the experiment. Nevertheless, open questions remain to answers: the purity of dsDNA and the stability of the protein will affect the results, but there is also the possibility of different ways of DNA fixation by Ku. e) In collaboration with *Fluidic Analytics*, we collected preliminary data to test their new instrument, Fluidity One-W with the Ku-DNA interaction. This is a novel technique in solution based in diffusional sizing of a complex in a microfluidic system. For this experiment we used the same 18 bp dsDNA-FAM as before (AUC, MST) at 10 nM concentration, and 1/3 dilution of Ku70/Ku80 from 200 to 0.09 nM concentration. We were able to measure R_h (DNA alone, complex) and K_D values.

Tables

Table S1. Summary of the results for the alphaRep proteins interaction using different techniques.

	AUC-FDS	SEC-MALS*	ITC		MST	switchSENSE		BLI		SPR*
His-A3	**Blue-NHS**	**Dimer**	**Monomer/high affinity**	**Dimer /low affinity**	**Red-His**	**Rep2***	**Rep17**	**Monomer**		**Monomer**
Ratio	1:1	1:1	1:1	1:1	N/A	1:1	1:1	N/A		N/A
K_D (nM)	13.4 ± 1.8	N/A	0.6 ± 0.1	24 ± 8	8.0	0.29 ± 0.01	0.98 ± 0.16	3.2 ± 1.1	3.3 ± 0.8	3.97 ± 1.38
k_{ON} ($M^{-1}s^{-1}$) k_{OFF} (s^{-1})	N/A	N/A	N/A	N/A	N/A	2.4 ± 0.1 10^{+6} 6.9 ± 0.2 10^{-4}	2.4 ± 0.2 10^{+6} 2.3 ± 0.3 10^{-3}	2.6 ± 0.7 10^{+5} 7.6 ± 0.7 10^{-4}	N/A	2.31 ± 1.79 10^{+5} 4.28 ± 0.36 10^{-3}
Other information	S (A3) = 2.6 ± 0.1 S (A3/Rep17) = 3.0 ± 0.1	R_h (A3) dimer = 3nm Mw (Rep2) = 11.6 kDa Mw (A3) = 44.8 kDa Mw (A3/Rep2) = 65.5 kDa	ΔH = 11.6 ± 0.5 kcal/mol	ΔH = 15.4 ± 0.7 kcal/mol	N/A	D_h (A3)monomer = 3 nm D_h (A3-Rep2) = 3.8 nm	N/A	N/A	N/A	N/A

In the last column in grey, previous SPR data obtained by P. Minard's team.*Rep2

Table S2. Summary of the results obtained for the Ku-DNA interaction using the different techniques.

	AUC-FDS	ITC		SEC-MALS	BLI		MST	switch SENSE	SPR	Diffusional sizing
DNA(bp)	**18***	**18**	**42**	**42**	**42****		**18***	**48**	**200****	**18***
Ratio Ku vs DNA	1:1	1:1	2:1	2:1, 1:1	N/A		N/A	1:1	20:1	1:1
K_D (nM)	12.9 ± 3.2	3.5 ± 0.8	3.6 ± 0.4	N/A	0.4 ± 0.1	5.2 ± 0.2	2.8	1.0 ± 0.2	7.3 ± 3.0	2.5
k_{ON} ($M^{-1}s^{-1}$) k_{OFF} (s^{-1})	N/A	N/A	N/A	N/A	$1.9 \pm 0.1\ 10^{+6}$ $7.2 \pm 0.3\ 10^{-4}$	N/A	N/A	$2.6 \pm 0.2\ 10^{+6}$ $2.3 \pm 0.3\ 10^{-4}$	$7.8 \pm 4.0\ 10^{+6}$ $1.5 \pm 0.8\ 10^{-4}$	N/A
Other information	S (DNA) = 2.2 ± 0.1 S (1:1) = 7.3 ± 0.2	5.1 ± 0.1 kcal/ mol	23.9 ± 4.9 kcal/mol	Mw (DNA)= 26.1 kDa Mw (Ku) = 144.4 kDa Mw (1:1) = 171.0 kDa Mw (2:1) = 306.2 kDa	N/A	N/A	N/A	D_h = 8.9nm	N/A	Rh = 7.1nm

The last two columns came from additional data: Preliminary SPR obtained by Charbonnier's team, and MDF in collaboration with Fluidic Analytics. DNA modified *FAM or **Biotin.

Macromolecular interactions *in vitro*, comparing classical and novel approaches

Christophe Velours[1,2*], Magali Aumont-Nicaise[1*], Stephan Uebel[3], Patrick England[4], Adrian Velazquez-Campoy[5,6,7,8,9], David Stroebel[10], Guillaume Bec[11], Pierre Soule[12], Christophe Quétard[13], Christine Ebel[14], Alain Roussel[15], Jean-Baptiste Charbonnier[1], Paloma Fernández Varela[1#]

[1]Université Paris-Saclay, CEA, CNRS, Institute for Integrative Biology of the Cell (I2BC), 91198, Gif-sur-Yvette, France. [2]Microbiologie Fondamentale et Pathogénicité, MFP CNRS UMR 5234, University of Bordeaux, 146 rue Léo Saignat 33076 Bordeaux, France. [3]Bioorganic Chemistry & Biophysics Core Facility, Max-Planck-Institute of Biochemistry, Martinsried, Germany. [4]Molecular Biophysics platform, Institut Pasteur, Paris, France. [5]Institute of Biocomputation and Physics of Complex Systems (BIFI), Joint Units IQFR-CSIC-BIFI, and GBsC-CSIC-BIFI, Universidad de Zaragoza, Zaragoza, 50018, Spain. [6]Departamento de Bioquímica y Biología Molecular y Celular, Universidad de Zaragoza, 50009, Zaragoza, Spain. [7]Instituto de Investigación Sanitaria Aragón (IIS Aragón), 50009, Zaragoza, Spain. [8]Centro de Investigación Biomédica en Red en el Área Temática de Enfermedades Hepáticas y Digestivas (CIBERehd), 28029, Madrid, Spain. [9]Fundación ARAID, Gobierno de Aragón, 50009, Zaragoza, Spain. [10]Institut de biologie de l'Ecole normale supérieure (IBENS), Paris, France. [11]Institut de Biologie Moléculaire et Cellulaire (IBMC), Strasbourg, France. [12]NanoTemper Technologies GmbH, Munich, Germany. [13]ForteBio-Sartorius, Dourdan, France. [14]Univ. Grenoble Alpes, CNRS, CEA, IBS, Grenoble, France .[15]Architecture et Fonction des Macromolécules Biologiques (AFMB), Marseille, France.

**Contributed equally*

#Corresponding author: paloma.fernandez-varela@i2bc.paris-saclay.fr ORCID: 0000-0001-5078-7102

Abstract

Biophysical quantification of protein interactions is central to unveil molecular mechanisms of cellular processes. Researchers can choose from a wide panel of biophysical methods, including classical and more novel ones. A real-life proof-of-concept was carried out during an ARBRE-MOBIEU training school held in June 2019 in Gif-sur-Yvette, France (https://mosbio.sciencesconf.org/). Twenty European students benefited from a one-week training with lessons and practical sessions on six complementary approaches: (i) Analytical UltraCentrifugation with or without a Fluorescence Detector System (AUC-FDS), (ii) Isothermal Titration Calorimetry (ITC), (iii) Size Exclusion Chromatography coupled to Multi-Angle Light Scattering (SEC-MALS), (iv) Bio-Layer Interferometry (BLI), (v) MicroScale Thermophoresis (MST) and, (vi) switchSENSE. They implemented all these methods on two examples of macromolecular interactions: firstly, a protein-protein interaction between an artificial alphaRep binder, and its target protein, also an alphaRep; secondly, a protein-DNA interaction

between a DNA repair complex, Ku70/Ku80 (hereafter called Ku), and its cognate DNA ligand. The students acknowledged that the workshop provided them with a clearer understanding of the advantages and limitations of the different techniques and will help them in the future to choose the approaches that are most relevant or informative ~~to~~ for their projects.

Keywords

Molecular scale biophysics, macromolecular interactions, artificial binders, double-stranded DNA breaks repair factors

Introduction

Macromolecular interactions play a central role in the activation/inactivation of most cellular mechanisms. These interactions can be measured *in cellulo*, or *in vitro,* and predicted *in silico*. The classical *in cellulo* methods (such as tap-tag or two-hybrid) allow large-scale studies, but in order ~~to~~ the characterization of ~~confirm that~~ a direct interaction between two macromolecules ~~occurs~~relies on the ~~between two macromolecules,~~ quantitative *in vitro* measurements ~~are needed~~. These measurements allow to characterize interactions not only in terms of affinity, but also to determine additional kinetic and thermodynamic parameters, as well as to define the hydrophobic or hydrophilic nature of the interface. They also give access to the stoichiometry of the assembly and allow to map the regions involved by using different constructs or mutants. *In vitro* measurements can also be useful to evaluate the the drugability of the interaction site or to understand the role of ~~post-translational modifications or other~~endogenous regulatory events on the formation of complexes (post-translational modifications). These measurements are essential to set-up predictive ~~By~~ *in silico* docking ~~analysis~~tools. Conversely, by *in silico* analysis, ~~we can predict~~ the structure of macromolecular complexes ~~or~~ as well as the impact of functional substitutions can be predicted, helping to optimize experimental design (Andreani and Guerois, 2014).

The original idea of the project presented here originated during the organization of a European Training School in Molecular Scale Biophysics (https://mosbio.sciencesconf.org/) within the MOBIEU COST Action. We proposed to the participants to compare different techniques allowing to measure macromolecular interactions *in vitro*. Nowadays, there is a large panel of possibilities, and it becomes difficult to choose which technology will be the

best adapted when embarking into a new project. Each approach presents advantages and drawbacks, and it is therefore difficult for the user to choose from the beginning which one will be most adapted to the properties of the interaction partners. In the workshop, we focused on six approaches (Fig. 1). Choosing between the different techniques can be considered in a progressive manner. If none of the interaction partners can be easily labeled or immobilized on a surface, approaches in which ~~the macromolecules~~both partners are in solution (AUC, ITC, and SEC-MALS) should be favored (Fig. 1, top). However, several of them require large quantities of biological material. When a partner can be immobilized easily on a bio-surface, without affecting its function, approaches like BLI, switchSENSE and Surface Plasmon Resonance (SPR) will be often tested, since they offer the possibility to use small amounts of the immobilized partner (called ligand) (Fig. 1, middle). Finally, when the partners can be labeled, again without affecting their function, fluorescent probes can be grafted allowing the use of reduced amounts of material and facilitated signal analysis (AUC FDS, MST, or Microfluidic diffusional sizing (MDS)) (Fig. 1, bottom).The choice of the optimal approach may further rely on additional criteria including the solubility of the partners, the instrument environment or non-specific interactions with instrument surfaces. Finally, it should be stressed that it is preferable to perform measurements using several orthogonal techniques to fully validate and characterize a biological interaction, and specify its features, such as stoichiometry, kinetics or thermodynamics.

Figure 1. Decisional tree to help choosing the biophysical approach ~~that~~ best suited for~~s~~ the study of a specific molecular interaction.

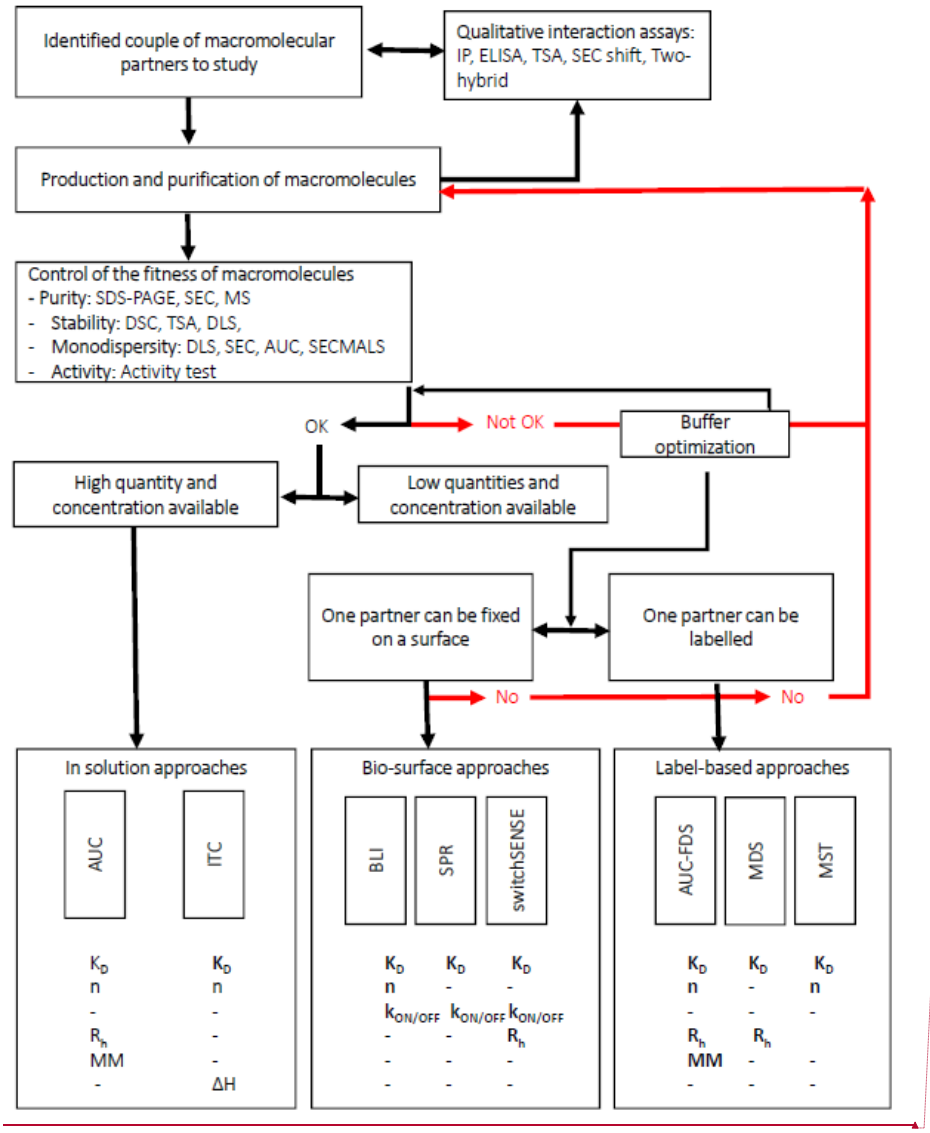

88

Formatted: English (United States)

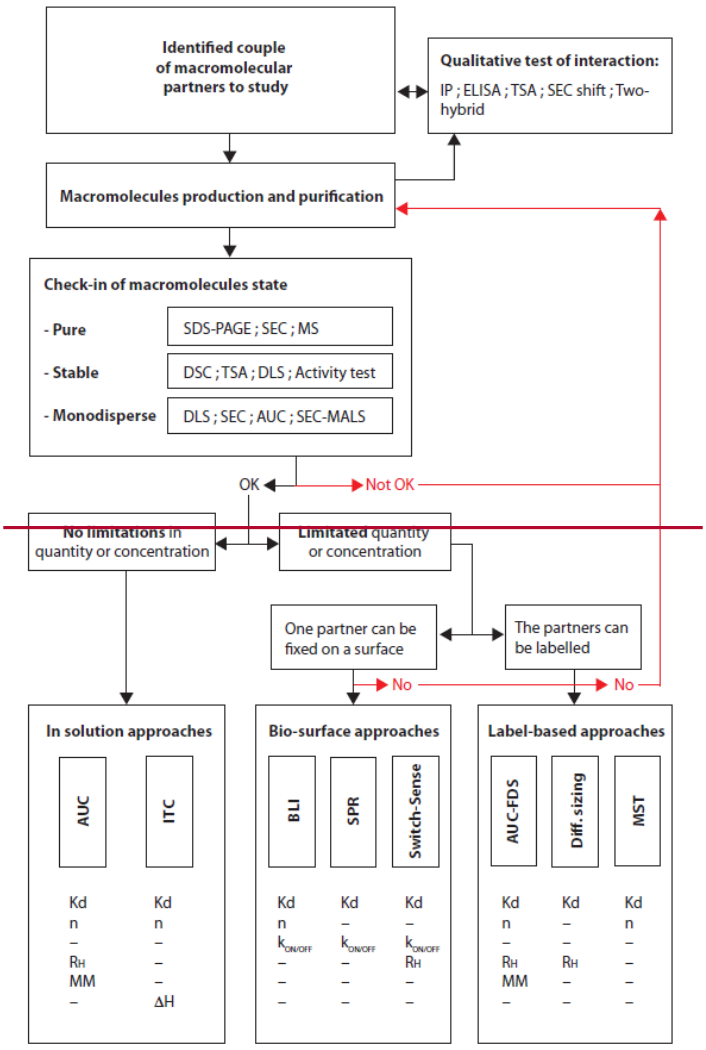

To determine whether two macromolecular partners potentially interact, first indication of a binding event could be obtained with qualitative methods (top right): Immunoprecipitation (IP) from cell extracts; Thermal Shift Assay (TSA); Size Exclusion Chromatography (SEC) shift, measuring the elution volume change after complex formation; Two-hybrid assay, *in cellulo*. The production and purification of the macromolecular partners should aim at reaching high purity, time-stability and monodispersity of the preparation for the interaction measurements to be reliable. Mass-Spectrometry (MS); Differential Scanning Calorimetry (DSC) ; TSA; Dynamic Light Scattering (DLS); Activity test (for instance an enzymatic assay); Analytical UltraCentrifugation (AUC); Size Exclusion Chromatography coupled with Multi-Angle Light Scattering (SEC-MALS). Macromolecular interaction methods ~~Six approaches were used in the training school. They~~ can be classified in three main groups: measurements in solution and label free: -(AUC; Isothermal Titration Calorimetry (ITC) (bottom, left)), on biosensor with a partner graft on a surface: (Bio-Layer Interferometry (BLI), Surface Plasmon Resonance (SPR); switchSENSE technology (bottom, middle)), and methods with a partner labeled with a fluorescent probe (AUC-FDS (AUC-Fluorescence

Formatted: Font: Not Bold
Formatted: Font: Not Bold
Formatted: Font: Not Bold
Formatted: Right: 0", Widow/Orphan control, Adjust space between Latin and Asian text, Adjust space between Asian text and numbers, Pattern: Clear (White)
Formatted: Font: Not Bold
Formatted: Font: Not Bold
Formatted: Font: Not Bold
Formatted: Font: Not Bold
Formatted: Font: Not Bold
Formatted: Font: Not Bold
Formatted: Font: Not Bold
Formatted: Font: Not Bold
Formatted: Font: Not Bold
Formatted: Font: Not Bold, Italic
Formatted: Font: Not Bold
Formatted: Font: Not Bold
Formatted: Font: Not Bold
Formatted: Font: Not Bold
Formatted: Font: Not Bold
Formatted: Font: Not Bold
Formatted: Font: Not Bold
Formatted: Font: Not Bold
Formatted: Font: Not Bold
Formatted: Font: Not Bold

Detector System); Microfluidic Diffusional Sizing (MDS); MicroScale Thermophoresis (MST) (bottom, right)). These ~~six~~ approaches give access to different parameters of the interaction and present some specific limitations. ~~.~~ If a high quality sample (pure, stable, monodisperse) is available in large quantity (up to mg amount) one may start with label-free and in solution approaches. Otherwise, if material is limited for one partner, surface ~~approaches~~ and labeling approaches are a good alternative~~. Finally, when labeling is possible, MST and AUC-FDS are~~ and highly complementary~~. approaches~~ to cross-validate interaction~~s~~ measurements. Surface approaches are best candidates to get access to the kinetic parameters of interaction. Six of these approaches were used in the training school. ~~The six approaches give access to different parameters of the interaction and present some specific limitations. AUC: Analytical Ultracentrifugation; ITC: Isothermal Titration Calorimetry, SEC-MALS: Size Exclusion Chromatography with Multi Angle Light Scattering; BLI: Bio Layer Interferometry; MST: MicroScale Thermophoresis; AUC-FDS: Analytical Ultracentrifugation with a Fluorescence Detector System; S: Sedimentation coefficient; K_D,~~ D~~d~~issociation constant (K_D); ~~n,~~ stoichiometry (n); association and dissociation rates (k_{ON}, k_{OFF}); ~~Dh,~~ hydrodynamic radius~~diameter or~~ (Rh)~~, hydrodynamic radius; k_{ON}, k_{OFF}; association and dissociation rates; MT mass transport~~; Molecular mass (MM).

Formatted: Subscript

Formatted: Not Superscript/ Subscript

Formatted: Subscript

Formatted: Subscript

Formatted: Font: (Default) Segoe UI, 10.5 pt, Not Bold, Font color: Black

In this training school, we used as examples two different macromolecular interactions systems, that have been well characterized in our laboratories using several of the approaches discussed here. One is an interaction between two proteins, and the other a protein-DNA interaction, both with an affinity in the nanomolar range. Reference data were initially produced in our laboratories. A group of 20 participants reproduced our measurements during the five-day MoSBio Training School.

The first project comes from P. Minard's team, who uses an original family of artificial helicoidal repeat proteins, called alphaRep (Guellouz et al., 2013). AlphaRep libraries allow to select tight binders against a variety of targets by phage display. The alphaRep's are highly soluble proteins, easily expressed in *E. coli*, which display a very high thermal stability. These proteins are cysteine-free and, thus do not contain disulfide bonds. They are composed by repeated motifs made with two antiparallel alpha helices. Clusters of variable side chains, mainly in the second helix, are positioned on the same face of the motifs. The ensemble of all these variable motifs forms a library of surfaces from which tight binders can be extracted against a given target. The alphaRep's have been used for several applications, such as chaperones for crystallization and structural studies of difficult targets (Valerio-Lepiniec et al., 2015; Di Meo et al., 2017; Chevrel et al., 2018; Campanacci et al., 2019), as well as in biophysical and live cell ~~applications~~ studies (Léger et al., 2019; Prasad et al., 2019; Fernandez et al., 2020; Léger et al., 2020). New applications of these artificial binders are currently being explored in relation with~~to~~ their ability to be expressed in eukaryotic cells. Here we analyzed the interactions between two alphaRep's (Rep2 and Rep17) selected against a protein target, (A3), which is itself an alphaRep. The interaction between the alphaReps has been extensively characterized before in the laboratory by ITC, SEC-MALS and AUC, but also by Circular Dichroism (CD), SPR and Fluorescence Resonance energy Transfer (FRET) (not used in this training school) (Guellouz et al.,2013; Di Meo et al., 2017; Léger et al., 2019). Both A3 / Rep2 and A3 / Rep17 interactions were tested previously to determine which one was the most appropriate for the training. Because~~, and~~ the former is weaker than the latter, we focused only on the only A3 / Rep17 interaction ~~. D~~during the training ~~only A3 / Rep17 interaction was measured~~.

The second project comes from J.B. Charbonnier's team. It concerns proteins involved in DNA repair, and more precisely, in the classical Non-Homologous End Joining (c-NHEJ), the main

Double-Strand Break (DSB) repair pathway in human. The Ku70/Ku80 (Ku) heterodimer plays a central role in the recognition of DSB ends, as it is the first repair factor that interacts with them. Ku binds tightly to DNA ends in a sequence independent manner thanks to its ring-shaped structure (Walker et al., 2001). Ku then iteratively recruits different NHEJ partners (ligase 4, nucleases and polymerases) (Chang et al., 2017; Frit et al., 2019). Ku also contributes to the tethering (synapse) between the two DSB ends to avoid misrepair with other DSB ends. J.B. Charbonnier's team (Tadi et al., 2016; Nemoz et al., 2018) has recently described the recruitment mechanism of some NHEJ factors by Ku at the molecular level. DSBs, despite being deleterious DNA lesions, are generated on purpose during radiotherapy or in genome editing by CRISPR-Cas9. Understanding the molecular basis of the c-NHEJ is thus central to improve these major biotechnological applications. Here we analyzed the interaction between Ku and DNA substrates of different lengths, to determine the most appropriate for~~to~~ the training and to study the threading of Ku on DNA. The characterization of the interaction between Ku and DNA h~~w~~as been extensively studied in the laboratory by ITC, MST (Tadi et al., 2016; Nemoz et al., 2018; Gontier et al., 2021~~, Chapter of MiMB, *in press*~~), switchSENSE, AUC, BLI (data not published) and, more recently by other techniques not used during the training school (SPR, MDS or FRET). One Ku occupies about 18 bp ~~on DNA. S~~and several Ku molecules can thread on DNA when ~~the~~ its size ~~of the DNA~~ is longer than 18bp, ~~and a long DNA can be covered by~~with one Ku molecule every 18bp.

We present in this article the results obtained by 20 students during a European Training School in Molecular Scale Biophysics that took place from June 3rd to 7th, 2019 at I2BC at Gif-sur-Yvette, France. We report the protocols used to analyze the two systems under study (protein/protein and protein/DNA interactions) using the six biophysical methods mentioned above. The results obtained by the students during ~~this~~ the one-week course are shown and compared to our previous published data when available. Finally, we compare the advantages and drawbacks of the different approaches used during this training school and present some feedback~~s~~ from the students, allowing to have a global overview of the pros and cons of these six complementary biophysical approaches.

Materials and Methods

Biophysical approaches in solution that do not require labeling of an interaction partner

Size Exclusion Chromatography with Multi-Angle Laser Light Scattering detection (SEC-MALS): SEC-MALS allows to determine the absolute molar mass of the components ~~of a protein/multiprotein~~present in a macromolecular sample. It indicates if elution peaks are homogenous ~~in term of protein composition~~ or if they are composed of mixtures, either of different oligomers or of different conformers. SEC-MALS allows size determination if an online Dynamic Light Scattering (DLS) detector is included in the setup (Folta-Stogniew, 2006). In order to determine stoichiometry in a macromolecular hetero-complex, differences in extinction coefficients are required. An experimental determination of extinction coefficient by analyzing each partner separately, will be more precise than *in-silico* prediction. For a more precise estimation of molar mass of complex components, you need to know the refractive index increment (dn/dc value) of each complex partner at the wavelength of the MALS system laser. We used an HPLC system from *Shimadzu* coupled to a MALS detector (miniDAWN TREOS) plus a DLS detector (QELS), and a refractometer (optilab T-rEX) from *Wyatt technologies* ~~(Fig. S1)~~. To run an experiment, one needs 1 L of running buffer to equilibrate the column and detectors, ~~and~~ from 2 mg/mL of protein (for MW of 20 kDa), down to 0.5 mg/mL (if the MW is higher than 150 kDa). Depending ~~of~~ on the column used, the volume of the sample (30 µL for Bio-SEC-3 *Agilent*, 50 µL for KW-803/804 *Shodex*, and 100 µL for Superose 6, Superdex 75 or Superdex 200 increase 10/300 GL *Cytiva*) and the time of elution can differ. A run (including an equilibration step and a control BSA sample) takes typically a few hours and consumes ~~about~~ 40-200 µg of sample.

Isothermal Titration Calorimetry (ITC): ITC allows the direct, and thorough thermodynamic characterization of interactions between molecules in solution with no limitation of partner size and without labeling (Holdgate, 2001; Krell, 2008; Velazquez-Campoy and Freire, 2006) ~~and without labeling~~. ITC ~~is an equilibrium solution technique~~allows to quantify dissociation constants (K_D)~~ values~~, but also other interaction parameters (enthalpy, entropy, stoichiometry, and heat capacity). ITC is not affected by the optical properties of the samples, but may be very sensitive to the composition of the buffer (e.g.~~ presence of DMSO or~~ in particular to mismatches between partner sample solutions). In a microcalorimeter the two cells (reference and sample) needs to be kept at exactly the same temperature. A heat sensing

Formatted: Font: 12 pt

Formatted: Font: 12 pt, Italic

Formatted: Font: 12 pt, Not Bold, Italic

Formatted: Font: 12 pt, Not Bold

Formatted: Font: 12 pt

Formatted: Font: 12 pt

Formatted: Font: 12 pt

device detects temperature difference between the cells when binding occurs, upon serial injection of a ligand, and give feedback to the heaters, which compensate for this difference and return the cells to equal temperature. Each injection gives then rise to a peak of emitted or absorbed heat whose surface is proportional to the amount of binding. For the ITC experiments, we used three instrument models: VP-ITC, ITC200 and PEAQ-ITC all from *Malvern Panalytical* ~~(Fig. S1)~~. One of the interacting partners is placed in a cell (1.4 mL for the VP-ITC, 200 µL for the ITC200 and PEAQ-ITC) and the other in a syringe (300 µL for the VP-ITC, 40 µL for the ITC200 and PEAQ-ITC). Sequential injections are made from ~~a~~ the syringe (5-10 µL for the VP-ITC, 1-2 µL for the ITC200 and PEAQ-ITC) into the cell. ~~In~~ To produce the data ~~described~~ reported here, we used 80-990 µg of the molecule in the cell, and 130-320 µg of the molecule in the syringe. The transient heat effect due to complex formation (and other potential unspecific phenomena) upon partner injection is measured as the titration progresses, from which the binding isotherm is constructed.

Biophysical approaches with a partner immobilized on a surface

Bio-Layer Interferometry (BLI): BLI is a fast, high throughput and label-free technology for measuring biomolecular interactions by analyzing the interference pattern of white light reflected from a layer of immobilized macromolecules on a biosensor tip ~~and~~ *versus* an internal reference (Abdiche et al., 2018). It enables real-time ~~analysis for~~ determination of affinity, kinetic parameters and concentration, with one of the binding partners immobilized onto the biosensor surface (ligand) and the other in solution (analyte). This microfluidic-free technology is particularly adapted for performing binding assays in crude lysates or cell culture media. We used an Octet RED96e during the training, and ~~previously~~ an RED384 during the preparation phase, both from *FortéBio* ~~(Fig. S1)~~. In all cases, one of the interaction partners will be non-covalently captured on a glass sensor probe. The sensor will then be incubated in microplate wells containing the second interaction partner in solution. A light beam is sent through the sensor, and the reflected beam is analyzed using an interferometric detector, that measures the spectral shift due to the variations of density (optical thickness) that the biolayer undergoes upon association and dissociation of the complex. The real-time monitoring of these variations allows to record a « sensorgram », from which the kinetic rates (k_{ON} and k_{OFF}), as well as the equilibrium constant K_D can be determined through mathematical curve fitting. We used 1-5 µg/mL of ligand to load NTA sensors for 20-120 s, for low density, or 120-600 s,

Formatted: Font: 11 pt

Formatted: Font: Italic

Formatted: Font: 12 pt

Formatted: Font: 12 pt

Formatted: Font: 12 pt

Formatted: Font: 12 pt

for high density, and a range of at least 7 ~~(~~2-fold dilutions (starting at 100-200 nM) of the analyte with an association time of 600-900 s. We consumed ~~per run~~ about 8 µg of protein A3, and 400 ng of 42 bp biotinylated DNA per run for the immobilization, and about 2-14 µg of the respective analytes. The concentration of ligand could be reduced (at least by 2) in favor of a longer incubation. The consumption of the analyte, depends on the affinity of the interaction, as the concentrations used should range from K_D /1~~2~~0 to 10 x K_D.

switchSENSE: switchSENSE technology is based on short DNA nanolevers (48 bp in our case), which are immobilized on gold electrodes in a microfluidic channel. The intrinsically negatively charged DNA nanolevers can be electrically actuated ("switched") on the gold surface to oscillate at high frequencies (Knezevic et al., 2012). A switchSENSE microfluidic biochip contains four flow channels, each containing six gold electrodes. Switching of the DNA is mediated by alternating the voltage across the gold surface. The motion of the levers is tracked in real time (µs scale) via electrically triggered time correlated single photon counting (E-TCSPC) detecting a fluorescent probe (dye) present on top of the immobilized DNA strands. The recorded fluorescence intensity correlates to the orientation of the DNA nanolever relative to the surface as the fluorescence is gradually quenched upon approaching the gold electrode due to energy transfer. ~~time-resolved single photon counting detecting a fluorescent probe present on the immobilized DNA strands.~~ The complementary DNA strands can be cross-linked to a ligand via amine or thiol coupling or click-chemistry. By hybridization of this conjugated complementary strand to the surface-tethered DNA nanolever, the surface is functionalized with the ligand of interest. Upon binding of an analyte, the hydrodynamic friction of the levers is ~~affected~~ increased and subsequently the movement of the levers is slowed down. This change in switching speed is used by the system to determine the size (D_h) or conformational changes of ligands and complexes. The kinetics of molecular interactions (k_{ON}, k_{OFF}, K_D) can be ~~followed~~ monitored using two measurement modes: dynamic or static. In the first case, analyte binding is measured through the change of the oscillation rate of the electrically actuated DNA nanolevers (changes in dynamic response). In the second case, the DNA nanolevers are kept at an upright position, in a constant electric field, and analyte in close proximity to a dye can alter ~~the~~ its local chemical environment resulting in a fluorescence change (also called Fluorescence Proximity Sensing). Binding is then measured thanks to the fluorescence intensity variation of the functionalized nanolever. For the switchSENSE

Formatted: Font: 11 pt, English (United Kingdom), Pattern: Clear

Formatted: Font: 12 pt

experiments, we used a DRX[2] device from *Dynamic Biosensors* with two LED light sources (for the excitation of red and green fluorophores) ~~(Fig. S1)~~. In all cases, a hundred µg of protein where enough to generate cross-linked complementary strands (cNL-DNA) for several round of experiments, since one measurement needs only 40 µL of 100 nM DNA-protein conjugate. A sizing measurement classically takes less than an hour. The ~~amount~~ quantity of analyte needed for a kinetic experiment depends on the overall affinity, ~~which delimits~~the flow rates, and the association~~/dissociation~~ time~~s to be used~~. ~~During association, a~~A too slow flow rate can ~~be the cause for~~ result in mass transport limitation ~~effect and~~ during ~~ad~~issociation and ~~inadequate flow rate can result~~ in re-binding effects during dissociation. Here we used flow rates of 100-500 µL/min, association times of 80-300 s, and 1500 s of dissociation time. ~~In sample quantities, w~~We used 150 ng of the cross-linked ligands, and 2-20 µg of its partner for a series of 3 concentrations.

Biophysical approaches with a labeled partner

Analytical UltraCentrifugation with Fluorescence Detection (AUC-FDS): AUC is a powerful technique for the characterization of macromolecules and macromolecular self- and hetero-association processes in solution. It was used here with labeled protein or DNA, but it can be used with non-labeled material like SEC-MALS and ITC. An analytical ultracentrifuge is a high-speed centrifuge equipped with one or more detectors (absorbance/interference, fluorescence) allowing to monitor sedimentation in real time. Two types of complementary experiments can be performed, sedimentation velocity and sedimentation equilibrium (Zhao et al., 2013). Sedimentation velocity experiments allow to determine the size distribution of species, their aggregation and oligomerization, sedimentation coefficients, hydrodynamic radius, shape and molar masses, their stoichiometry and K_D (by isotherm fitting of sedimentation coefficients measured at various concentrations). Sedimentation equilibrium ~~is~~ experiments are suited for well-defined samples, and gives molar mass and K_D information. The centrifugation speed can be set between 600 and 260 000 g allowing to study all sizes of macromolecules. The duration of sedimentation experiments ranges from 2 h to several days ~~(Fig. S1)~~. dn/dc and UV extinction coefficients values, which are needed to analyse data obtained with absorbance and interference optics, can be determined from the protein sequence using the SEDFIT calculator module (Schuck, 2000). For the AUC-FDS experiments we used a ProteomeLab XL-I ultracentrifuge from *Beckman Coulter*

Formatted: Font: (Default) +Body (Calibri), 11 pt, Font color: Black, English (United Kingdom), Pattern: Clear (White)

Formatted: Font: (Default) Calibri, 12 pt

Formatted: Font: (Default) Calibri, 12 pt

Formatted: Font: (Default) Calibri, 12 pt

Formatted: Font: (Default) Calibri, 12 pt

Formatted: Font: (Default) Calibri, 11 pt

equipped with a Fluorescence Detection System (FDS) from *AVIV Instruments* ~~(Fig. S1)~~. A sedimentation velocity experiment requires 100-450 µL of sample at 0.3 to 1.5 OD, for absorbance/interference detection, and 5-60 nM concentration, for fluorescence detection, whereas sedimentation equilibrium requires 130 µL at 0.2 to 0.5 OD. In interference, the limit of detection is 0.1 mg/mL, but in absorbance it depends on the sample extinction coefficient~~s~~. To characterize an interaction using the AUC fluorescence detector, a range of 2 nM to 2 µM is typically used. When the affinity is very high, a range between 2 pM and 2 nM is chosen, but a blocking agent - e.g. BSA at 1 mg / mL - is added in the sample to avoid non-specific adsorption and loss of fluorescent dye. To produce the data described here, we used about 1-3.5 µg of the fluorescent molecule and 8-80 µg of the non-fluorescent molecule.

Microscale Thermophoresis (MST): MST is a novel technology for the analysis of biomolecules based on the modification of fluorescence intensity induced by the temperature, due to Temperature Related Intensity Changes (TRIC) and the directed movement of particles in a microscopic temperature gradient (thermophoresis) (Asmari et al., 2018; Jerabek-Willemsen et al., 2011). Thermophoresis is influenced by a combination of changes at the level of the hydration shell, shape, charge…, of biomolecules (all the parameters that influence the Soret coefficient) ~~of biomolecules~~, which result in differences of movement along the temperature gradient as well as ~~the~~ of brightness of the fluorescent tag. MST provides information on the binding affinities with good accuracy and sensitivity in the pM to mM range. This technology allows immobilization-free measurement of interactions in any buffer and complex biological liquid, but requires one of the two partners to be labeled with a fluorescent dye to measure protein-protein interactions (there is also a label free instrument that detects the intrinsic fluorescence of proteins). Any size of unlabeled molecules can be used (from ions, to large proteins). MST experiments are performed in capillaries, thus require a low sample consumption. Method development for MST is usually fast and consists of three steps: (i) ensure there is enough fluorescence signal intensity. (ii) Check your sample for sticking to the capillaries. (iii) Establish the noise floor of your experiment by measuring MST of just your target without ligand at the final settings (final concentration, excitation laser and 'MST power' = IR laser LED power to be used). We used a Monolith NT.115 blue/green and a red/blue from *NanoTemper Technologies*, ~~(Fig. S1). MST experiments, performed in~~

Formatted: Font: (Default) Calibri, 12 pt
Formatted: Font: (Default) Calibri, 12 pt
Formatted: Font: (Default) Calibri, 12 pt
Formatted: Font: (Default) Calibri, 12 pt
Formatted: Font: (Default) Calibri, 12 pt
Formatted: Font: (Default) Calibri, 12 pt
Formatted: Font: 12 pt

~~capillaries, require a low sample consumption (~~200 µL at 20 nM of the fluorescent molecule~~,~~ and 20 µL of the non-fluorescent molecule at the highest concentration needed~~,~~ (depending on the expected K_D). To produce the data described here, we used about 50-350 ng of the fluorescent molecule and 6-12 µg of the non-fluorescent molecule.

Formatted: Font: 11 pt, English (United Kingdom)

Sample preparation

To perform biophysical characterization measurements, samples of high purity, stability and monodispersity are needed (Fig. S1). We chose well characterized systems from our laboratories, and the concentration ranges employed to accurately determine binding parameters were already known.

AlphaReps are recombinant proteins produced by standard overexpression procedures in *E.coli* (Guellouz et al., 2013). For our experiments, we used the following alphaRep proteins: A3, which is the target and Rep17 and Rep2, which are the binders. Because A3 forms homodimers at high concentration, it was used as ligand for real-time biosensors approaches (BLI, switchSENSE) and was the labeled partner in AUC-FDS and MST experiments. In the conditions used, we assumed A3 is a monomer~~, as t~~. The simultaneous presence of the monomeric and dimeric forms would make the analysis difficult.~~.~~ A3 dimers are unable to interact with Rep17, and it is only when they dissociate into monomers that, the interaction with Rep17 occurs. A dissociation constant of 37 nM for the A3 / A3 dimer was measured by AUC (Léger et al., 2019). This is why we observe several events in ITC: the dissociation of the A3 dimer and the interaction with Rep17.

Ku is a recombinant protein produced by standard overexpression procedures in insect cells (Nemoz et al., 2018). For our experiments, we used different lengths of dsDNA depending on the assay format. Shorter DNA are not adapted for biosensor approaches, since a DNA too close to the surfaces will hinder its interaction with Ku. DNA is practical to work with, because it is easy to modify and is commercially available. For immobilizationed on BLI biosensors and for detection in AUC-FDS and MST, we ordered biotinylated and 5-Carbofluorescein (5-FAM)-labeled DNA oligonucleotides, respectively.

~~To perform biophysical characterization measurements, samples of high purity, stability and monodispersity are needed (Fig. S2).~~ All proteins were dialyzed to eliminate glycerol from the

storage buffer, which can interfere with the measurements. We chose the pH and ionic strength of the buffer for the best solubility of the samples. To simplify as much as possible, we used the dialysis buffer (20 mM Tris-HCl pH 8, 150 mM NaCl, 5 mM β-mercaptoethanol) as running buffer in most experiments. Due to the particularities of each approach and measurement devices, there are some limitation in the buffer choice. In some cases, blocking agents were required, such as 1mg/mL BSA, especially for low protein concentrations (in the nM range), to prevent surface adsorption. To reduce surface tension in capillaries and microfluidic devices, ~~as well as~~ detergents were required, such as 0.1 % Tween-20~~, to reduce surface tension (capillaries, chip, biosensors)~~. For AUC-FDS, we had to avoid Tris-HCl or HEPES above 20 mM, which can cause problems at 230 nm wavelength, and be aware of other absorbent molecules (nucleotides, old DTT or β-mercaptoethanol). For MST experiments, we used the commercial MST buffers (50 mM Tris-HCl pH 7.4, 150 mM NaCl, 10 mM $MgCl_2$, 0.05 % Tween-20) for Ku-DNA and, Roti®-Stock 1x PBS (10 mM Na_2HPO_4, 2 mM KH_2PO_4 pH 7.6137 mM NaCl, 2.7 mM KCl, 0.005% Tween 20) for A3-Rep17. For switchSENSE sizing experiments D_h estimation, a low salt buffer is required (10 mM Tris-HCl, 40 mM NaCl, 0.05 % Tween-20, 50 µM EGTA, 50 µM EDTA).

In order for new users to determine the concentration ranges to work with in an unknown system, preliminary experiments need to be done using a broad range, observe the results and in consequence refine the initial conditions to a narrow range that could better suit the system in question. If an interaction partner is difficult to produce or not stable at high concentration, in solution approaches will be the one to keep in constant concentration during titration of its partner. In the other approaches must be the one to try first to immobilize or label. Reverse configuration can be always tested to improve or confirm the results.

Results

Biophysical measurements of alphaRep interactions

We characterized the interaction of A3 with its binders ~~Rep2 and~~ Rep17 (Rep2 was also used during the preparation of the training) using the following techniques presented in the Fig. 1: in solution approaches, which do not require labeling (SEC-MALS and ITC), in solution approaches that require labeled protein or DNA (MST and AUC-FDS), and surface approaches (BLI and switchSENSE). The students performed the measurements presented here during the training (Fig. 2, Fig. S2~~3~~ and Table S1). ~~The studied interactions data represent limited value due to students measuring and protein concentration as common denominators, but added benefits of putting the techniques in context. For most of them, additional measurements and controls are needed.~~ When available, we mention the values that have been reported for some approaches in previous studies~~articles~~.

AlphaRep interactions measured by label free in solution approaches

Due to time limitations, the SEC-MALS experiments were performed ~~in our platform~~ prior to the training. We used a Superdex 200 increase 10/300 GL column (*Cytiva*), and compared three different runs with A3 alone, Rep2 alone and A3-Rep2 complex at 2 mg/mL ~~concentration~~ each. A3 eluted as a dimer with a molar mass of 44.8 ± 0.4 kDa and, a hydrodynamic radius of 3.0 ± 0.2 nm. Rep2 eluted as a monomer with a molar mass of 11.6 ± 0.9 kDa. The Rep2 concentration was insufficient, in view of the small molar mass, to make accurate sizing measurement by DLS. Finally, the A3-Rep2 complex eluted before the free proteins, with a molar mass of 65.5 ± 0.4 kDa and hydrodynamic radius of 4.0 ± 0.2 nm (Fig. 2b). The stoichiometry was determined by using the protein conjugate method (Loiseau et al., 2017). Accurate mass can be calculated from MALS data with this method, which uses two concentration detectors simultaneously (a refractometer and UV spectrophotometer), and information about refractive index increment (dn/dc) and UV extinction coefficient of each component. In our case, the complex corresponds to one dimer of A3 and two Rep2 molecules.

Preparatory ITC experiments were performed ~~in our platform~~ on a PEAQ-ITC instrument with A3 in the cell at 18 µM and Rep17 in the syringe at 187 µM (Fig. S2~~3~~a). Three different groups of students did a triplicate measurement ~~(Fig. 2c)~~ during the training using the same PEAQ-

ITC~~same~~ instrument. We observed bi-phasic thermograms, and isotherms were fitted using a model of two identical binding sites with cooperativity. This cooperativity could stem from the propensity of A3 to form homodimers at µM concentration as shown by SEC-MALS (Freire et al., 2009; Vega et al., 2015). We could estimate two K_D values, the first K_D corresponds to an interaction with a tight affinity (K_{D1} from 0.48~~5~~ ~~–~~to 0.66~~7~~ nM) and the second one to a weaker affinity (K_{D2} from 16 ~~–~~to 32 nM) (Fig. 2c). With the obtained parameters for each site, described in the table at the bottom of thermograms, an average global affinity (Wyman and Gill, 1990) could be calculated (geometric mean of both dissociation constants: $K_{D,av}$ = sqrt(K_{D1} x K_{D2}), which for each assay was 3.9 nM, 3.1 nM, and 3.2 nM, close to that obtained with other techniques. Data were analyzed during the training using the Origin software and the new PEAQ ITC software for comparison.

AlphaRep interactions measured by biophysical approaches with a partner immobilized on a surface

Preliminary~~Comparable~~ analysis using SPR ~~classical technology~~, were carried out ~~in our platform using~~ a ProteON XPR36 instrument from *Biorad* (data not published, Fig. S2~~3~~b).

Before the training p~~P~~reliminary BLI experiments were performed ~~before the training~~ on an Octet RED384 instrument where His-tagged A3 protein was captured on Ni-NTA sensors at 5 µg/mL for 20 s and Rep17 concentration ~~ranges~~ ranged from 200 nM to 1.56 nM. In these conditions, in which A3 is most probably in a monomeric form, the calculated kinetic rates were k_{ON} of 1.3 10^{+5} $M^{-1}s^{-1}$, k_{OFF} of 5.9 10^{-3} s^{-1} and K_D of 22.4 nM (data not shown). We observed that the fit was not correct with a single site model and that residuals showed systematic errors. During the training, a duplicate experiment was performed on an Octet RED96e in a buffer containing 1 mg/mL BSA and 0.1 % Tween-20 to limit the non-specific binding. In this case, the fitting was improved (Fig. 2d). We obtained the following preliminary values: k_{ON} of 2.6 ± 0.7 10^{+5} $M^{-1}s^{-1}$, k_{OFF} of 7.6 ± 0.7 10^{-4} s^{-1}, K_D of 3.2 ± 1.1 nM. The K_D measured from the plateau of the curve (steady state) was of 3.3 ± 0.8 nM, close to the one obtained from kinetics (Fig. S2~~3~~c).

For the switchSENSE experiments, we first coupled A3 with the DNA strand (cNL-B48), which was complementary to the surface-tethered DNA strand on the chip. In this case, the surface-tethered DNA strand was labeled with a red fluorescent probe (NLB48-red dye). The DNA-

protein conjugate was purified using an anion-exchange-chromatography (Fig. S2~~3~~d, top left). We then hybridized the A3-cNLB48 with the NLB48 on the sensor surface at a concentration of 100 nM. The hybridization step could be monitored in real-time by measuring the fluorescence increase (Fig. S2~~3~~d, top right). Preliminary kinetic experiments were done using the dynamic mode (switching of the nanolevers) ~~in our platform~~. Rep2 alphaRep was used as analyte at three different concentrations ranging from 100 nM to 11.1 nM. Preliminary kinetic rates were calculated from a global fit for the three concentrations: k_{ON} of 2.40 ± 0.05 10^{+6} $M^{-1}s^{-1}$, k_{OFF} of 6.86 ± 0.23 10^{-4} s^{-1} and K_D of 0.29 ± 0.01 nM (Fig. S2~~3~~d, bottom, left). For each analyte concentration, it was possible to perform a sizing experiment to measure the hydrodynamic diameter of the ligand A3, before or after association with Rep2. The D_h of the dimeric form of A3 calculated from the crystal structure (PDB 6FT) is found to be equal to 4.8 nm. Due to protein dilution, we expect A3 to be present as a monomer on the DNA conjugated strand. Indeed, the D_h of 3.0 ± 0.1 nm measured in our switchSENSE experiments is compatible with a monomeric form of A3 (Fig. S2~~3~~d, bottom, right). The D_h = 3.8 ± 0.1 nm measured for the complex A3-Rep2 corresponds to an increase of 0.8 nm when compared to the hydrodynamic diameter of the monomeric form of A3 (Fig. S2~~3~~d, bottom, left). During the training, kinetic experiments in static mode (nanolevers in up position) were performed, as before for Rep2, with Rep17 concentration ranging from 100 nM to 11.1 nM~~in the same conditions as before for Rep2, but with Rep17 alphaRep as ligand~~. The calculated kinetic values measured in this case were in the same range than the ones obtained previously with Rep2: k_{ON} of 2.35 ± 0.17 10^{+6} $M^{-1}s^{-1}$, k_{OFF} of 2.30 ± 0.34 10^{-3} s^{-1} and K_D of 0.98 ± 0.16 nM (Fig. 2e). During the training, students did not have time to run a sizing experiment.

~~Comparable analysis using SPR classical technology, were carried out in our platform using a ProteON XPR36 instrument from *Biorad* (data not published, Fig. S3b).~~

AlphaRep interactions measured by biophysical approaches with a labeled partner

Because AUC-FDS experiment ~~were~~ was time consuming, data were collected before the training ~~in our platform~~. We first labeled A3 with the dye NT495 using the commercial *NanoTemper* Monolith Protein Labeling Kit BLUE-NHS (Amine Reactive). In these conditions, we were able to use a low concentration of A3 (5 nM). At this nanomolar concentration, A3 is a monomer as observed before by switchSENSE. We used variable concentrations of Rep17

from 0.5 nM to 0.5 µM, and an An-50 Ti rotor at 42 000 rpm (130 000 g) speed. The sedimentation coefficients for A3 and A3-Rep17 complex were 2.16 ± 0.08 S and 2.96 ± 0.05 S, respectively and the calculated K_D at equilibrium was 13.4 ± 1.8 nM (Fig. 2fe).

Finally, for the MST experiment, we decided to use ~~another~~ the ~~dye *from NanoTemper* Monolith His-Tag Labeling Kit~~ Red-tris-NTA 2nd Generation dye from the *NanoTemper* Monolith His-Tag Labeling Kit, this site-specific non covalent labeling substantially improved the signal respect to the 1st Generation dyes, and respected better the integrity of protein. Red-tris-NTA labeled A3 could not be used in AUC-FDS experiment, because its excitation and emission maxima are out of the fluorescence detector range (488nm and 505-565 nm respectively). In the~~is~~ MST experiment, labeled A3 was at ~~70~~ 35 nM, and the highest concentration of Rep17 was 8 µM. The titration curves we obtained allowed us to measure a K_D of 8.0 ± 4.3 nM (Fig. 2g). ~~Using the labeled A3 produced for the AUC-FDS at 20 nM did not provide us with substantial results due to high inhomogeneity in the sample preparation (Fig S3e), thus leading to a strong noise and suggesting that this labeling of A3 influences the interaction on the time scale of the MST measurement. Interestingly, we observed a titration curve with a K_D at 10.5 ± 2.4 µM, which could be linked to an additional interaction between A3-Rep17 complexes at the highest Rep17 concentration of 288 µM or some steric hindrance of the fluorescent probe. Orthogonal confirmation would help to better understand the origin of this K_D difference, unfortunately none of the other approaches were performed at such high concentration.~~

Figure 2. Biophysical measurements of alphaRep interactions.

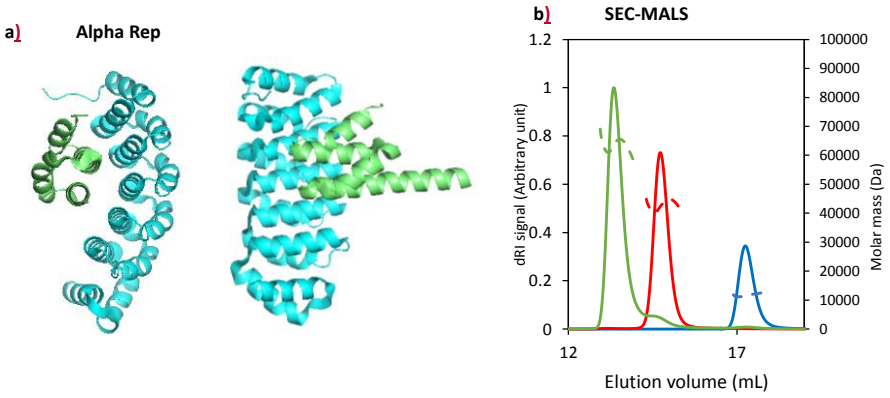

Formatted: Font: Not Italic

Formatted: Superscript

Formatted: Strikethrough

c) ITC

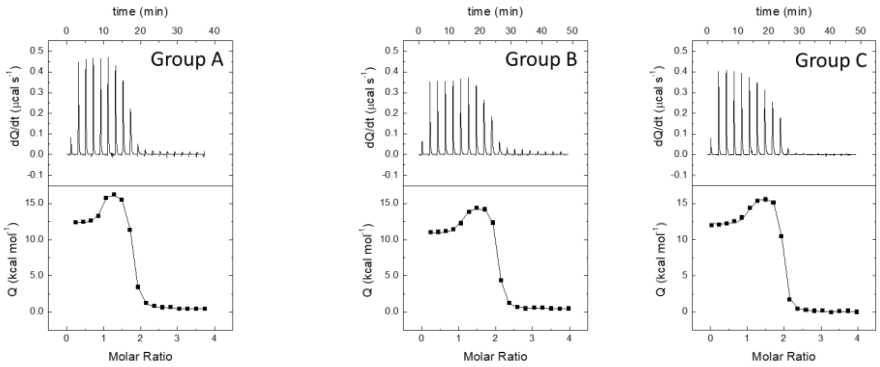

	K (M^{-1})	K_D (nM)	ΔH (kcal/mol)	α	Δh (kcal/mol)	n
Group A	$2.1 \cdot 10^9$	0.48	12.0	0.015	4.3	0.84
Group B	$1.7 \cdot 10^9$	0.59	10.5	0.036	3.6	0.98
Group C	$1.5 \cdot 10^9$	0.66	12.2	0.041	3.8	0.94

	K_{D1} (nM)	ΔH_1 (kcal/mol)	K_{D2} (nM)	ΔH_2 (kcal/mol)
Group A	0.48	12.0	32	16.3
Group B	0.59	10.5	16	14.1
Group C	0.66	12.2	16	16.0

d) BLI

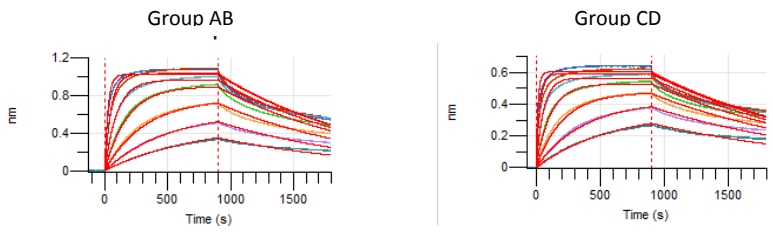

e) switchSENSE

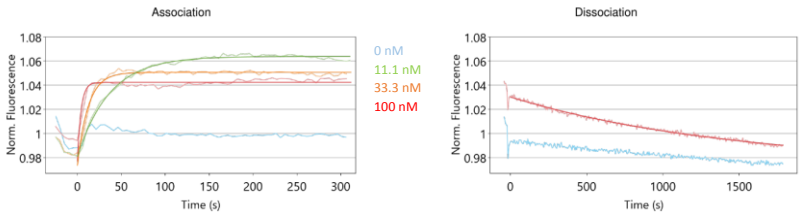

f) AUC-FDS g) MST

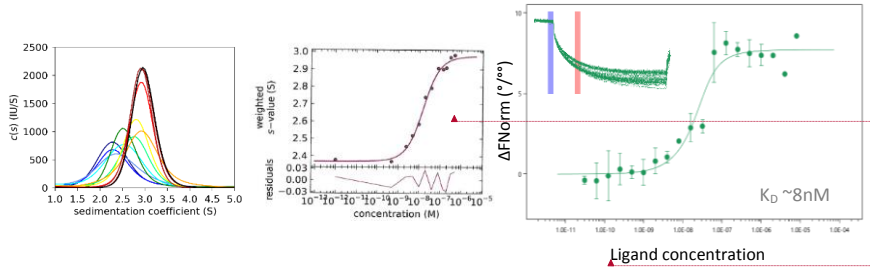

Formatted: Font: 9 pt

Formatted: Font: 9 pt

a) Crystal structure of A3 alphaRep (a-A3, blue) in complex with Rep2 (bA3-2, green) (PDB: 4JW2) at 90° view (left). b) SEC-MALS analysis. Elution profiles and molar masses of Rep2 in blue, A3 in red, and the complex of A3-dimer and two molecules of Rep2 in green. c) PEAQ-ITC data of A3-Rep17 interaction obtained during the training for three groups (A, B and C). K, K_D, and ΔH were the association constant, the dissociation constant, and the interaction enthalpy of either of the two binding sites when the A3 dimer was unoccupied. α and Δh were the cooperative interaction constant and the cooperative interaction enthalpy, which reflect the binding cooperative phenomenon (a factor that modulates the binding affinity and a term that modulates the binding enthalpy to the second site when there was a site already occupied, respectively). n was the active (or binding-competent) fraction of protein, since the stoichiometry was already included in the model. K_{D1} and ΔH_1 were the intrinsic site-specific dissociation constant and binding enthalpy for the first binding site ($K_{D1} = K_D$, $\Delta H_1 = \Delta H$). K_{D2} and ΔH_2 were the intrinsic site-specific dissociation constant and binding enthalpy for the second binding site ($K_{D2} = K_{D1} / \alpha$, $\Delta H_2 = \Delta H_1 + \Delta h$). d) Octet RED96e BLI kinetic analysis of A3-Rep17 interaction in duplicate. Colors code of Rep17 concentration: 3.13 nM (teal), 6.25 nM (purple), 12.5 nM (orange), 25 nM (green), 50 nM (cyan), 100 nM (red), 200 nM (blue). e) switchSENSE kinetics analysis of A3-Rep17 interaction on dynamic mode, at three Rep17 concentrations. Normalized association (left) and dissociation (right) data were represented in function of time. f) AUC-FDS distribution of sedimentation coefficients (left) with labeled A3 at 5 nM and increasing concentrations of Rep17 from 0.5 nM to 0.5 µM, obtained with the program SEDFIT (Schuck, 2000) and GUSSI (Brautigam, 2015). Colors code of Rep17 concentrations: 0 µM (navy blue), 0.5 nM (blue), 1 nM (cornflower blue), 2 nM (cyan), 4 nM (green), 8 nM (springgreen), 16 nM (yellow), 32 nM (orange), 64 nM (red), 128 nM (maroon), 256 nM (brown) and 0.5 µM (black). AUC-FDS K_D calculation (right), by fitting with isotherm tool in the program SEDPHAT. g) MST analysis with red fluorophore. Inset, MST traces from relative fluorescence versus time, MST on used was 10 s (red band).

In summary, the students obtained ~~preliminary results~~ in one week ~~with the six~~using several complementary approaches, results that were consistent in stoichiometry, and to a lesser extent, in kinetic rates or affinity (Table S1). They could observe that the required ~~amount of material~~quantity of sample, ligand or analyte, for each approach differs significantly. They also observed that some approaches gave highly complementary information on the system studied (Fig. S2~~3~~). For example, ITC shows that the interaction is cooperative when A3 alphaRep is used at the high concentration needed for ITC (18µM). This cooperativity, linked to the dimeric state of A3, was not observed with monomeric ligand immobilized on BLI or switchSENSE. They observed higher K_D values with AUC-FDS and MST, where one of the partner is labeled, reflecting possible steric hindrance between the fluorophore and the interaction site. This was particularly true with the covalent amine labeling strategy where the K_D measured by MST was three order of magnitude higher.

Biophysical measurements of Ku-DNA interactions

We determined the interaction of the heterodimeric full-length protein Ku with four double-strand DNAs (dsDNAs) of different lengths: 18 bp, 42 bp, 48 bp, and 200 bp (Fig. 3, Fig. S34). Ku binds DNA through its ring-shaped structure (Fig. 3a). The main observations made during the training for the Ku-DNA interactions ~~, using the same six approaches, as for the alphaRep interactions,~~ are shown in Fig. 3 and Table S2.

Ku-DNA interactions measured by label-free in solution biophysical approaches

For SEC-MALS, we used a Superdex 200 increase 10/300 GL column (*Cytiva*)~~the same column~~ as above and ran first a quadruplicate experiment with Ku alone, resulting in an average molar mass of 144.4 kDa (Fig. S34a). We then ran a duplicate experiment with Ku and a 1.2 excess of 42 bp DNA. We obtained three peaks: the first corresponded to 2 Ku : 1 DNA complex (average Mw of 306.2 kDa), the second corresponded to 1 Ku : 1 DNA (average Mw of 171.0 kDa), and the last corresponded to the excess of dsDNA alone (average Mw of 26.1 kDa). This suggests that there is an equilibrium between 2:1 and 1:1 Ku-DNA complexes (Fig. 3b) with stoichiometries determined by using the protein conjugated method (Loiseau et al.; 2017). The presence of these two types of complexes could be explain by the use of a non-saturating Ku concentration.

For ITC experiments, we used in our laboratory two different sizes of dsDNA, 18 bp and 42 bp (Gontier et al., 2021~~, Chapter of MiMB, *in press*~~). Due to time limitations students repeated the measurement only with the 42 bp. We used a VP-ITC instrument which consumes more sample, but was more sensitive to study these protein-DNA interactions. The heat effects were positive (endothermic interaction) and small (0.2 µcal.sec^{-1}) (Fig. 3c). Students did two runs, the first at 20 µM and the second at 40 µM concentration of DNA in the syringe, and in both cases Ku at 4 µM in the cell. We obtained a mean K_D at equilibrium of 3.7 ± 0.7 nM with a molar ratio of 0.34 ± 0.02 and a ΔH of 24.4 ± 2.7 kcal/mol. The molar ratio was in good agreement with a ratio of 0.5 expected for the interaction of two Ku molecules with a DNA of 42 bp. No evidence for cooperativity was observed. All the data were analyzed using the Origin software and the new PEAQ ITC software for comparison.

Ku-DNA interactions measured by biophysical approaches with a partner immobilized on a surface

Preparatory BLI experiments were performed on an Octet RED384 instrument. First~~ly~~, we tried the ~~same~~ strategy that was used for the A3 alphaRep protein, i.e. ~~captured~~ capturing the Ku heterodimer on Ni-NTA sensors. We did not observe any binding with an 18 bp DNA as analyte (data not shown). We hypothesized that the DNA binding site may not be accessible when Ku is immobilized through its His-tag. We therefore tested another strategy, which relied on the capture of a biotinylated 42 bp DNA on Streptavidin sensors (at 10 nM for 120 s), which were then incubated with Ku protein as analyte (at concentrations in 200 nM to 1.56 nM range). In these conditions, we observed an interaction, with an estimated K_D around 40 nM (data not shown). We repeated the experiment in duplicate during the training on an Octet RED96e using an optimized buffer with 1mg/mL BSA and 0.1 % Tween-20, and Ku protein concentrations ranging from 200 nM to 3 nM. The results of the two runs were consistent, with apparent kinetic rates, k_{ON} of 1.91 ± 0.02 10^{+6} $M^{-1}s^{-1}$, k_{OFF} of 7.17 ± 0.33 10^{-4} s^{-1}, and a K_D of 0.37 ± 0.01 nM (Fig. 3d). However, the deviation between the fitted curves and the experimental data was high, indicating that the interaction mechanism was more complex than a simple 1:1 binding. For instance, the association and the dissociation processes could be limited by the diffusion of Ku towards and from the biosensor surface (mass transport limitation). We therefore analyzed the concentration-dependence of the steady state responses and measured a K_D of 5.2 ± 0.2 nM (Fig. S3~~4~~b). As several curves did not reach~~ed~~ a steady state, this K_D value could however be overestimated and experiments should be reproduced with longer association times. Taking everything into account, BLI binding constants were at this stage only qualitative.

Preliminary switchSENSE experiments were done before the training by forming an 80 bp dsDNA on the sensor. For that, we hybridized an 80-mer DNA with a 32-mer DNA. This DNA was complementary to the NL48 ssDNA on the chip (Fig. S3~~4~~c, top, left). We performed kinetic analyses in duplicate using static mode and Ku protein at 500 nM concentration. We obtained the following kinetic rates: k_{ON} of 9.3 ± 0.1 10^{+4} $M^{-1}s^{-1}$, k_{OFF} of 2.8 ± 0.1 10^{-4} s^{-1}, and K_D of 3.1 ± 0.1 nM (Fig. S3~~4~~c, bottom). We monitored the dissociation over a long time (5000 s) to measure a significant proportion of dissociated Ku molecules. In between, we performed a sizing measurement. The calculated value (D_h = 8.9 ± 0.3 nm) was in good agreement with the one obtained from the crystal structure of the Ku-DNA complex (PDB: 1JEQ; D_h = 8.9 nm) (Fig. S3~~4~~c, top, right). During the training, we performed experiments in dynamic mode using a 48

bp DNA (without overhang). We used a Ku concentration range from 200 nM to 22.2 nM with 1/3 serial dilution this time. In these conditions, the protein was closer to the fluorophore at the tip of the 48 bp DNA on the chip. We measured in these conditions a k_{ON} of 2.6 ± 0.2 10^{+6} $M^{-1}s^{-1}$, a k_{OFF} of 2.3 ± 0.3 10^{-3} s^{-1}, and a K_D of 1.0 ± 0.2 nM (Fig. 3e). During the training, students did not have time to run a sizing experiment.

Comparable preliminary data were obtained by SPR ~~in our platform~~ using a ProteON XPR36 instrument from *Biorad* (Fig. S34d, left), and ~~in Institut Pasteur platform using~~ a Biacore T200 instrument from *Cytiva* (Fig. S34d, right).

Ku-DNA interactions measured by biophysical approaches with a labeled partner

For AUC-FDS, we used an 18 bp DNA labeled with fluorescein (FAM) in 5'. We titrated the DNA (60nM) with Ku ~~protein from~~ (concentration range from 0.5 nM to 0.5 µM) ~~concentrations with 60nM of DNA~~. The sedimentation profile showed two species, corresponding to the DNA alone (2.15 ± 0.05 S) and to the 1:1 protein-DNA complex (7.25 ± 0.15 S), and we were able to determine the K_D at equilibrium (12.9 ± 3.2 nM) (Fig. 3f).

For MST, we used the same 18 bp labeled DNA ~~same labeled 18 bp DNA~~ as for AUC-FDS, but at 10 nM ~~concentration~~; and titrated it with Ku (concentration range from 2 µM) ~~concentration~~. Training participants performed four runs in total, in duplicates or triplicate ~~measurements~~ (Fig. 3g). We could see some variability in the curves that might originate from the pipetting of the different students. All curves were fitted globally resulting in a K_D of 2.8 nM.

Comparable data were obtained in parallel of the training with a novel technology, microfluidic diffusional sizing (MDS) in collaboration with Fluidic Analytics (Fig. S34e). The Fluidity One-W instrument measures the rate of diffusion of macromolecules under steady state laminar flow in a microfluidic chip. In a diffusion chamber with two parallel streams, the migration of a labeled partner depends on its size. At the end, the streams are re-split and ~~from~~ the fluorescence ratio ~~of the fluorescence~~ between the two allows to calculate~~m,~~ R_h ~~is calculated~~. The~~n, changes in average size after titrat~~ variation of R_h observed when titrating ~~an unlabeled binding partner against~~ the labeled partner by the unlabeled one allows to generate~~, give~~ a binding curve and to calculate a K_D value.

Figure 3. Biophysical measurements of Ku-DNA interactions.

a) **Ku-DNA**

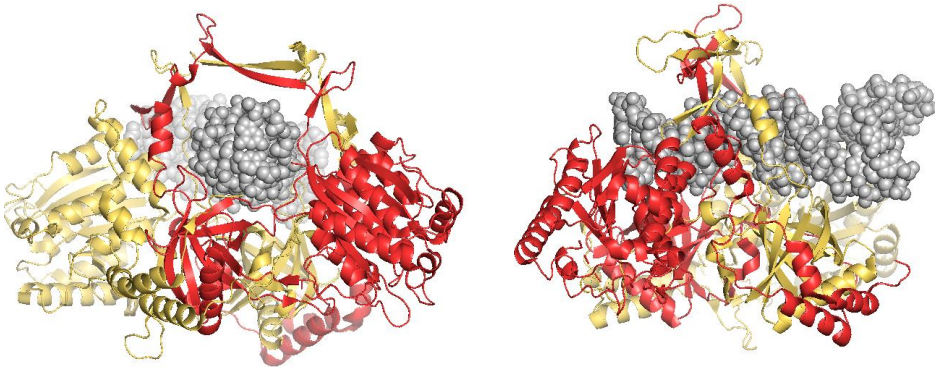

b) SEC-MALS

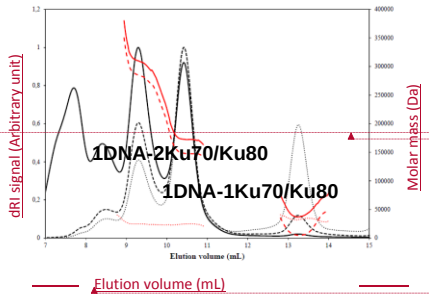

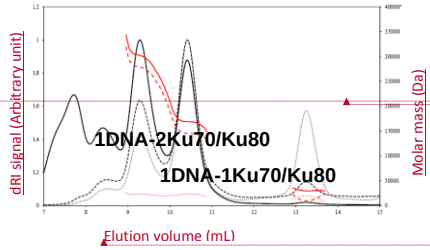

		Peak 1	Peak 2	Peak 3
Group C	Protein molar mass	279.1	145.7	9.6
	DNA molar mass	23.3	23.3	19.9
	Total molar mass	302.3	169.0	29.6
Group D	Protein molar mass	285.3	148.4	4.8
	DNA molar mass	24.7	24.6	32.3
	Total molar mass	310.1	172.9	37.1

c) ITC

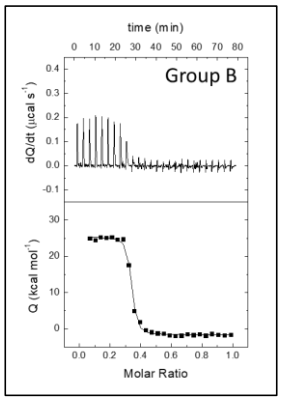

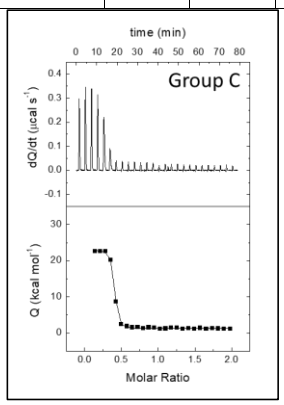

	K (M^{-1})	K_D (nM)	ΔH (kcal/mol)	n
Group B	$3.4\ 10^8$	3.0	27.1	0.32
Group C	$2.3\ 10^9$	4.3	21.7	0.37

d) BLI: Group AB and Group CD

Formatted: Font: 8 pt
Formatted: Font: 8 pt
Formatted: Font: 8 pt
Formatted: Font: 8 pt
Formatted: Font: 8 pt
Formatted: Font: 8 pt
Formatted: Font: 10 pt
Formatted: Font: 10 pt

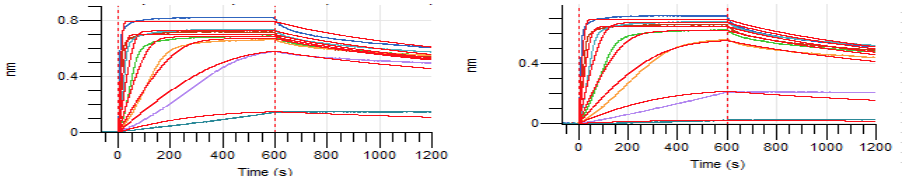

e) **switchSENSE**

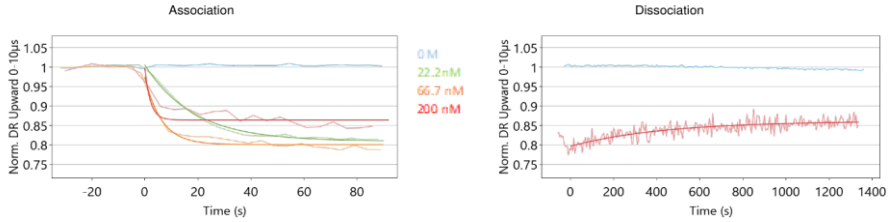

f) **AUC-FDS**

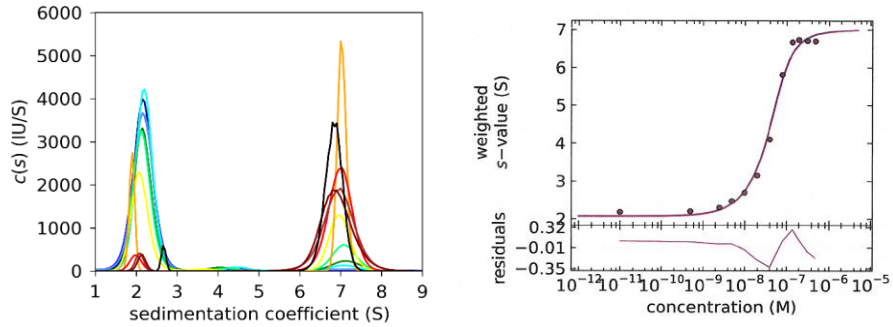

g) **MST**

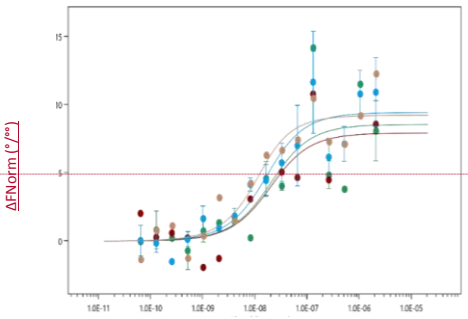

GROUPS	Excitation Power	K_D	K_D Confidence	Std. Error of Regression	Signal to Noise
A1-B1	60	$1.53\ 10^{-08}$	$1.86\ 10^{-08}$	2.77	3.33
A2	40	$1.49\ 10^{-08}$	$1.73\ 10^{-08}$	2.01	4.33
B2-C2-D2	100	$1.14\ 10^{-08}$	$7.26\ 10^{-09}$	1.61	6.31
D1	100	$6.15\ 10^{-09}$	$4.3\ 10^{-09}$	1.56	6.37

a) Crystal structure of the Ku- DNA complex (PDB: 1JEQ). View down the DNA helix (left) and side view (right), with Ku70 colored in red, Ku80 in yellow cartoons and DNA in grey spheres. b) SEC-MALS elution profiles and molar masses of Ku-DNA complex in duplicate. Representation of elution volumes in mL and molar mass in g/mol.

Formatted: Font: 10 pt

Formatted: Font: 10 pt

Formatted: Font: 8 pt

Formatted: Font: 8 pt

c) VP-ITC data in duplicate. d) Octet RED96e BLI kinetics data in duplicate. Colors code of Ku concentration: 3.13 nM (teal), 6.25 nM (purple), 12.5 nM (orange), 25 nM (green), 50 nM (cyan), 100 nM (red), 200 nM (blue). e) switchSENSE dynamic mode data for three Ku concentrations. F) AUC-FDS measurement of Ku-DNA interaction. AUC-FDS distribution of sedimentation coefficients (left) with labeled DNA at 60 nM and increasing concentrations of Ku from 0.5 nM to 0.5 µM, obtained with the program SEDFIT (Schuck, 2000) and GUSSI (Brautigam, 2015). Colors code of Ku concentration: 0 µM (navy blue), 0.5 nM (blue), 1 nM (cornflower blue), 2 nM (cyan), 4 nM (green), 8 nM (springgreen) , 16 nM (yellow), 32 nM (orange), 64 nM (red), 128 nM (maroon), 256 nM (brown) and 0.5 µM (black). AUC-FDS K_D calculation by fitting with isotherm tool in the program SEDPHAT (right). g) MST analysis. Representation of ligand concentration against ΔFNorm °/°° (left). Superposition of several run in the similar conditions, but different excitation power and students. Summary of MST data (right).

In summary, for the Ku-DNA project, the students also obtained ~~also for the Ku-DNA project results~~ consistent results of~~in~~ stoichiometry, ~~and in the same range for~~ kinetic rates ~~or~~ and affinity (Fig. 3, Table S2). As for the alphaRep project, ~~they observed that~~ the ~~amount of material~~quantity of sample required varies between the different approaches. ITC, SEC-MALS and AUC-FDS were very efficient for measuring the stoichiometry of Ku on DNA with one Ku molecule bound every 18-21bp DNA. They observed that measurements on surfaces, either by BLI or switchSENSE, were successful only when the DNA was immobilized. They could observe that switchSENSE allows a quite accurate estimation of the Ku size (Fig. S34d, bottom). Oligonucleotides with a fluorescent probe in 5' or 3' are inexpensive and allow to follow the interaction between a fluorescent DNA and a protein quite easily by MST or AUC-FDS, without major steric hindrance between the fluorescent probe and the interaction sites.

Discussion

The study presented here compares six different *in vitro* biophysical approaches to characterize the architecture (in terms of size or stoichiometry) and binding parameters (k_{ON}, k_{OFF}, K_D) of two different types of complexes (protein-protein and protein-DNA). It was designed to provide a rather complete overview of six different techniques in a short period. During a week, 20 participants performed this study in the context of ~~a~~ the MoSBio Training School (ARBRE-MOBIEU COST Action). During the first day of the training school, experts of each field presented the projects, the theory and examples of applications for the three classical techniques (AUC, SEC-MALS, ITC), and the three more recent ones (MST, BLI, switchSENSE). An additional presentation about, sample quality control, a relevant subject regarding reproducibility of experimental measurements, completed the first day of the training (Raynal et al., 2014). The remainder of the week was dedicated fulltime to practical sessions where the participants could perform experiments on instruments, analyze results and discuss with experts. All six approaches, except AUC, and SEC-MALS for the alphaRep

Formatted: Subscript

Formatted: Subscript

Formatted: Subscript

interaction, were successfully used during the training school to study two important types of macromolecular interactions (~~protein-protein~~alphaReps and Ku~~protein~~-DNA). The training allowed the students, first, to compare the quantity of material consumed for each technique, and, second, to understand the parameters that can be measured by each of them (Fig. 4). This first edition of the MoSBio Training School was positively assessed ~~by~~ both by ~~experts~~ trainers and ~~participants~~trainees. It was a unique opportunity to compare advantages and limitations of this large ensemble of techniques. A new edition will be scheduled soon. The participants were able to use all instruments quite easily by themselves, with the exception of AUC, which requires a little more expertise and longer run times. Finally, this study showed that a nanomolar range affinity ~~is~~ can be easily ~~to be~~ assessed with all tested techniques. The students could observe that the K_D vary significantly with the technique used, though the K_D measured were all in the nanomolar range. The maximal and minimal values of K_D measured between the alphaRep and the different techniques differ by a factor 21. The extreme K_D differ by a factor 13 for the K_D measured between Ku and DNA. We observed that in these two systems the presence of a label on one partner, in MST and AUC-FDS approaches, comes with a higher K_D than without label. During the training school, the students could observe the variability on the K_D values measured in the different groups or with the different approaches (see Fig. 2 and Fig. 3). The training was also an opportunity to discuss on the techniques that are more favorable ~~Nevertheless, this is not the case when we want~~ to measure lower ~~K_D~~ (pM) or higher ~~K_D~~ (µM) K_D values.

Formatted: Font color: Auto

The results presented here for the alphaRep-proteins and Ku-DNA complexes highlight the advantages and drawbacks of each approach. The quantity~~amount~~ of required ~~material~~ sample was not limited in our case, but the participants clearly observed that the amounts of protein and DNA used for each approach are very different (Fig. 4). AUC, SEC-MALS and ITC are the most sample-consuming techniques. The ITC200 and PEAQ-ITC instruments were an important progress for ITC in this regard, but we observed that for interactions with very weak heat exchange like Ku-DNA, the more sensitive, but more sample-consuming VP-ITC was still needed to obtain good results. Surface methods like BLI and switchSENSE require only small amounts of the immobilized protein. For the study of high affinity systems (in the nM range) like those characterized here, the consumption of analyte is small too. For weaker affinities (higher K_D in the µM range) the required ~~amount~~quantity of analyte will however rise

significantly to cover concentrations from 1/10 of the K_D to 10 times the K_D. The MST technique consumes very small volumes of material once the labeling step is successfully achieved. Anyway, the time and sample consumption for a given technique must be evaluated not just for a single successful experiment, but must also ~~considering t~~take into account he experimental design and optimization stage.

Figure 4. Comparison of results obtained for the alphaReps and the Ku-DNA interaction with the six approaches.

Alpha Reps	**SEC-MALS**	**200 µg A3, 200 µg Rep2** Molar mass Stoichiometry: (A3-dimer): 2 Rep2	ITC	**80 µg A3, 130 µg Rep17** Biphasic curve Cooperativity (A3 dimer) K_{D1}, K_{D2}, ΔH, -TΔs
	BLI	**8 µg A3, 2 µg Rep17** A3-monomer K_D, k_{ON}, k_{OFF}	Switch-SENSE	**150 ng A3, 2-20 µg Rep17** A3-monomer Size (D_h) K_D, k_{ON}, k_{OFF}
	AUC-FDS	**1 µg A3, 8 µg Rep17** Sedimentation coefficient Stoichiometry K_D	**MST**	**620 ng A3, 6 µg Rep17** (One labeling failed) K_D
Ku-DNA	**SEC-MALS**	**40µg of DNA, 200 µg Ku** Molar mass Stoichiometry: 1 Ku /18-21 bp	**ITC**	**990 µg Ku, 320 µg DNA** Biphasic curve Stoichiometry: 1 Ku /18-21bp K_D, ΔH,-TΔS
	BLI	**400 ng DNA, 14 µg Ku** (Failed with Ku immobilized) K_D, k_{ON}, k_{OFF}	**Switch-SENSE**	**150 ng DNA, 2-20 µg Ku** (Ligand is the nanolever) Size (D_h) K_D, k_{ON}, k_{OFF}
	AUC-FDS	**3.5 µg DNA, 80 µg Ku** (DNA easily labeled) Sedimentation coefficient Stoichiometry K_D	**MST**	**50 µg DNA, 12 µg Ku** (DNA easily labeled) K_D

~~**SEC-MALS**~~	~~**AlphaReps**~~ ~~✓ 200 µg A3, 200 µg Rep2~~ ~~➢ Molar mass~~ ~~➢ Stoichiometry: (A3-dimer): 2 Rep2~~	~~**ITC**~~	~~**AlphaReps**~~ ~~✓ 80 µg A3, 130 µg Rep17~~ ~~✓ Biphasic curve~~ ~~➢ Cooperativity (A3 dimer)~~ ~~➢ K_{D1}, K_{D2}, ΔH, -TΔs~~
	~~**Ku-DNA**~~ ~~✓ 40µg of DNA, 200 µg Ku~~ ~~➢ Molar mass~~ ~~➢ Stoichiometry: 1 Ku /18-21 bp~~		~~**Ku-DNA**~~ ~~✓ 990 µg Ku, 320 µg DNA~~ ~~✓ Biphasic curve~~ ~~➢ Stoichiometry: 1 Ku /18-21bp~~ ~~➢ K_D, ΔH, TΔS~~
~~**BLI**~~	~~**AlphaReps**~~ ~~✓ 8 µg A3, 2 µg Rep17~~ ~~✓ A3-monomer~~ ~~➢ K_D, k_{ON}, k_{OFF}~~	~~**switchSENSE**~~	~~**AlphaReps**~~ ~~✓ 150 ng A3, 2-20 µg Rep17~~ ~~✓ A3-monomer~~ ~~✓ Size (D_h)~~

			✓ K_D, k_{ON}, k_{OFF}
	Ku-DNA ✓ 400 ng DNA, 14 µg Ku ✓ Failed with Ku immobilized ➢ K_D, k_{ON}, k_{OFF}		**Ku-DNA** ✓ 150 ng DNA, 2-20 µg Ku ✓ Ligand is the nanolever ✓ Size (D_H) ➢ K_D, k_{ON}, k_{OFF}
AUC-FDS	**AlphaReps** ✓ 1 µg A3, 8 µg Rep17 ➢ Sedimentation coefficient ➢ Stoichiometry ➢ K_D	**MST**	**AlphaReps** ✓ 620 ng A3, 6 µg Rep17 ✓ One labeling failed ➢ K_D
	Ku-DNA ✓ 3.5 µg DNA, 80 µg Ku ✓ DNA easily labeled ➢ Sedimentation coefficient ➢ Stoichiometry ➢ K_D		**Ku-DNA** ✓ 50 µg DNA, 12 µg Ku ✓ DNA easily labeled ➢ K_D

The experiments performed by the students on the two systems of study with the six approaches were successful. Quantity of materialsThe sample quantities used for the different approaches are indicate, as well as very different. Here are the amount needed per run. The training highlighted the parameters that can be deduced from the different approaches.

All experimental approaches used in this study can provide K_D values of the interaction. Interestingly, they also provide additional information that may orient the users to one or the other according to the main questions raised in their specific projects. In the two examples we studied, the stoichiometry issue is an important point, since the A3 alphaRep is a dimer when its concentration is in the µM range, while it is a monomer in the nM range. According to this oligomeric state, we can observe some cooperative binding of its partner or not, or somewhich influences on the binding parameters. In this regards, ITC, SEC-MALS and AUC allow characterizing the ratio between the dimeric alphaRep target and its binders or between Ku and DNA of increasing lengths, and confirm the information provided by theirir crystal structures of the complexes. The sizing measurement in switchSENSE can also provide some information regarding the stoichiometry or /conformation.

Kinetic parameters are important data to estimate the half-time of a complex, which is an important interaction parameter gaining attention recently. BLI and switchSENSE (as well as SPR) proved to be efficient in this study to determine k_{ON} and k_{OFF}. We observed that the switchSENSE allows to characterize very tight interactions with small k_{OFF} values (k_{OFF} about 10^{-4} s) by monitoring the dissociation over a long time period (5000 s). Thermodynamic parameters (enthalpy, entropy and Gibbs free energy) also provide key information about

macromolecular interactions, notably about the polar/apolar nature of the interface between a protein and its ligand. The Ku-DNA thermograms for example indicate that the interaction is entropically driven with a positive and unfavorable enthalpy probably linked to desolvation of the DNA and Ku surface upon binding. ~~The MoSBio training school over a week with 20 students proved to be a very rich occasion for such discussions.~~

The choice of one technique over another depends mainly on the questions one wants to answer. Some practical issues can also guide the choice of the method, such as the quantity and solubility of protein and ligands available, the possibility to immobilize or to label one of the interaction partners, and the time available. The presence of an instrument and experts in house or nearby the user is another criterion. Noteworthy, all these approaches are available in many research institutions in Europe, especially in those engaged in Structural Biology studies. If needed, these approaches are also available through ~~network~~ research infrastructures, like MOSBRI and Instruct in Europe or FRISBI in France. Finally, there are research networks, like ARBRE-MOBIEU, allowing ~~and~~ to foster~~ing~~ fruitful exchanges with experts in the different fields. The MoSBio training school over a week with 20 students proved to be a very rich occasion for such discussions.

Studying macromolecular interactions *in vitro* ~~are~~ is extremely complementary to *in cellulo* analyses. Interactions observed in cells or in cellular extracts ~~need~~ often need further *in vitro* ~~validation~~ characterization ~~and~~ of target engagement ~~to confirm the specificity of the proposed interaction~~. Training schools, as the one described in this article, are central to further disseminate the importance of biophysical studies in cell~~ular~~ biology laboratories. This training school contributed to initiate students from various fields ~~on~~ to biophysical approaches and showed in a short period the added-value of quantitative measurements of protein interactions.

By mutagenesis, Nuclear Magnetic Resonance (NMR) shift or Hydrogen-Deuterium Exchange-Mass Spectrometry (HDX-MS), one can determine the residues involved in the interaction, and structural analysis can yield information about their topology. One can play with the experimental conditions (pH, ionic strength, temperature) to expand the knowledge about the nature of the interaction under study (electrostatic and/or hydrophobic, exo- or endothermic, presence/absence of conformational changes, coupling with additional binding equilibria). Furthermore, pharmacological studies require this kind of biophysical approaches. Finally,

molecular scale biophysics data can also be ~~also~~ used to implement *in silico* simulations to predict other interactions in basic research. A second edition of this Training School will be held as soon as possible. The extremely positive feedback~~s~~ from the students, as well as ~~and~~ from the academic experts and industrials participating in this school, highlights the need for a better understanding of the theoretical bases ~~and hands-on experimental practical~~ of such a panel of biophysical methods coupled to hands-on experimental practice.

References

Abdiche Y, Malashock D, Pinkerton A, Pons J.(2018) Determining kinetics and affinities of protein interactions using a parallel real-time label-free biosensor, the Octet. *Anal Biochem*. 377(2):209-17

Andreani J, Guerois R. (2014) Evolution of protein interactions: from interactomes to interfaces. *Arch Biochem Biophys*. 554:65-75

Asmari M, Ratih R, Alhazmi HA, El Deeb S. (2018) Thermophoresis for characterizing biomolecular interaction. *Methods* 146:107-119

Brautigam, CA. (2015) Chapter Five - Calculations and Publication-Quality Illustrations for Analytical Ultracentrifugation Data. In *Methods in Enzymology*, Cole, J. L., Ed. Academic Press: Vol. 562, pp 109-133

Campanacci V, Urvoas A, Consolati T, Cantos-Fernandes S, Aumont-Nicaise M, Valerio-Lepiniec M, Surrey T, Minard P, Gigant B. (2019) Selection and Characterization of Artificial Proteins Targeting the Tubulin α Subunit. *Structure*. 27(3):497-506

Chang HHY, Pannunzio NR, Adachi N, Lieber MR. (2017) Non-homologous DNA end joining and alternative pathways to double-strand break repair. *Nat Rev Mol Cell Biol* 18(8):495-506

Chevrel A, Mesneau A, Sanchez D, Celma L, Quevillon-Cheruel S, Cavagnino A, Nessler S, Li de la Sierra-Gallay I, van Tilbeurgh H, Minard P, Valerio-Lepiniec M, Urvoas A. (2018) Alpha repeat proteins (αRep) as expression and crystallization helpers. *J Struct Biol*. 201(2):88-99

Di Meo T, Ghattas W, Herrero C, Velours C, Minard P, Mahy JP, Ricoux R, Urvoas A. (2017) αRep A3: A Versatile Artificial Scaffold for Metalloenzyme Design. *Chemistry*. 23(42):10156-10166

Fernandez M, Urvoas A, Even-Hernandez P, Burel A, Mériadec C, Artzner F, Bouceba T, Minard P, Dujardin E, Marchi V. (2020) Hybrid gold nanoparticle-quantum dot self-assembled nanostructures driven by complementary artificial proteins. *Nanoscale*. 12(7):4612-4621

Folta-Stogniew E. (2006) Oligomeric states of proteins determined by size-exclusion chromatography coupled with light scattering, absorbance, and refractive index detectors. *Methods Mol. Biol. 328*, 97-112

Freire E, Schön A, Velazquez-Campoy A. (2009) Isothermal titration calorimetry: general formalism using binding polynomials. *Methods Enzymol*. 455:127-55

Frit P, Ropars V, Modesti M, Charbonnier JB, Calsou P. (2019) Plugged into the Ku-DNA hub: The NHEJ network. *Prog Biophys Mol Biol*. 147:62-76

Gontier A, Varela PF, Nemoz C, Ropars V, Aumont-Nicaise M, Desmadril M, Charbonnier JB. (2021) Measurements of Protein-DNA Complexes Interactions by Isothermal Titration Calorimetry (ITC) and Microscale Thermophoresis (MST). *Methods Mol. Biol. 2247*, 125-143

Guellouz A, Valerio-Lepiniec M, Urvoas A, Chevrel A, Graille M, Fourati-Kammoun Z, Desmadril M, van Tilbeurgh, Minard P. (2013) Selection of Specific Protein Binders for Pre-Defined Targets from an Optimized Library of Artificial Helicoidal Repeat Proteins (alphaRep). *PLoS One*. 8(8):e71512

Holdgate GA. (2001) Making cool drugs hot: isothermal titration calorimetry as a tool to study binding energetics. *Biotechniques* 31(1):164-170

Jerabek-Willemsen M, Wienken CJ, Braun D, D, Baaske P, Duhr S. (2011) Molecular interaction studies using microscale thermophoresis. *Assay Drug Dev Technol* 9(4):342-353

Knezevic J, Langer A, Hampel PA, Kaiser W, Strasser R, Rant U. (2012) Quantitation of Affinity, Avidity, and Binding Kinetics of Protein Analytes with a Dynamically Switchable Biosurface *J. Am. Chem. Soc.* 134 (37), 15225–15228

Formatted: Indent: Left: 0", Hanging: 0.1"

Formatted: French (France)

Formatted: Font: (Default) Calibri, 12 pt, Font color: Auto, French (France)

Formatted: Font: (Default) Calibri, 12 pt, Font color: Auto

Formatted: Font: (Default) Calibri, 12 pt, Font color: Auto, English (United States)

Formatted: Font: (Default) Calibri, 12 pt, Font color: Auto

Formatted: English (United States)

Krell T. (2008) Microcalorimetry: a response to challenges in modern biotechnology. *Microb Biotechnol* 1(2):126-136

Léger C, Di Meo T, Aumont-Nicaise M, Velours C, Durand D, Li de la Sierra-Gallay I, van Tilbeurgh H, Hildebrandt N, Desmadril M, Urvoas A, Valerio-Lepiniec M, Minard P. (2019) Ligand-induced conformational switch in an artificial bidomain protein scaffold. *Sci Rep*. 9(1):1178

Léger C, Yahia-Ammar A, Susumu K, Medintz IL, Urvoas A, Valerio-Lepiniec M, Minard P, Hildebrandt N. (2020) Picomolar Biosensing and Conformational Analysis Using Artificial Bidomain Proteins and Terbium-to-Quantum Dot Förster Resonance Energy Transfer. *ACS Nano*. 14(5):5956-5967

Loiseau L, Fyfe C, Aussel L, Hajj Chehade M, Hernández SB, Faivre B, Hamdane D, Mellot-Draznieks C, Rascalou B, Pelosi L, Velours C, Cornu D, Lombard M, Casadesús J, Pierrel F, Fontecave M, Barras F. (2017) The UbiK protein is an accessory factor necessary for bacterial ubiquinone (UQ) biosynthesis and forms a complex with the UQ biogenesis factor UbiJ. *J Biol Chem.* 292(28):11937-11950

Nemoz C, Ropars V, Frit P, Gontier A, Drevet P, Yu J, Guerois R, Pitois A, Comte A, Delteil C, Barboule N, Legrand P, Baconnais S, Yin Y, Tadi S, Barbet-Massin E, Berger I, Le Cam E, Modesti M, Rothenberg E, Calsou P, Charbonnier JB. (2018). XLF and APLF bind Ku at two remote sites to ensure DNA repair by non-homologous end joining. *Nat Struct Mol Biol.* 25(10):971-980

Prasad J, Viollet S, Gurunatha KL, Urvoas A, Fournier AC, Valerio-Lepiniec M, Marcelot C, Baris B, Minard P, Dujardin E. (2019) Directed evolution of artificial repeat proteins as habit modifiers for the morphosynthesis of (111)-terminated gold nanocrystals. *Nanoscale*. 11(37):17485-17497

Raynal B, Lenormand P, Baron B, Hoos S, England P. (2014) Quality assessment and optimization of purified protein samples: why and how? Microb Cell Fact. 13:180

Schuck, P. (2000) Size-distribution analysis of macromolecules by sedimentation velocity ultracentrifugation and lamm equation modeling. *Biophys. J.* 78, 1606-1619

Tadi SK, Tellier-Lebegue C, Nemoz C, Drevet P, Audebert S, Roy S, Meek K, Charbonnier JB, Modesti M. (2016) PAXX Is an Accessory c-NHEJ Factor that Associates with Ku70 and Has Overlapping Functions with XLF. *Cell Rep* 17(2):541-555

Valerio-Lepiniec M, Urvoas A, Chevrel A, Guellouz A, Ferrandez Y, Mesneau A, de la Sierra-Gallay IL, Aumont-Nicaise M, Desmadril M, van Tilbeurgh H, Minard P. (2015) The αRep artificial repeat protein scaffold: a new tool for crystallization and live cell applications. *Biochem Soc Trans*. 43(5):819-24

Vega S, Abian O, Velazquez-Campoy A. (2015) A unified framework based on the binding polynomial for characterizing biological systems by isothermal titration calorimetry. *Methods. Apr.* 76:99-115

Velazquez-Campoy A, Freire E. (2006) Isothermal titration calorimetry to determine association constants for high-affinity ligands. *Nat Protoc* 1(1):186-191

Walker JR, Corpina RA, Goldberg J. (2001) Structure of the Ku heterodimer bound to DNA and its implications for double-strand break repair. *Nature* 412(6847):607-614

Wyman J, Gill SJ. (1990) Binding and linkage: Functional chemistry of biological macromolecules. *Mill Valley, CA: University Science Books*

Zhao H, Brautigam CA, Ghirlando R, Schuck P. (2013) Overview of current methods in sedimentation velocity and sedimentation equilibrium analytical ultracentrifugation. *Curr Protoc Protein Sci*. Chapter 20

846

Declarations

Funding JBC is supported by ARC program (SLS220120605310), ANR (ANR-12-SVSE8-012), INCA DomRep (PLBIO 2012-280), and by the French Infrastructure for Integrated Structural Biology (FRISBI) ANR-10-INBS-05.

Conflicts of interest/Competing interests The authors declare no competing interest. Pierre Soule (NanoTemper) and Christophe Quétard (FortéBio) helped during the training without commercial interest

Ethics approval Not applicable.

Consent to participate The authors consent to participate to this project.

Consent for publication The authors consent to publish the work reported in this paper.

Availability of data and material Data can be obtained by requesting the corresponding author.

Code availability Not applicable.

Authors' contributions PFV, PE, SU, CE, AVC, AR, JBC authors contributed to the study conception and design. Material preparation, data collection and analysis were performed by CV, MAN, SU, PE, AVC, DS, GB, PS, CQ, CE, AR. The first draft of the manuscript was written by PFV and all authors commented on previous versions of the manuscript. All authors read and approved the final manuscript.

Acknowledgments

We thank: members of Philippe Minard's and Jean-Baptiste Charbonnier's teams at I2BC for the sample preparation, Bruno Baron and Bertrand Raynal from *Institut Pasteur, Paris* for all their expert advices in molecular scale biophysics, and Eric Ennifar from *Institut de Biologie Moléculaire et Cellulaire, Strasbourg* for sharing its expertise in the study of biomolecular machineries using biophysical approaches. Friederike Möller and Hanna Müller-Landau from *Dynamic Biosensors*, Aymeric Audfray from Malvern Panalytical, Mathilde Belnou from *NanoTemper technologies*, and Stephanie Bourgeois and coworkers from *Fluidic Analytics* for their availability and all the fruitful discussion. We kindly thank all the participants to the MoSBio Training School, all the sponsors without whom this successful event had not been possible, and finally the keynote speakers, Julie Ménétrey and Terence Strick who shared their projects with us. Most of preparatory experiments were performed in the I2BC, PIM platform (https://www.pluginlabs-universiteparissaclay.fr/fr/results/keywords/PIM), while some others were performed in Institut Pasteur, PFBMI platform.

Supplementary material

Figures

Figure S1. Flyer of the Molecular Scale Biophysics (MoSBio):

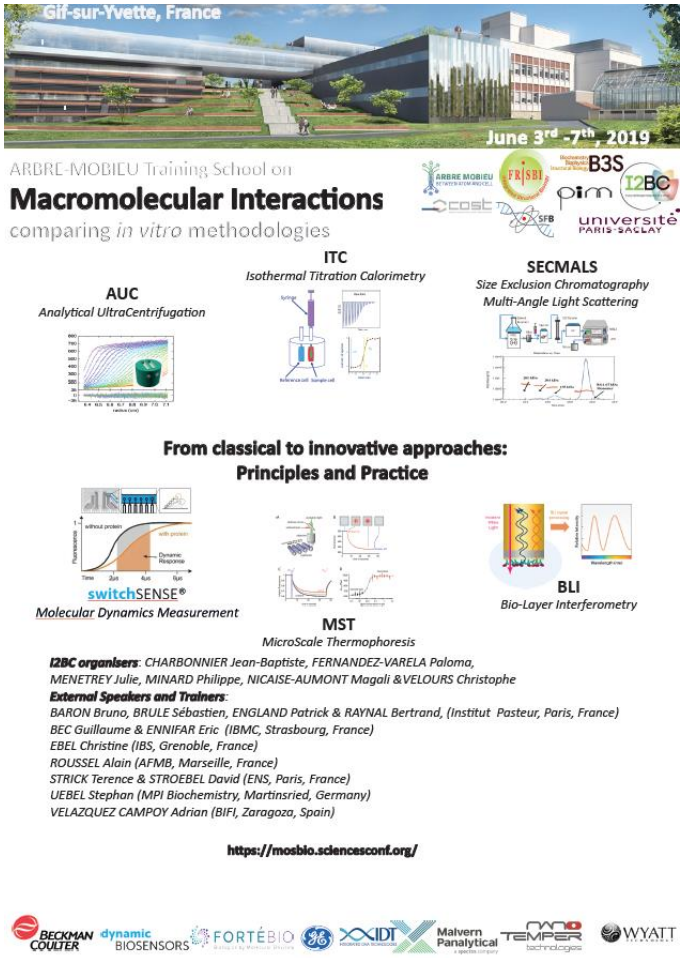

Macromolecular interactions *in vitro*, comparing classical and innovative approaches training school. Students during this training were able to use different approaches: Hydrodynamic (AUC-FDS, MST, SEC-MALS); Real time biosensor (BLI, switchSENSE) and Thermodynamic (ITC) to measure *in vitro* macromolecular interactions (protein-protein and protein-DNA). Experts on these approaches came from France and Europe as speakers and trainers. This event was made possible thanks to several networks and sponsors.

Figure ~~S2~~S1. Unfolding profile plot of Ku70/Ku80.

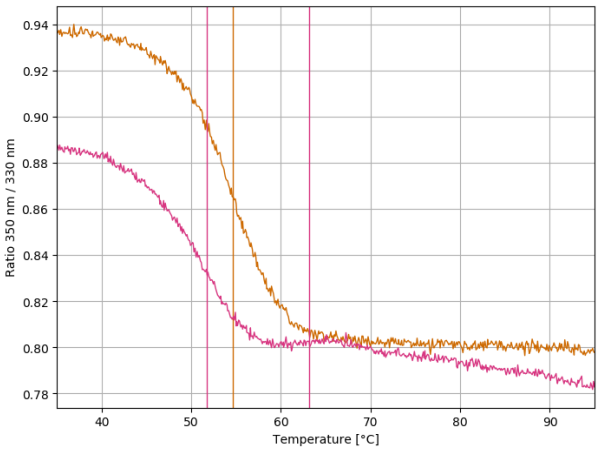

Quality and stability of samples are crucial to obtain accurate biophysical data. For all the biophysical studies shown in this manuscript, we used a full-length version of Ku (called KuFL), but for structural studies we used a shorter version where the C-terminus of each monomer is deleted (called KuCC). We took advantage of the new technology of *NanoTemper*, the Tycho NT.6 instrument, present during the training, to compare the thermal stability of these two versions of Ku protein by a fast measurement. Fluorescence intensity is recorded at 330 nm and 350 nm (emission profile of the Tryptophan residues). The brightness ratio 350 nm / 330 nm plotted against the temperature is called the unfolding profile plot and inflexion temperatures can be derived representing unfolding events. Tryptophan fluorescence of KuFL (orange) and KuCC (pink) were follow during a ramp of temperature of 35-95°C. KuFL showed a higher temperature of unfolding than KuCC (vertical bars). Thus, KuFL appears to be more stable than KuCC by a few degrees.

Figure S2~~3~~. Additional biophysical measurements of alphaRep interactions.

a) ITC

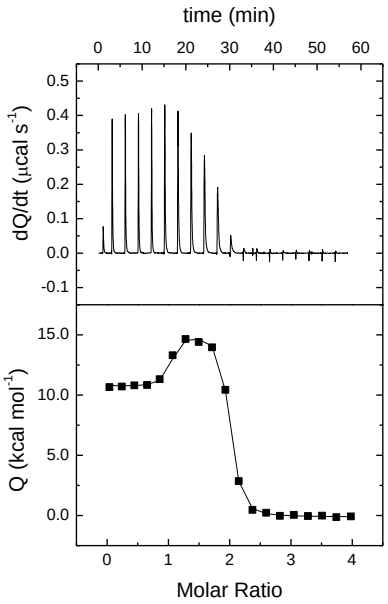

K (M^{-1})	K_D (nM)	ΔH (kcal/mol)	α	Δh (kcal/mol)	n
$1.4 \cdot 10^9$	0.71	10.9	0.024	4.4	0.95
~~K (M^{-1})~~	~~K_D (nM)~~	~~ΔH (kcal/mol)~~	~~α~~	~~Δh (kcal/mol)~~	~~n~~
~~$1.4 \cdot 10^9$~~	~~0.71~~	~~10.9~~	~~0.024~~	~~4.4~~	~~0.95~~

Formatted Table

b) SPR

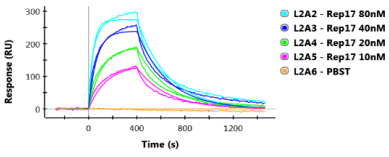

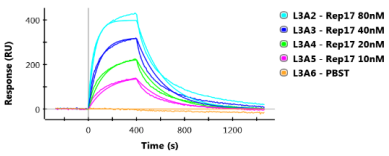

c) BLI

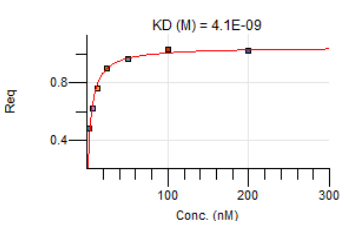

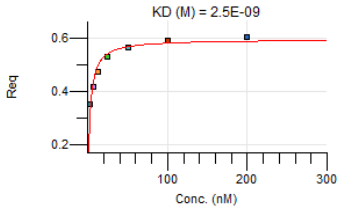

d) switchSENSE

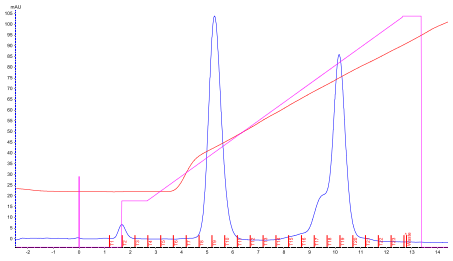

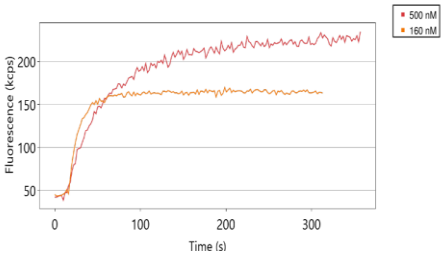

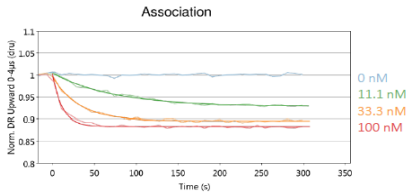

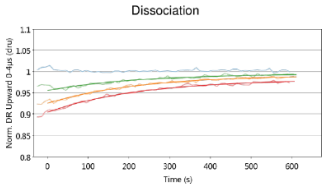

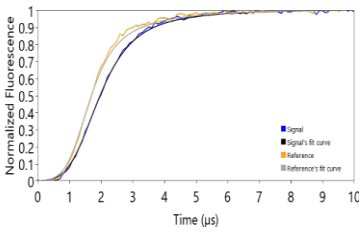

D_h^{ave} = 3.02 ± 0.05 nm (n=8)

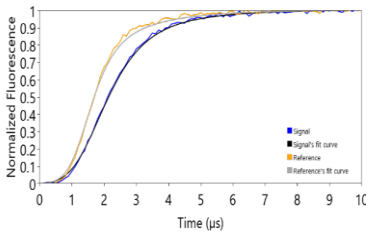

D_h^{ave} = 3.82 ± 0.09 nm (n=4)

~~e MST~~

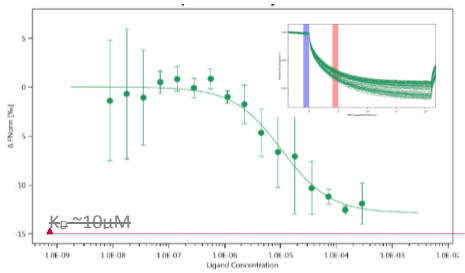

a) PEAQ-ITC data obtained before the training in our laboratory. K, K_D, and ΔH were the association constant, the dissociation constant, and the interaction enthalpy of either of the two binding sites when the dimer was unoccupied. α and Δh were the cooperative interaction constant and the cooperative interaction enthalpy, which modulate the binding cooperative phenomenon (a factor that modulates the binding affinity and a term that modulates the binding enthalpy to the second site when there was a site already occupied, respectively). n was the active (or binding-competent) fraction of protein, since the stoichiometry was already included in the model. K_{D1} and ΔH_1 were the intrinsic site-specific dissociation constant and binding enthalpy for the first binding site ($K_{D1} = K_D$, $\Delta H_1 = \Delta H$). K_{D2} and ΔH_2 were the intrinsic site-specific dissociation constant and binding enthalpy for the second binding site ($K_{D2} = K_{D1} / \alpha$, $\Delta H_2 = \Delta H_1 + \Delta h$). b) Sensograms of alphaRep A3-Rep17 interaction measured in duplicate on a ProteON XPR36 instrument from *Biorad*. For this experiment, association and dissociation times were 400 s and 1000 s, respectively with a flow rate of 50 µL/min in phosphate buffered saline with 0.1 % Tween-20 (PBST) using His-Tag capturing (HTG) chip to immobilized A3 at 6.25 or 12.5 µg/mL during 80 s (inducing 60 RU and 95 RU, respectively). Rep17 ranges from 10 to 80 nM concentration. A k_{ON} of 2.8 10^{+5} $M^{-1}s^{-1}$, a k_{OFF} of 3.9 10^{-3} s^{-1} and a K_D of 13.8 nM were measured in the first run, and a k_{ON} of 1.8 10^{+5} $M^{-1}s^{-1}$, a k_{OFF} of 4.6 10^{-3} s^{-1} and a K_D of 25.9 nM in the second one. c) Octet RED96e BLI steady-state analysis in duplicate. Colors code of Rep17 concentrations: 3.13 nM (teal), 6.25 nM (purple), 12.5 nM (orange), 25 nM (green), 50 nM (cyan), 100 nM (red), 200 nM (blue). d~~D~~) Sample preparation for switchSENSE experiments. Anion-exchange chromatogram of the A3 cross-linked protein (up, left). The cross-linked protein was the shoulder of the final peak that correspond to the free DNA. Hybridization of the cross-linked ssDNA-A3 on the chip, which carries a red fluorescent probe (up, right). Red profile corresponds to the control (free cNLB48 without protein) and the orange one to the cross-linked cNLB48-A3 conjugate. switchSENSE dynamic mode data of A3-Rep2 at three concentrations (middle, left). Normalized association (left) and dissociation (right) data were represented in function of time. switchSENSE sizing measurement of A3 hydrodynamic diameter (D_h) (bottom, left), and of the A3-Rep17 complex (bottom, right). Measured signal curve is in blue (conjugated DNA), the associated fitted curve in blank, reference signal (cNLB48) is in orange, and the associated fitted curve in grey. ~~d) MST analysis with blue fluorophore. Inset, MST traces, MST on used was 10 s (red band).~~

Formatted: Strikethrough

Formatted: Strikethrough

Formatted: Strikethrough

Figure S34. Additional biophysical measurements of Ku-DNA interactions.

a) **SEC-MALS**

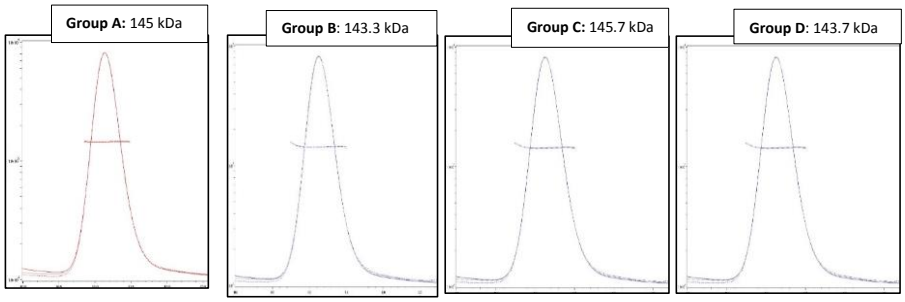

b) **BLI**

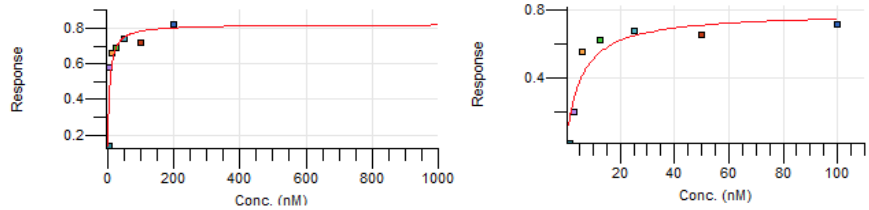

c) **switchSENSE**

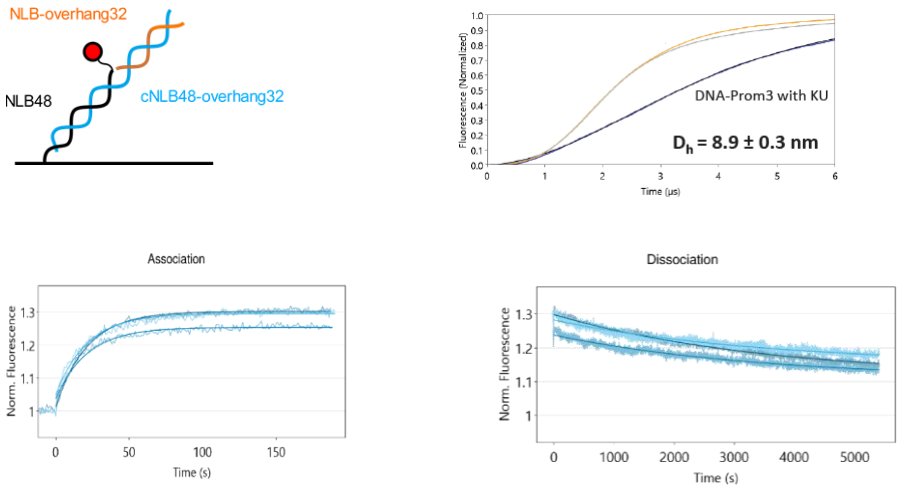

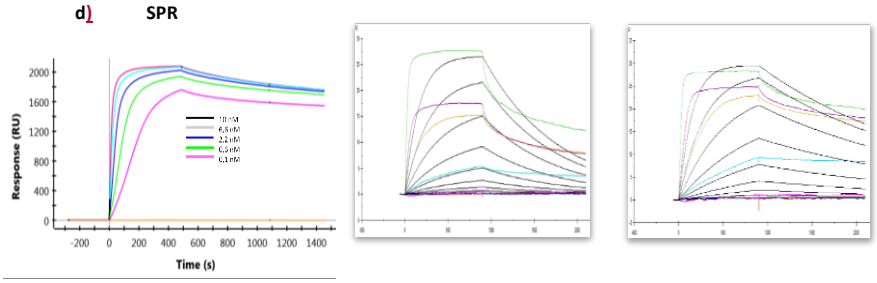

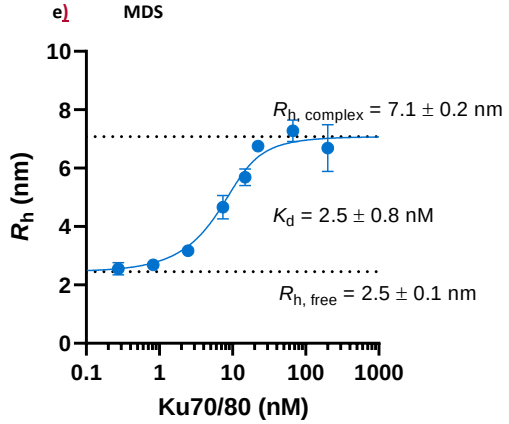

a) SEC-MALS elution profiles and molar masses of Ku alone in quadruple. b) Octet RED96e BLI steady-state data in duplicate. Colors code of Ku concentration: 3.13 nM (teal), 6.25 nM (purple), 12.5 nM (orange), 25 nM (green), 50 nM (cyan), 100 nM (red), 200 nM (blue). c) switchSENSE measurement set up (top, left). By hybridization of complementary DNA carrying the target sequence as overhang, the surface is functionalized with the sequence of interest. switchSENSE static mode data of 1 Ku concentration in duplicate (bottom). switchSENSE sizing data (top, right). Reference (bare DNA) is depicted in yellow. DNA-protein-complex is depicted in blue. d) SPR sensograms by ProteON XPR36 of Ku-200 bp dsDNA interaction measured (right). A 200 bp biotinylated DNA was immobilized on a Streptavidin (NLC) chip. Ku70/Ku80 ranged from 0.1 to 10 nM concentrations, one heterodimer may induce 200 RU. A k_{ON} of 7.8 ± 4 10^{+6} $M^{-1}s^{-1}$, a k_{OFF} of 1.5 10^{-4} s^{-1} and a K_D of 7.3 ± 3 nM were measured. This experiment showed the threading of Ku on DNA, approximately 10 heterodimers bound to this 200 bp DNA. SPR sensograms by BIAcore T200 of Ku-42 bp dsDNA (middle) and, Ku-60 bp dsDNA (left) interaction measured by biotinylated DNA immobilized in a serie S sensor chip SA at 10 nM concentration. Same buffer as in switchSENSE experiment adding 0.2 mg/mL of BSA, flow rates of 20 to 100 µL/min, and Ku at 5 nM as higher concentration for 900 s of association and dissociation. A k_{ON} of 1.0 10^{+6} $M^{-1}s^{-1}$, a k_{OFF} of 11.7 10^{-4} s^{-1} and a K_D of 1.2 nM (R_{max} of 32.9 RU) were measured for the 42 bp DNA and, a k_{ON} of 1.4 10^{+6} $M^{-1}s^{-1}$, a k_{OFF} of 5.0 10^{-4} s^{-1} and a K_D of 35.4 nM (R_{max} of 31.6 RU) for the 60 bp DNA. Colors code of Ku concentrations: 5 nM (light green), 2.5 nM (purple), 1.25 nM (orange), 0.625 nM (cyan), 0.3125 (pink), 0.156 (dark green), 0.078 (blue), 0.039 (red). The differences observed in the results depend mainly on the setup strategy of the experiment. Nevertheless, open questions remain to answers: the purity of dsDNA and the stability of the protein will affect the results, but there is also the possibility of different ways of DNA fixation by Ku. e) In collaboration with *Fluidic Analytics*, we collected preliminary data to test their new instrument, Fluidity One-W with the Ku-DNA interaction. This is a novel technique in solution based in diffusional sizing of a complex in a microfluidic system. For this experiment we used the ~~same~~ 18 bp dsDNA-FAM as before (AUC, MST) at 10 nM concentration, and 1/3 dilution of Ku70/Ku80 from 200 to 0.09 nM concentration. We were able to measure R_h (DNA alone, complex) and K_D values.

Tables

Table S1. Summary of the results for the interaction between alphaRep proteins ~~interaction~~ using different techniques.

	AUC-FDS	SEC-MALS*	ITC		MST	switchSENSE		BLI		~~SPR*~~
His-A3	**Blue-NHS**	**Dimer**	**Monomer /high affinity**	**Dimer /low affinity**	**Red-His**	**Rep2***	**Rep17**	**Monomer**		**Monomer**
Ratio	1:1	1:1	1:1	1:1	N/A	1:1	1:1	N/A		N/A
K_D (nM)	13.4 ± 1.8	N/A	0.6 ± 0.1	21.3 ± 7.5	8.0	0.29 ± 0.01	0.98 ± 0.16	3.2 ± 1.1	3.3 ± 0.8	3.97 ± 1.38
k_{ON} ($M^{-1}s^{-1}$) k_{OFF} (s^{-1})	N/A	N/A	N/A	N/A	N/A	2.4 ± 0.1 10^{+6} 6.9 ± 0.2 10^{-4}	2.4 ± 0.2 10^{+6} 2.3 ± 0.3 10^{-3}	2.6 ± 0.7 10^{+5} 7.6 ± 0.7 10^{-4}	Steady-state	2.31 ± 1.79 10^{+5} 4.28 ± 0.36 10^{-3}
Other information	S (A3) = 2.6 ± 0.1 S (A3/Rep17) = 3.0 ± 0.1	Mw (Rep2) = 11.6 kDa Mw (A3) = 44.8 kDa R_h (A3) dimer = 3nm Mw (A3/Rep2) = 65.5 kDa R_h (A3/Rep2) = 3.8 nm	ΔH = 11.6 ± 0.6 kcal/mol	ΔH = 15.5 ± 1.0 kcal/mol	N/A	D_h (A3)monomer = 3 nm D_h (A3-Rep2) = 3.8 nm	N/A	N/A	N/A	N/A

In the last column in grey, previous SPR data obtained by P. Minard's team.*Rep2

Formatted Table

Table S2. Summary of the results ~~obtained~~ for the interaction Ku-DNA ~~interaction~~ using the different techniques.

	AUC-FDS	ITC		SEC-MALS	BLI		MST	switch SENSE		SPR	~~Diffusiona l sizing~~MDS
DNA(bp)	**18***	**18**	**42**	**42**	**42****		**18***	**48**	80	**200****	**18***
Ratio Ku vs DNA	1:1	1:1	2:1	2:1, 1:1	N/A		N/A	1:1		20:1	1:1
K_D (nM)	12.9 ± 3.2	3.5 ± 0.8	3.~~76~~ ± 0.~~74~~	N/A	0.4 ± 0.1	5.2 ± 0.2	~~2.8~~11.9	1.0 ± 0.2	3.1 ± 0.1	7.3 ± 3.0	2.5 ± 0.8
k_{ON} ($M^{-1}s^{-1}$) k_{OFF} (s^{-1})	N/A	N/A	N/A	N/A	1.9 ± 0.1 10^{+6} 7.2 ± 0.3 10^{-4}	N/A	N/A	2.6 ± 0.2 10^{+6} 2.3 ± 0.3 10^{-3}	~~92~~.3 ± 0.~~13~~ 10^{-4} 2.8 ± 0.1 10^{-4}	7.8 ± 4.0 10^{+6} 1.5 ± 0.8 10^{-4}	N/A
Other information	S (DNA) = 2.2 ± 0.1 S (1:1) = 7.3 ± 0.2	ΔH = 10.95~~.~~ ~~1 ± 0.1~~ kcal/mol n = 0.95	ΔH = 2~~43~~.~~49~~ ± 2~~4~~.~~79~~ kcal/mol n = 0.34 ± 0.02	Mw (DNA)= 26.1 kDa Mw (Ku) = 144.4 kDa Mw (1:1) = 171.0 kDa Mw (2:1) = 306.2 kDa	N/A	N/A	N/A	N/A ~~D_h = 8.9nm~~	D_h = 8.9nm	N/A	Rh = 7.1 ± 0.2 nm

The last two columns came from additional data: Preliminary SPR obtained by Charbonnier's team, and MDF in collaboration with Fluidic Analytics. DNA modified *FAM or **Biotin.

Formatted Table

Macromolecular interactions *in vitro*, comparing classical and novel approaches

Christophe Velours[1,2*], Magali Aumont-Nicaise[1*], Stephan Uebel[3], Patrick England[4], Adrian Velazquez-Campoy[5,6,7,8,9], David Stroebel[10], Guillaume Bec[11], Pierre Soule[12], Christophe Quétard[13], Christine Ebel[14], Alain Roussel[15], Jean-Baptiste Charbonnier[1], Paloma Fernández Varela[1#]

[1]Université Paris-Saclay, CEA, CNRS, Institute for Integrative Biology of the Cell (I2BC), 91198, Gif-sur-Yvette, France. [2]Microbiologie Fondamentale et Pathogénicité, MFP CNRS UMR 5234, University of Bordeaux, 146 rue Léo Saignat 33076 Bordeaux, France. [3]Bioorganic Chemistry & Biophysics Core Facility, Max-Planck-Institute of Biochemistry, Martinsried, Germany. [4]Molecular Biophysics platform, Institut Pasteur, Paris, France. [5]Institute of Biocomputation and Physics of Complex Systems (BIFI), Joint Units IQFR-CSIC-BIFI, and GBsC-CSIC-BIFI, Universidad de Zaragoza, Zaragoza, 50018, Spain. [6]Departamento de Bioquímica y Biología Molecular y Celular, Universidad de Zaragoza, 50009, Zaragoza, Spain. [7]Instituto de Investigación Sanitaria Aragón (IIS Aragón), 50009, Zaragoza, Spain. [8]Centro de Investigación Biomédica en Red en el Área Temática de Enfermedades Hepáticas y Digestivas (CIBERehd), 28029, Madrid, Spain. [9]Fundación ARAID, Gobierno de Aragón, 50009, Zaragoza, Spain. [10]Institut de biologie de l'Ecole normale supérieure (IBENS), Paris, France. [11]Institut de Biologie Moléculaire et Cellulaire (IBMC), Strasbourg, France. [12]NanoTemper Technologies GmbH, Munich, Germany. [13]ForteBio-Sartorius, Dourdan, France. [14]Univ. Grenoble Alpes, CNRS, CEA, IBS, Grenoble, France .[15]Architecture et Fonction des Macromolécules Biologiques (AFMB), Marseille, France.

**Contributed equally*

#Corresponding author: paloma.fernandez-varela@i2bc.paris-saclay.fr ORCID: 0000-0001-5078-7102

Abstract

Biophysical quantification of protein interactions is central to unveil molecular mechanisms of cellular processes. Researchers can choose from a wide panel of biophysical methods, including classical and more novel ones. A real-life proof-of-concept was carried out during an ARBRE-MOBIEU training school held in June 2019 in Gif-sur-Yvette, France (https://mosbio.sciencesconf.org/). Twenty European students benefited from a one-week training with lessons and practical sessions on six complementary approaches: (i) Analytical UltraCentrifugation with or without a Fluorescence Detector System (AUC-FDS), (ii) Isothermal Titration Calorimetry (ITC), (iii) Size Exclusion Chromatography coupled to Multi-Angle Light Scattering (SEC-MALS), (iv) Bio-Layer Interferometry (BLI), (v) MicroScale Thermophoresis (MST) and, (vi) switchSENSE. They implemented all these methods on two examples of macromolecular interactions: firstly, a protein-protein interaction between an artificial alphaRep binder, and its target protein, also an alphaRep; secondly, a protein-DNA interaction

between a DNA repair complex, Ku70/Ku80 (hereafter called Ku), and its cognate DNA ligand. The students acknowledged that the workshop provided them with a clearer understanding of the advantages and limitations of the different techniques and will help them in the future to choose the approaches that are most relevant or informative for their projects.

Keywords

Molecular scale biophysics, macromolecular interactions, artificial binders, double-stranded DNA breaks repair factors

Introduction

Macromolecular interactions play a central role in the activation/inactivation of most cellular mechanisms. These interactions can be measured *in cellulo*, or *in vitro,* and predicted *in silico*. The classical *in cellulo* methods (such as tap-tag or two-hybrid) allow large-scale studies, but the characterization of a direct interaction between two macromolecules relies on the quantitative *in vitro* measurements. These measurements allow to characterize interactions not only in terms of affinity, but also to determine additional kinetic and thermodynamic parameters, as well as to define the hydrophobic or hydrophilic nature of the interface. They also give access to the stoichiometry of the assembly and allow to map the regions involved by using different constructs or mutants. *In vitro* measurements can also be useful to evaluate the drugability of the interaction site or to understand the role of endogenous regulatory events on the formation of complexes (post-translational modifications). These measurements are essential to set-up predictive *in silico* docking tools. Conversely, by *in silico* analysis, the structure of macromolecular complexes as well as the impact of functional substitutions can be predicted, helping to optimize experimental design (Andreani and Guerois, 2014).

The original idea of the project presented here originated during the organization of a European Training School in Molecular Scale Biophysics (https://mosbio.sciencesconf.org/) within the MOBIEU COST Action. We proposed to the participants to compare different techniques allowing to measure macromolecular interactions *in vitro*. Nowadays, there is a large panel of possibilities, and it becomes difficult to choose which technology will be the best adapted when embarking into a new project. Each approach presents advantages and

drawbacks, and it is therefore difficult for the user to choose from the beginning which one will be most adapted to the properties of the interaction partners. In the workshop, we focused on six approaches (Fig. 1). Choosing between the different techniques can be considered in a progressive manner. If none of the interaction partners can be easily labeled or immobilized on a surface, approaches in which both partners are in solution (AUC, ITC, and SEC-MALS) should be favored (Fig. 1, top). However, several of them require large quantities of biological material. When a partner can be immobilized easily on a bio-surface, without affecting its function, approaches like BLI, switchSENSE and Surface Plasmon Resonance (SPR) will be often tested, since they offer the possibility to use small amounts of the immobilized partner (called ligand) (Fig. 1, middle). Finally, when the partners can be labeled, again without affecting their function, fluorescent probes can be grafted allowing the use of reduced amounts of material and facilitated signal analysis (AUC FDS, MST, or Microfluidic diffusional sizing (MDS)) (Fig. 1, bottom).The choice of the optimal approach may further rely on additional criteria including the solubility of the partners, the instrument environment or non-specific interactions with instrument surfaces. Finally, it should be stressed that it is preferable to perform measurements using several orthogonal techniques to fully validate and characterize a biological interaction, and specify its features, such as stoichiometry, kinetics or thermodynamics.

Figure 1. Decisional tree to help choosing the biophysical approach best suited for the study of a specific molecular interaction.

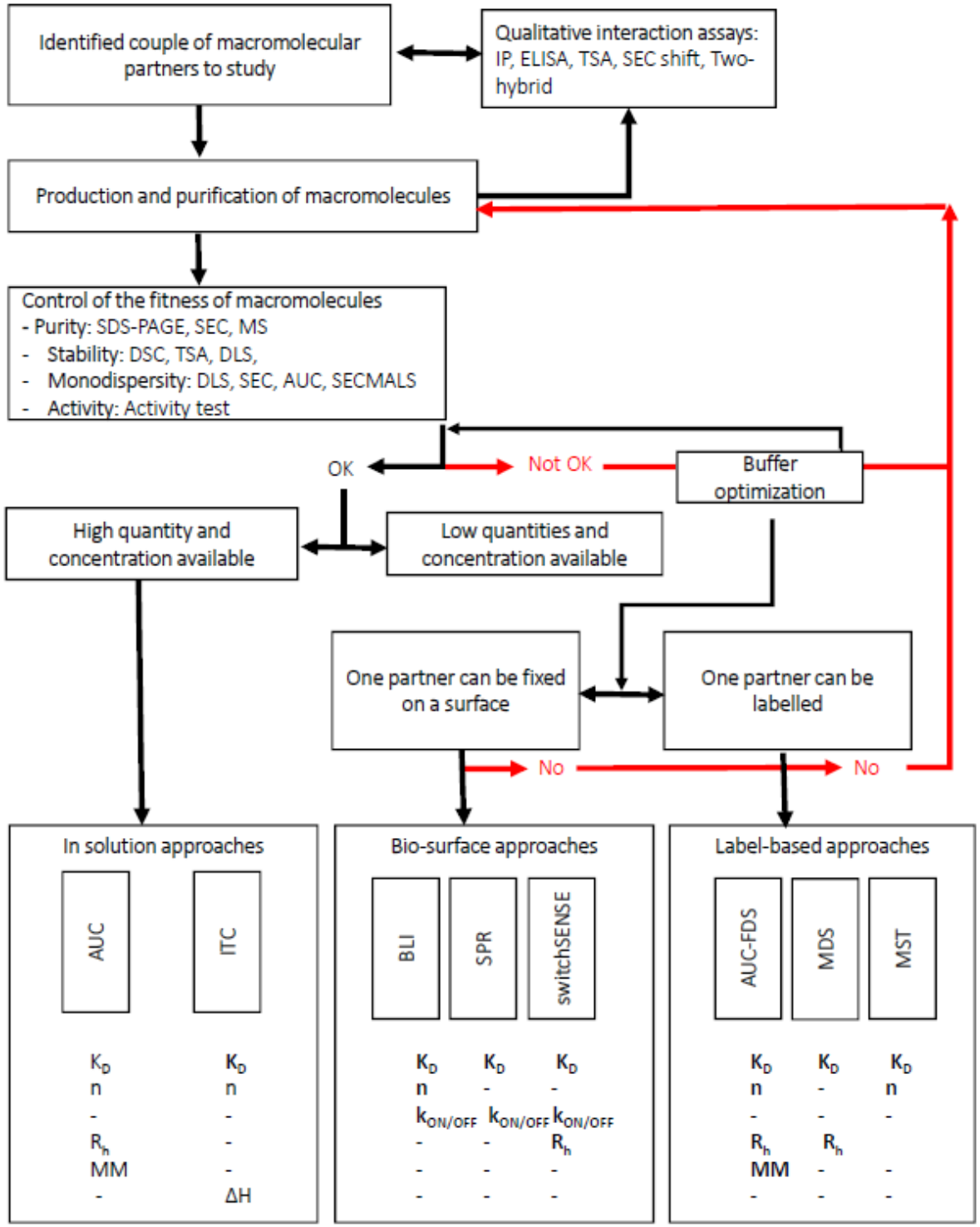

To determine whether two macromolecular partners potentially interact, first indication of a binding event could be obtained with qualitative methods (top right): Immunoprecipitation (IP) from cell extracts; Thermal Shift Assay (TSA); Size Exclusion Chromatography (SEC) shift, measuring the elution volume change after complex formation; Two-hybrid assay, *in cellulo*. The production and purification of the macromolecular partners should aim at reaching high purity, time-stability and monodispersity of the preparation for the interaction measurements to be reliable. Mass-Spectrometry (MS); Differential Scanning Calorimetry (DSC) ; TSA; Dynamic Light Scattering (DLS); Activity test (for instance an enzymatic assay); Analytical UltraCentrifugation (AUC); Size Exclusion Chromatography coupled with Multi-Angle Light Scattering (SEC-MALS). Macromolecular interaction methods can be classified in three main groups: measurements in solution and label free (AUC; Isothermal Titration

Calorimetry (ITC) (bottom, left)), on biosensor with a partner graft on a surface (Bio-Layer Interferometry (BLI); Surface Plasmon Resonance (SPR); switchSENSE technology (bottom, middle)), and methods with a partner labeled with a fluorescent probe (AUC-Fluorescence Detector System (AUC-FDS); Microfluidic Diffusional Sizing (MDS); MicroScale Thermophoresis (MST) (bottom, right)). These approaches give access to different parameters of the interaction and present some specific limitations. If a high quality sample (pure, stable, monodisperse) is available in large quantity (up to mg amount) one may start with label-free and in solution approaches. Otherwise, if material is limited for one partner, surface and labeling approaches are a good alternative and highly complementary to cross-validate interaction measurements. Surface approaches are best candidates to get access to the kinetic parameters of interaction. Six of these approaches were used in the training school. Dissociation constant (K_D); stoichiometry (n); association and dissociation rates (k_{ON}, k_{OFF}); hydrodynamic radius (Rh); Molecular mass (MM).

In this training school, we used as examples two different macromolecular interactions systems, that have been well characterized in our laboratories using several of the approaches discussed here. One is an interaction between two proteins, and the other a protein-DNA interaction, both with an affinity in the nanomolar range. Reference data were initially produced in our laboratories. A group of 20 participants reproduced our measurements during the five-day MoSBio Training School.

The first project comes from P. Minard's team, who uses an original family of artificial helicoidal repeat proteins, called alphaRep (Guellouz et al., 2013). AlphaRep libraries allow to select tight binders against a variety of targets by phage display. The alphaRep's are highly soluble proteins, easily expressed in *E. coli*, which display a very high thermal stability. These proteins are cysteine-free and, thus do not contain disulfide bonds. They are composed by repeated motifs made with two antiparallel alpha helices. Clusters of variable side chains, mainly in the second helix, are positioned on the same face of the motifs. The ensemble of all these variable motifs forms a library of surfaces from which tight binders can be extracted against a given target. The alphaRep's have been used for several applications, such as chaperones for crystallization and structural studies of difficult targets (Valerio-Lepiniec et al., 2015; Di Meo et al., 2017; Chevrel et al., 2018; Campanacci et al., 2019), as well as in biophysical and live cell studies (Léger et al., 2019; Prasad et al., 2019; Fernandez et al., 2020; Léger et al., 2020). New applications of these artificial binders are currently being explored in relation with their ability to be expressed in eukaryotic cells. Here we analyzed the interactions between two alphaRep's (Rep2 and Rep17) selected against a protein target, (A3), which is itself an alphaRep. The interaction between the alphaReps has been extensively characterized before in the laboratory by ITC, SEC-MALS and AUC, but also by Circular Dichroism (CD), SPR and Fluorescence Resonance energy Transfer (FRET) (not used in this training school) (Guellouz et al.,2013; Di Meo et al., 2017; Léger et al., 2019). Both A3 / Rep2 and A3 / Rep17 interactions were tested previously to determine which one was the most appropriate for the training. Because the former is weaker than the latter, we focused only on the only A3 / Rep17 interaction during the training.

The second project comes from J.B. Charbonnier's team. It concerns proteins involved in DNA repair, and more precisely, in the classical Non-Homologous End Joining (c-NHEJ), the main Double-Strand Break (DSB) repair pathway in human. The Ku70/Ku80 (Ku) heterodimer plays

a central role in the recognition of DSB ends, as it is the first repair factor that interacts with them. Ku binds tightly to DNA ends in a sequence independent manner thanks to its ring-shaped structure (Walker et al., 2001). Ku then iteratively recruits different NHEJ partners (ligase 4, nucleases and polymerases) (Chang et al., 2017; Frit et al., 2019). Ku also contributes to the tethering (synapse) between the two DSB ends to avoid misrepair with other DSB ends. J.B. Charbonnier's team (Tadi et al., 2016; Nemoz et al., 2018) has recently described the recruitment mechanism of some NHEJ factors by Ku at the molecular level. DSBs, despite being deleterious DNA lesions, are generated on purpose during radiotherapy or in genome editing by CRISPR-Cas9. Understanding the molecular basis of the c-NHEJ is thus central to improve these major biotechnological applications. Here we analyzed the interaction between Ku and DNA substrates of different lengths, to determine the most appropriate for the training and to study the threading of Ku on DNA. The characterization of the interaction between Ku and DNA has been extensively studied in the laboratory by ITC, MST (Tadi et al., 2016; Nemoz et al., 2018; Gontier et al., 2021), switchSENSE, AUC, BLI (data not published) and, more recently by other techniques not used during the training school (SPR, MDS or FRET). One Ku occupies about 18 bp and several Ku molecules can thread on DNA when its size is longer than 18bp, with one Ku molecule every 18bp.

We present in this article the results obtained by 20 students during a European Training School in Molecular Scale Biophysics that took place from June 3rd to 7th, 2019 at I2BC at Gif-sur-Yvette, France. We report the protocols used to analyze the two systems under study (protein/protein and protein/DNA interactions) using the six biophysical methods mentioned above. The results obtained by the students during the one-week course are shown and compared to our previous published data when available. Finally, we compare the advantages and drawbacks of the different approaches used during this training school and present some feedback from the students, allowing to have a global overview of the pros and cons of these six complementary biophysical approaches.

Materials and Methods

Biophysical approaches in solution that do not require labeling of an interaction partner

Size Exclusion Chromatography with Multi-Angle Laser Light Scattering detection (SEC-MALS): SEC-MALS allows to determine the absolute molar mass of the components present in a macromolecular sample. It indicates if elution peaks are homogenous or if they are composed of mixtures, either of different oligomers or of different conformers. SEC-MALS allows size determination if an online Dynamic Light Scattering (DLS) detector is included in the setup (Folta-Stogniew, 2006). In order to determine stoichiometry in a macromolecular hetero-complex, differences in extinction coefficients are required. An experimental determination of extinction coefficient by analyzing each partner separately, will be more precise than *in-silico* prediction. For a more precise estimation of molar mass of complex components, you need to know the refractive index increment (dn/dc value) of each complex partner at the wavelength of the MALS system laser. We used an HPLC system from *Shimadzu* coupled to a MALS detector (miniDAWN TREOS) plus a DLS detector (QELS), and a refractometer (optilab T-rEX) from *Wyatt technologies*. To run an experiment, one needs 1 L of running buffer to equilibrate the column and detectors, from 2 mg/mL of protein (for MW of 20 kDa), down to 0.5 mg/mL (if the MW is higher than 150 kDa). Depending on the column used, the volume of the sample (30 µL for Bio-SEC-3 *Agilent*, 50 µL for KW-803/804 *Shodex*, and 100 µL for Superose 6, Superdex 75 or Superdex 200 increase 10/300 GL *Cytiva*) and the time of elution can differ. A run (including an equilibration step and a control BSA sample) takes typically a few hours and consumes 40-200 µg of sample.

Isothermal Titration Calorimetry (ITC): ITC allows the direct, and thorough thermodynamic characterization of interactions between molecules in solution with no limitation of partner size and without labeling (Holdgate, 2001; Krell, 2008; Velazquez-Campoy and Freire, 2006). ITC allows to quantify dissociation constants (K_D), but also other interaction parameters (enthalpy, entropy, stoichiometry, and heat capacity). ITC is not affected by the optical properties of the samples, but may be very sensitive to the composition of the buffer (e.g in particular to mismatches between partner sample solutions). In a microcalorimeter the two cells (reference and sample) needs to be kept at exactly the same temperature. A heat sensing device detects temperature difference between the cells when binding occurs, upon serial injection of a ligand, and give feedback to the heaters, which compensate for this difference

and return the cells to equal temperature. Each injection gives then rise to a peak of emitted or absorbed heat whose surface is proportional to the amount of binding. For the ITC experiments, we used three instrument models: VP-ITC, ITC200 and PEAQ-ITC all from *Malvern Panalytical*. One of the interacting partners is placed in a cell (1.4 mL for the VP-ITC, 200 µL for the ITC200 and PEAQ-ITC) and the other in a syringe (300 µL for the VP-ITC, 40 µL for the ITC200 and PEAQ-ITC). Sequential injections are made from the syringe (5-10 µL for the VP-ITC, 1-2 µL for the ITC200 and PEAQ-ITC) into the cell. To produce the data reported here, we used 80-990 µg of the molecule in the cell, and 130-320 µg of the molecule in the syringe. The transient heat effect due to complex formation (and other potential unspecific phenomena) upon partner injection is measured as the titration progresses, from which the binding isotherm is constructed.

Biophysical approaches with a partner immobilized on a surface

Bio-Layer Interferometry (BLI): BLI is a fast, high throughput and label-free technology for measuring biomolecular interactions by analyzing the interference pattern of white light reflected from a layer of immobilized macromolecules on a biosensor tip *versus* an internal reference (Abdiche et al., 2018). It enables real-time determination of affinity, kinetic parameters and concentration, with one of the binding partners immobilized onto the biosensor surface (ligand) and the other in solution (analyte). This microfluidic-free technology is particularly adapted for performing binding assays in crude lysates or cell culture media. We used an Octet RED96e during the training, and an RED384 during the preparation phase, both from *FortéBio*. In all cases, one of the interaction partners will be non-covalently captured on a glass sensor probe. The sensor will then be incubated in microplate wells containing the second interaction partner in solution. A light beam is sent through the sensor, and the reflected beam is analyzed using an interferometric detector, that measures the spectral shift due to the variations of density (optical thickness) that the biolayer undergoes upon association and dissociation of the complex. The real-time monitoring of these variations allows to record a « sensorgram », from which the kinetic rates (k_{ON} and k_{OFF}), as well as the equilibrium constant K_D can be determined through mathematical curve fitting. We used 1-5 µg/mL of ligand to load NTA sensors for 20-120 s, for low density, or 120-600 s, for high density, and a range of at least 7 2-fold dilutions (starting at 100-200 nM) of the analyte with an association time of 600-900 s. We consumed about 8 µg of protein A3, and 400 ng of 42 bp

biotinylated DNA per run for the immobilization, and about 2-14 µg of the respective analytes. The concentration of ligand could be reduced (at least by 2) in favor of a longer incubation. The consumption of the analyte, depends on the affinity of the interaction, as the concentrations used should range from K_D /10 to 10 x K_D.

switchSENSE: switchSENSE technology is based on short DNA nanolevers (48 bp in our case), which are immobilized on gold electrodes in a microfluidic channel. The intrinsically negatively charged DNA nanolevers can be electrically actuated ("switched") on the gold surface to oscillate at high frequencies (Knezevic et al., 2012). A switchSENSE microfluidic biochip contains four flow channels, each containing six gold electrodes. Switching of the DNA is mediated by alternating the voltage across the gold surface. The motion of the levers is tracked in real time (µs scale) via electrically triggered time correlated single photon counting (E-TCSPC) detecting a fluorescent probe (dye) present on top of the immobilized DNA strands. The recorded fluorescence intensity correlates to the orientation of the DNA nanolever relative to the surface as the fluorescence is gradually quenched upon approaching the gold electrode due to energy transfer. The complementary DNA strands can be cross-linked to a ligand via amine or thiol coupling or click-chemistry. By hybridization of this conjugated complementary strand to the surface-tethered DNA nanolever, the surface is functionalized with the ligand of interest. Upon binding of an analyte, the hydrodynamic friction of the levers is increased and subsequently the movement of the levers is slowed down. This change in switching speed is used by the system to determine the size (D_h) or conformational changes of ligands and complexes. The kinetics of molecular interactions (k_{ON}, k_{OFF}, K_D) can be monitored using two measurement modes: dynamic or static. In the first case, analyte binding is measured through the change of the oscillation rate of the electrically actuated DNA nanolevers (changes in dynamic response). In the second case, the DNA nanolevers are kept at an upright position, in a constant electric field, and analyte in close proximity to a dye can alter its local chemical environment resulting in a fluorescence change (also called Fluorescence Proximity Sensing). Binding is then measured thanks to the fluorescence intensity variation of the functionalized nanolever. For the switchSENSE experiments, we used a DRX^2 device from *Dynamic Biosensors* with two LED light sources (for the excitation of red and green fluorophores). In all cases, a hundred µg of protein where enough to generate cross-linked complementary strands (cNL-DNA) for several round of experiments, since one

measurement needs only 40 µL of 100 nM DNA-protein conjugate. A sizing measurement classically takes less than an hour. The quantity of analyte needed for a kinetic experiment depends on the overall affinity, the flow rates, and the association time. A too slow flow rate can result in mass transport limitation during association and in re-binding effects during dissociation. Here we used flow rates of 100-500 µL/min, association times of 80-300 s, and 1500 s of dissociation time. We used 150 ng of the cross-linked ligands, and 2-20 µg of its partner for a series of 3 concentrations.

Biophysical approaches with a labeled partner

Analytical UltraCentrifugation with Fluorescence Detection (AUC-FDS): AUC is a powerful technique for the characterization of macromolecules and macromolecular self- and hetero-association processes in solution. It was used here with labeled protein or DNA, but it can be used with non-labeled material like SEC-MALS and ITC. An analytical ultracentrifuge is a high-speed centrifuge equipped with one or more detectors (absorbance/interference, fluorescence) allowing to monitor sedimentation in real time. Two types of complementary experiments can be performed, sedimentation velocity and sedimentation equilibrium (Zhao et al., 2013). Sedimentation velocity experiments allow to determine the size distribution of species, their aggregation and oligomerization, sedimentation coefficients, hydrodynamic radius, shape and molar masses, their stoichiometry and K_D (by isotherm fitting of sedimentation coefficients measured at various concentrations). Sedimentation equilibrium experiments are suited for well-defined samples, and give molar mass and K_D information. The centrifugation speed can be set between 600 and 260 000 g allowing to study all sizes of macromolecules. The duration of sedimentation experiments ranges from 2 h to several days. dn/dc and UV extinction coefficients values, which are needed to analyse data obtained with absorbance and interference optics, can be determined from the protein sequence using the SEDFIT calculator module (Schuck, 2000). For the AUC-FDS experiments we used a ProteomeLab XL-I ultracentrifuge from *Beckman Coulter* equipped with a Fluorescence Detection System (FDS) from *AVIV Instruments*. A sedimentation velocity experiment requires 100-450 µL of sample at 0.3 to 1.5 OD, for absorbance/interference detection, and 5-60 nM concentration, for fluorescence detection, whereas sedimentation equilibrium requires 130 µL at 0.2 to 0.5 OD. In interference, the limit of detection is 0.1 mg/mL, but in absorbance it depends on the sample extinction coefficient. To characterize an interaction using the AUC

fluorescence detector, a range of 2 nM to 2 µM is typically used. When the affinity is very high, a range between 2 pM and 2 nM is chosen, but a blocking agent - e.g. BSA at 1 mg / mL - is added in the sample to avoid non-specific adsorption and loss of fluorescent dye. To produce the data described here, we used about 1-3.5 µg of the fluorescent molecule and 8-80 µg of the non-fluorescent molecule.

Microscale Thermophoresis (MST): MST is a novel technology for the analysis of biomolecules based on the modification of fluorescence intensity induced by the temperature, due to Temperature Related Intensity Changes (TRIC) and the directed movement of particles in a microscopic temperature gradient (thermophoresis) (Asmari et al., 2018; Jerabek-Willemsen et al., 2011). Thermophoresis is influenced by a combination of changes at the level of the hydration shell, shape, charge…, of biomolecules (all the parameters that influence the Soret coefficient), which result in differences of movement along the temperature gradient as well as of brightness of the fluorescent tag. MST provides information on the binding affinities with good accuracy and sensitivity in the pM to mM range. This technology allows immobilization-free measurement of interactions in any buffer and complex biological liquid, but requires one of the two partners to be labeled with a fluorescent dye to measure protein-protein interactions (there is also a label free instrument that detects the intrinsic fluorescence of proteins). Any size of unlabeled molecules can be used (from ions, to large proteins). MST experiments are performed in capillaries, thus require a low sample consumption. Method development for MST is usually fast and consists of three steps: (i) ensure there is enough fluorescence signal intensity. (ii) Check your sample for sticking to the capillaries. (iii) Establish the noise floor of your experiment by measuring MST of just your target without ligand at the final settings (final concentration, excitation laser and « MST power » = IR laser LED power to be used). We used a Monolith NT.115 blue/green and a red/blue from *NanoTemper Technologies*, 200 µL at 20 nM of the fluorescent molecule and 20 µL of the non-fluorescent molecule at the highest concentration needed (depending on the expected K_D). To produce the data described here, we used about 50-350 ng of the fluorescent molecule and 6-12 µg of the non-fluorescent molecule.

Sample preparation

To perform biophysical characterization measurements, samples of high purity, stability and monodispersity are needed (Fig. S1). We chose well characterized systems from our

laboratories, and the concentration ranges employed to accurately determine binding parameters were already known.

AlphaReps are recombinant proteins produced by standard overexpression procedures in *E.coli* (Guellouz et al., 2013). For our experiments, we used the following alphaRep proteins: A3, which is the target and Rep17 and Rep2, which are the binders. Because A3 forms homodimers at high concentration, it was used as ligand for real-time biosensors approaches (BLI, switchSENSE) and was the labeled partner in AUC-FDS and MST experiments. In the conditions used, we assumed A3 is a monomer. The simultaneous presence of the monomeric and dimeric forms would make the analysis difficult. A3 dimers are unable to interact with Rep17, and it is only when they dissociate into monomers that, the interaction with Rep17 occurs. A dissociation constant of 37 nM for the A3 / A3 dimer was measured by AUC (Léger et al., 2019). This is why we observe several events in ITC: the dissociation of the A3 dimer and the interaction with Rep17.

Ku is a recombinant protein produced by standard overexpression procedures in insect cells (Nemoz et al., 2018). For our experiments, we used different lengths of dsDNA depending on the assay format. Shorter DNA are not adapted for biosensor approaches, since a DNA too close to the surfaces will hinder its interaction with Ku. DNA is practical to work with, because it is easy to modify and is commercially available. For immobilization on BLI biosensors and for detection in AUC-FDS and MST, we ordered biotinylated and 5-Carbofluorescein (5-FAM)-labeled DNA oligonucleotides, respectively.

All proteins were dialyzed to eliminate glycerol from the storage buffer, which can interfere with the measurements. We chose the pH and ionic strength of the buffer for the best solubility of the samples. To simplify as much as possible, we used the dialysis buffer (20 mM Tris-HCl pH 8, 150 mM NaCl, 5 mM β-mercaptoethanol) as running buffer in most experiments. Due to the particularities of each approach and measurement devices, there are some limitation in the buffer choice. In some cases, blocking agents were required, such as 1mg/mL BSA, especially for low protein concentrations (in the nM range), to prevent surface adsorption. To reduce surface tension in capillaries and microfluidic devices, detergents were required, such as 0.1 % Tween-20. For AUC-FDS, we had to avoid Tris-HCl or HEPES above 20 mM, which can cause problems at 230 nm wavelength, and be aware of other absorbent

molecules (nucleotides, old DTT or β-mercaptoethanol). For MST experiments, we used the commercial MST buffers (50 mM Tris-HCl pH 7.4, 150 mM NaCl, 10 mM $MgCl_2$, 0.05 % Tween-20) for Ku-DNA and, Roti®-Stock 1x PBS (10 mM Na_2HPO_4, 2 mM KH_2PO_4 pH 7.6137 mM NaCl, 2.7 mM KCl, 0.005% Tween 20) for A3-Rep17. For switchSENSE sizing experiments D_h estimation, a low salt buffer is required (10 mM Tris-HCl, 40 mM NaCl, 0.05 % Tween-20, 50 µM EGTA, 50 µM EDTA).

In order for new users to determine the concentration ranges to work with in an unknown system, preliminary experiments need to be done using a broad range, observe the results and in consequence refine the initial conditions to a narrow range that could better suit the system in question. If an interaction partner is difficult to produce or not stable at high concentration, in solution approaches will be the one to keep in constant concentration during titration of its partner. In the other approaches must be the one to try first to immobilize or label. Reverse configuration can be always tested to improve or confirm the results.

Results

Biophysical measurements of alphaRep interactions

We characterized the interaction of A3 with its binder Rep17 (Rep2 was also used during the preparation of the training) using the following techniques presented in the Fig. 1: in solution approaches, which do not require labeling (SEC-MALS and ITC), in solution approaches that require labeled protein or DNA (MST and AUC-FDS), and surface approaches (BLI and switchSENSE). The students performed the measurements presented here during the training (Fig. 2, Fig. S2 and Table S1). When available, we mention the values that have been reported for some approaches in previous studies.

AlphaRep interactions measured by label free in solution approaches

Due to time limitations, the SEC-MALS experiments were performed prior to the training. We used a Superdex 200 increase 10/300 GL column (*Cytiva*), and compared three different runs with A3 alone, Rep2 alone and A3-Rep2 complex at 2 mg/mL each. A3 eluted as a dimer with a molar mass of 44.8 ± 0.4 kDa and, a hydrodynamic radius of 3.0 ± 0.2 nm. Rep2 eluted as a monomer with a molar mass of 11.6 ± 0.9 kDa. The Rep2 concentration was insufficient, in view of the small molar mass, to make accurate sizing measurement by DLS. Finally, the A3-Rep2 complex eluted before the free proteins, with a molar mass of 65.5 ± 0.4 kDa and hydrodynamic radius of 4.0 ± 0.2 nm (Fig. 2b). The stoichiometry was determined by using the protein conjugate method (Loiseau et al., 2017). Accurate mass can be calculated from MALS data with this method, which uses two concentration detectors simultaneously (a refractometer and UV spectrophotometer), and information about refractive index increment (dn/dc) and UV extinction coefficient of each component. In our case, the complex corresponds to one dimer of A3 and two Rep2 molecules.

Preparatory ITC experiments were performed on a PEAQ-ITC instrument with A3 in the cell at 18 µM and Rep17 in the syringe at 187 µM (Fig. S2a). Three different groups of students did a triplicate measurement during the training using the same PEAQ-ITC instrument. We observed bi-phasic thermograms, and isotherms were fitted using a model of two identical binding sites with cooperativity. This cooperativity could stem from the propensity of A3 to form homodimers at µM concentration as shown by SEC-MALS (Freire et al., 2009; Vega et al., 2015). We could estimate two K_D values, the first K_D corresponds to an interaction with a tight

affinity (K_{D1} from 0.48 to 0.66 nM) and the second one to a weaker affinity (K_{D2} from 16 to 32 nM) (Fig. 2c). With the obtained parameters for each site, described in the table at the bottom of thermograms, an average global affinity (Wyman and Gill, 1990) could be calculated (geometric mean of both dissociation constants: $K_{D,av}$ = sqrt(K_{D1} x K_{D2}), which for each assay was 3.9 nM, 3.1 nM, and 3.2 nM, close to that obtained with other techniques. Data were analyzed during the training using the Origin software and the new PEAQ ITC software for comparison.

AlphaRep interactions measured by biophysical approaches with a partner immobilized on a surface

Preliminary analysis using SPR, were carried out a ProteON XPR36 instrument from *Biorad* (data not published, Fig. S2b).

Before the training preliminary BLI experiments were performed on an Octet RED384 instrument where His-tagged A3 protein was captured on Ni-NTA sensors at 5 µg/mL for 20 s and Rep17 concentration ranged from 200 nM to 1.56 nM. In these conditions, in which A3 is most probably in a monomeric form, the calculated kinetic rates were k_{ON} of 1.3 10^{+5} $M^{-1}s^{-1}$, k_{OFF} of 5.9 10^{-3} s^{-1} and K_D of 22.4 nM (data not shown). We observed that the fit was not correct with a single site model and that residuals showed systematic errors. During the training, a duplicate experiment was performed on an Octet RED96e in a buffer containing 1 mg/mL BSA and 0.1 % Tween-20 to limit the non-specific binding. In this case, the fitting was improved (Fig. 2d). We obtained the following preliminary values: k_{ON} of 2.6 ± 0.7 10^{+5} $M^{-1}s^{-1}$, k_{OFF} of 7.6 ± 0.7 10^{-4} s^{-1}, K_D of 3.2 ± 1.1 nM. The K_D measured from the plateau of the curve (steady state) was of 3.3 ± 0.8 nM, close to the one obtained from kinetics (Fig. S2c).

For the switchSENSE experiments, we first coupled A3 with the DNA strand (cNL-B48), which was complementary to the surface-tethered DNA strand on the chip. In this case, the surface-tethered DNA strand was labeled with a red fluorescent probe (NLB48-red dye). The DNA-protein conjugate was purified using an anion-exchange-chromatography (Fig. S2d, top left). We then hybridized the A3-cNLB48 with the NLB48 on the sensor surface at a concentration of 100 nM. The hybridization step could be monitored in real-time by measuring the fluorescence increase (Fig. S2d, top right). Preliminary kinetic experiments were done using the dynamic mode (switching of the nanolevers). Rep2 alphaRep was used as analyte at three

different concentrations ranging from 100 nM to 11.1 nM. Preliminary kinetic rates were calculated from a global fit for the three concentrations: k_{ON} of 2.40 ± 0.05 10^{+6} $M^{-1}s^{-1}$, k_{OFF} of 6.86 ± 0.23 10^{-4} s^{-1} and K_D of 0.29 ± 0.01 nM (Fig. S2d, bottom, left). For each analyte concentration, it was possible to perform a sizing experiment to measure the hydrodynamic diameter of the ligand A3, before or after association with Rep2. The D_h of the dimeric form of A3 calculated from the crystal structure (PDB 6FT) is found to be equal to 4.8 nm. Due to protein dilution, we expect A3 to be present as a monomer on the DNA conjugated strand. Indeed, the D_h of 3.0 ± 0.1 nm measured in our switchSENSE experiments is compatible with a monomeric form of A3 (Fig. S2d, bottom, right). The D_h = 3.8 ± 0.1 nm measured for the complex A3-Rep2 corresponds to an increase of 0.8 nm when compared to the hydrodynamic diameter of the monomeric form of A3 (Fig. S2d, bottom, left). During the training, kinetic experiments in static mode (nanolevers in up position) were performed, as before for Rep2, with Rep17 concentration ranging from 100 nM to 11.1 nM. The calculated kinetic values measured in this case were in the same range than the ones obtained previously with Rep2: k_{ON} of 2.35 ± 0.17 10^{+6} $M^{-1}s^{-1}$, k_{OFF} of 2.30 ± 0.34 10^{-3} s^{-1} and K_D of 0.98 ± 0.16 nM (Fig. 2e). During the training, students did not have time to run a sizing experiment.

AlphaRep interactions measured by biophysical approaches with a labeled partner

Because AUC-FDS experiment was time consuming, data were collected before the training. We first labeled A3 with the dye NT495 using the commercial *NanoTemper* Monolith Protein Labeling Kit BLUE-NHS (Amine Reactive). In these conditions, we were able to use a low concentration of A3 (5 nM). At this nanomolar concentration, A3 is a monomer as observed before by switchSENSE. We used variable concentrations of Rep17 from 0.5 nM to 0.5 µM, and an An-50 Ti rotor at 42 000 rpm (130 000 g) speed. The sedimentation coefficients for A3 and A3-Rep17 complex were 2.16 ± 0.08 S and 2.96 ± 0.05 S, respectively and the calculated K_D at equilibrium was 13.4 ± 1.8 nM (Fig. 2f).

Finally, for the MST experiment, we decided to use the Red-tris-NTA 2nd Generation dye from the *NanoTemper* Monolith His-Tag Labeling Kit, this site-specific non covalent labeling substantially improved the signal respect to the 1st Generation dyes, and respected better the integrity of protein. Red-tris-NTA labeled A3 could not be used in AUC-FDS experiment, because its excitation and emission maxima are out of the fluorescence detector range

(488nm and 505-565 nm respectively). In the MST experiment, labeled A3 was at 35 nM, and the highest concentration of Rep17 was 8 µM. The titration curves we obtained allowed us to measure a K_D of 8.0 ± 4.3 nM (Fig. 2g).

Figure 2. Biophysical measurements of alphaRep interactions.

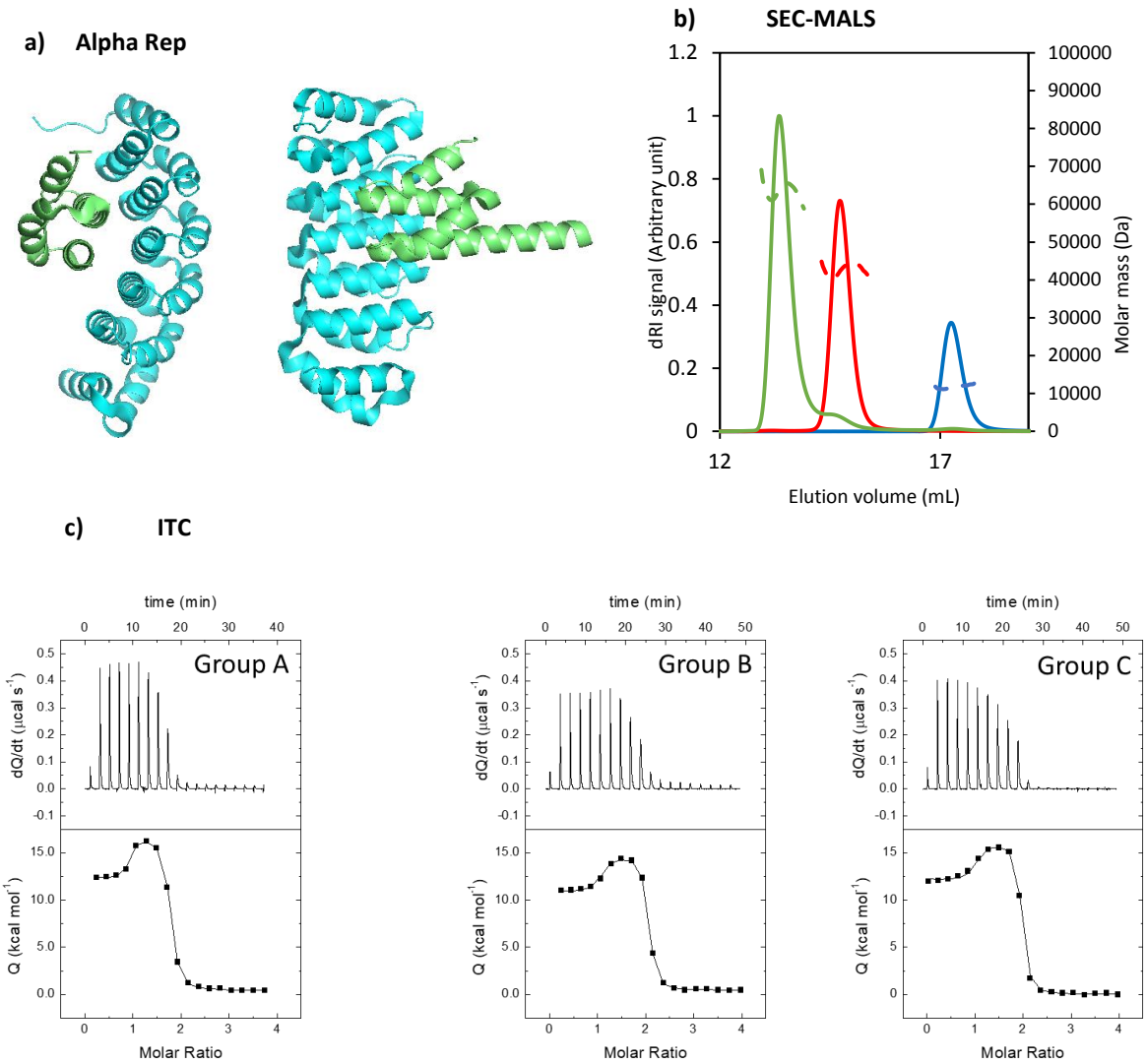

	K (M^{-1})	K_D (nM)	ΔH (kcal/mol)	α	Δh (kcal/mol)	n
Group A	$2.1 \cdot 10^9$	0.48	12.0	0.015	4.3	0.84
Group B	$1.7 \cdot 10^9$	0.59	10.5	0.036	3.6	0.98
Group C	$1.5 \cdot 10^9$	0.66	12.2	0.041	3.8	0.94

	K_{D1} (nM)	ΔH_1 (kcal/mol)	K_{D2} (nM)	ΔH_2 (kcal/mol)
Group A	0.48	12.0	32	16.3
Group B	0.59	10.5	16	14.1

Group C	0.66	12.2	16	16.0

d) BLI

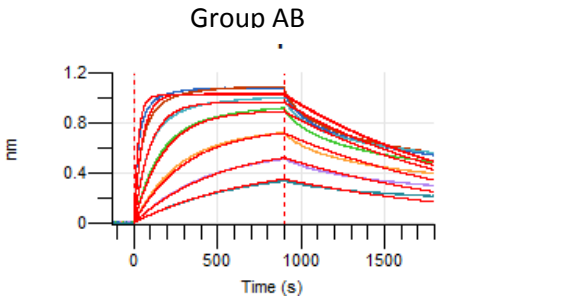

e) switchSENSE

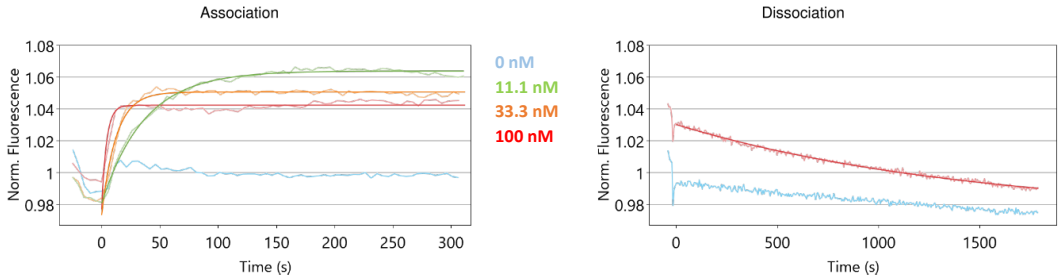

f) AUC-FDS **g) MST**

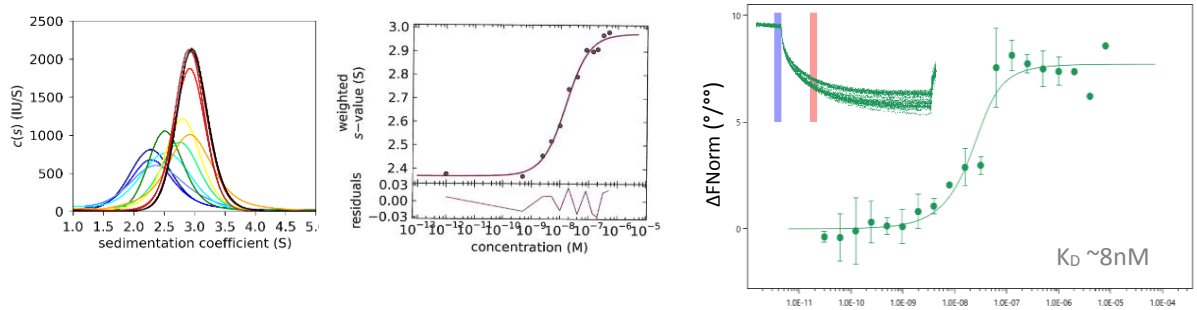

a) Crystal structure of A3 alphaRep (a-A3, blue) in complex with Rep2 (bA3-2 Ligand concentration) at 90° view (left). b) SEC-MALS analysis. Elution profiles and molar masses of Rep2 in blue, A3 in red, and the complex of A3-dimer and two molecules of Rep2 in green. c) PEAQ-ITC data of A3-Rep17 interaction obtained during the training for three groups (A, B and C). K, K_D, and ΔH were the association constant, the dissociation constant, and the interaction enthalpy of either of the two binding sites when the A3 dimer was unoccupied. α and Δh were the cooperative interaction constant and the cooperative interaction enthalpy, which reflect the binding cooperative phenomenon (a factor that modulates the binding affinity and a term that modulates the binding enthalpy to the second site when there was a site already occupied, respectively). n was the active (or binding-competent) fraction of protein, since the stoichiometry was already included in the model. K_{D1} and ΔH_1 were the intrinsic site-specific dissociation constant and binding enthalpy for the first binding site ($K_{D1} = K_D$, $\Delta H_1 = \Delta H$). K_{D2} and ΔH_2 were the intrinsic site-specific dissociation constant and binding enthalpy for the second binding site ($K_{D2} = K_{D1} / \alpha$, $\Delta H_2 = \Delta H_1 + \Delta h$). d) Octet RED96e BLI kinetic analysis of A3-Rep17 interaction in duplicate. Colors code of Rep17 concentration: 3.13 nM (teal), 6.25 nM (purple), 12.5 nM (orange), 25 nM (green), 50 nM (cyan), 100 nM (red), 200 nM (blue). e) switchSENSE kinetics analysis of A3-Rep17 interaction on dynamic mode, at three Rep17 concentrations. Normalized association (left) and dissociation (right) data were represented in function of time. f) AUC-FDS distribution of sedimentation coefficients (left) with labeled A3 at 5 nM and increasing concentrations of Rep17 from 0.5 nM to 0.5 µM, obtained with the program SEDFIT (Schuck, 2000) and GUSSI (Brautigam, 2015). Colors code of Rep17 concentrations: 0 µM (navy blue), 0.5 nM (blue), 1 nM (cornflower blue), 2 nM (cyan), 4 nM (green), 8 nM (springgreen), 16 nM (yellow), 32 nM (orange), 64 nM (red), 128 nM (maroon), 256 nM (brown) and 0.5 µM (black). AUC-FDS K_D calculation (right), by fitting with isotherm tool in the program SEDPHAT. g) MST

analysis with red fluorophore. Inset, MST traces from relative fluorescence versus time, MST on used was 10 s (red band).

In summary, the students obtained in one week using several complementary approaches, results that were consistent in stoichiometry, and to a lesser extent, in kinetic rates or affinity (Table S1). They could observe that the required quantity of sample, ligand or analyte, for each approach differs significantly. They also observed that some approaches gave highly complementary information on the system studied (Fig. S2). For example, ITC shows that the interaction is cooperative when A3 alphaRep is used at the high concentration needed for ITC (18µM). This cooperativity, linked to the dimeric state of A3, was not observed with monomeric ligand immobilized on BLI or switchSENSE. They observed higher K_D values with AUC-FDS and MST, where one of the partner is labeled, reflecting possible steric hindrance between the fluorophore and the interaction site.

Biophysical measurements of Ku-DNA interactions

We determined the interaction of the heterodimeric full-length protein Ku with four double-strand DNAs (dsDNAs) of different lengths: 18 bp, 42 bp, 48 bp, and 200 bp (Fig. 3, Fig. S3). Ku binds DNA through its ring-shaped structure (Fig. 3a). The main observations made during the training for the Ku-DNA interactions are shown in Fig. 3 and Table S2.

Ku-DNA interactions measured by label-free in solution biophysical approaches

For SEC-MALS, we used a Superdex 200 increase 10/300 GL column (*Cytiva*) as above and ran first a quadruplicate experiment with Ku alone, resulting in an average molar mass of 144.4 kDa (Fig. S3a). We then ran a duplicate experiment with Ku and a 1.2 excess of 42 bp DNA. We obtained three peaks: the first corresponded to 2 Ku : 1 DNA complex (average Mw of 306.2 kDa), the second corresponded to 1 Ku : 1 DNA (average Mw of 171.0 kDa), and the last corresponded to the excess of dsDNA alone (average Mw of 26.1 kDa). This suggests that there is an equilibrium between 2:1 and 1:1 Ku-DNA complexes (Fig. 3b) with stoichiometries determined by using the protein conjugated method (Loiseau et al.; 2017). The presence of these two types of complexes could be explain by the use of a non-saturating Ku concentration.

For ITC experiments, we used in our laboratory two different sizes of dsDNA, 18 bp and 42 bp (Gontier et al., 2021). Due to time limitations students repeated the measurement only with the 42 bp. We used a VP-ITC instrument which consumes more sample, but was more sensitive to study these protein-DNA interactions. The heat effects were positive (endothermic interaction) and small (0.2 µcal.sec^{-1}) (Fig. 3c). Students did two runs, the first at 20 µM and the second at 40 µM concentration of DNA in the syringe, and in both cases Ku at 4 µM in the cell. We obtained a mean K_D at equilibrium of 3.7 ± 0.7 nM with a molar ratio of 0.34 ± 0.02 and a ΔH of 24.4 ± 2.7 kcal/mol. The molar ratio was in good agreement with a ratio of 0.5 expected for the interaction of two Ku molecules with a DNA of 42 bp. No evidence for cooperativity was observed. All the data were analyzed using the Origin software and the new PEAQ ITC software for comparison.

Ku-DNA interactions measured by biophysical approaches with a partner immobilized on a surface

Preparatory BLI experiments were performed on an Octet RED384 instrument. First, we tried the strategy that was used for the A3 alphaRep protein, i.e. capturing the Ku heterodimer on Ni-NTA sensors. We did not observe any binding with an 18 bp DNA as analyte (data not shown). We hypothesized that the DNA binding site may not be accessible when Ku is immobilized through its His-tag. We therefore tested another strategy, which relied on the capture of a biotinylated 42 bp DNA on Streptavidin sensors (at 10 nM for 120 s), which were then incubated with Ku protein as analyte (at concentrations in 200 nM to 1.56 nM range). In these conditions, we observed an interaction, with an estimated K_D around 40 nM (data not shown). We repeated the experiment in duplicate during the training on an Octet RED96e using an optimized buffer with 1mg/mL BSA and 0.1 % Tween-20, and Ku protein concentrations ranging from 200 nM to 3 nM. The results of the two runs were consistent, with apparent kinetic rates, k_{ON} of 1.91 ± 0.02 10^{+6} $M^{-1}s^{-1}$, k_{OFF} of 7.17 ± 0.33 10^{-4} s^{-1}, and a K_D of 0.37 ± 0.01 nM (Fig. 3d). However, the deviation between the fitted curves and the experimental data was high, indicating that the interaction mechanism was more complex than a simple 1:1 binding. For instance, the association and the dissociation processes could be limited by the diffusion of Ku towards and from the biosensor surface (mass transport limitation). We therefore analyzed the concentration-dependence of the steady state responses and measured a K_D of 5.2 ± 0.2 nM (Fig. S3b). As several curves did not reach a steady state, this K_D value could however be overestimated and experiments should be reproduced with longer association times. Taking everything into account, BLI binding constants were at this stage only qualitative.

Preliminary switchSENSE experiments were done before the training by forming an 80 bp dsDNA on the sensor. For that, we hybridized an 80-mer DNA with a 32-mer DNA. This DNA was complementary to the NL48 ssDNA on the chip (Fig. S3c, top, left). We performed kinetic analyses in duplicate using static mode and Ku protein at 500 nM concentration. We obtained the following kinetic rates: k_{ON} of 9.3 ± 0.1 10^{+4} $M^{-1}s^{-1}$, k_{OFF} of 2.8 ± 0.1 10^{-4} s^{-1}, and K_D of 3.1 ± 0.1 nM (Fig. S3c, bottom). We monitored the dissociation over a long time (5000 s) to measure a significant proportion of dissociated Ku molecules. In between, we performed a sizing measurement. The calculated value (D_h = 8.9 ± 0.3 nm) was in good agreement with the one obtained from the crystal structure of the Ku-DNA complex (PDB: 1JEQ; D_h = 8.9 nm) (Fig. S3c, top, right). During the training, we performed experiments in dynamic mode using a 48 bp

549 DNA (without overhang). We used a Ku concentration range from 200 nM to 22.2 nM with 1/3
550 serial dilution this time. In these conditions, the protein was closer to the fluorophore at the
551 tip of the 48 bp DNA on the chip. We measured in these conditions a k_{ON} of 2.6 ± 0.2 10^{+6} $M^{-1}s^{-1}$, a k_{OFF} of 2.3 ± 0.3 10^{-3} s^{-1}, and a K_D of 1.0 ± 0.2 nM (Fig. 3e). During the training, students
553 did not have time to run a sizing experiment.

554 Comparable preliminary data were obtained by SPR using a ProteON XPR36 instrument from
555 *Biorad* (Fig. S3d, left), and a Biacore T200 instrument from *Cytiva* (Fig. S3d, right).

556 **Ku-DNA interactions measured by biophysical approaches with a labeled partner**

557 For AUC-FDS, we used an 18 bp DNA labeled with fluorescein (FAM) in 5'. We titrated the DNA
558 (60nM) with Ku (concentration range from 0.5 nM to 0.5 µM). The sedimentation profile
559 showed two species, corresponding to the DNA alone (2.15 ± 0.05 S) and to the 1:1 protein-
560 DNA complex (7.25 ± 0.15 S), and we were able to determine the K_D at equilibrium (12.9 ± 3.2
561 nM) (Fig. 3f).

562 For MST, we used the same 18 bp labeled DNA as for AUC-FDS, but at 10 nM; and titrated it
563 with Ku (concentration range from 2 µM). Training participants performed four runs in total,
564 in duplicates or triplicate (Fig. 3g). We could see some variability in the curves that might
565 originate from the pipetting of the different students. All curves were fitted globally resulting
566 in a K_D of 11.9 nM.

567 Comparable data were obtained in parallel of the training with a novel technology,
568 microfluidic diffusional sizing (MDS) in collaboration with Fluidic Analytics (Fig. S3e). The
569 Fluidity One-W instrument measures the rate of diffusion of macromolecules under steady
570 state laminar flow in a microfluidic chip. In a diffusion chamber with two parallel streams, the
571 migration of a labeled partner depends on its size. At the end, the streams are re-split and the
572 fluorescence ratio between the two allows to calculate R_h. The variation of R_h observed when
573 titrating the labeled partner by the unlabeled one allows to generate a binding curve and to
574 calculate a K_D value.

Figure 3. Biophysical measurements of Ku-DNA interactions.

a) **Ku-DNA**

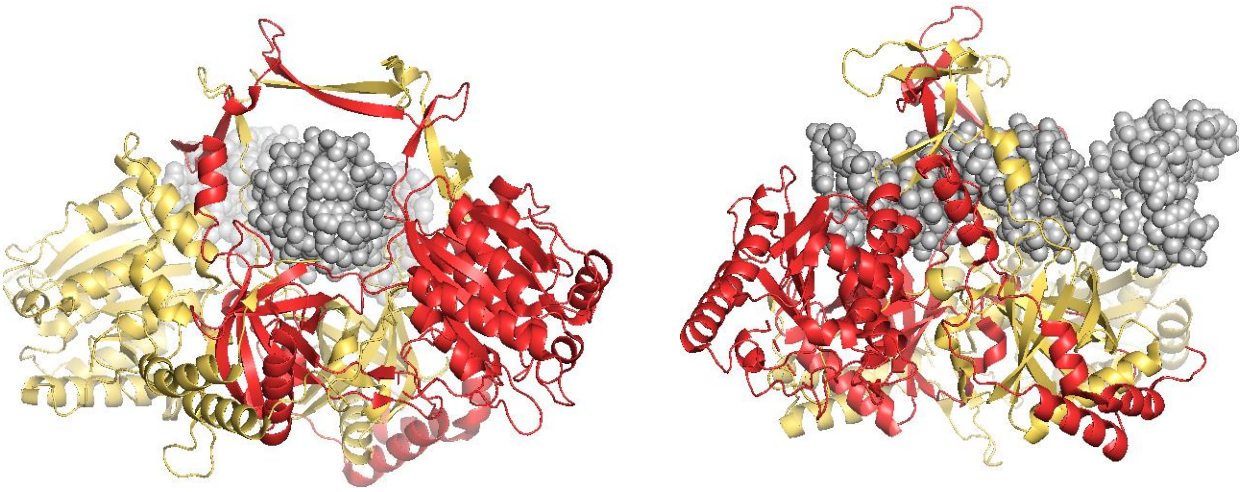

b) **SEC-MALS**

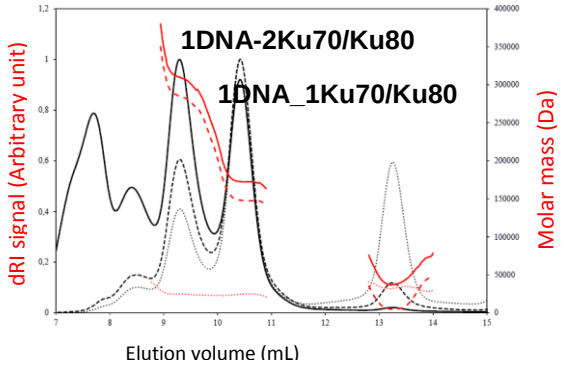

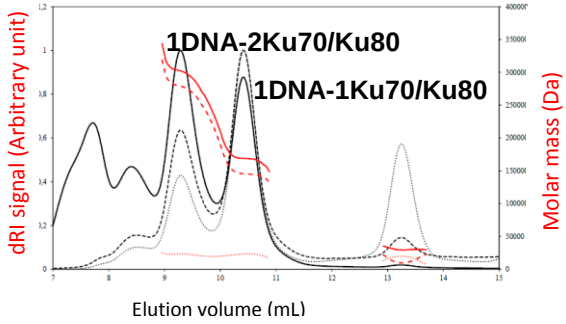

		Peak 1	Peak 2	Peak 3
Group C	**Protein molar mass**	279.1	145.7	9.6
	DNA molar mass	23.3	23.3	19.9
	Total molar mass	302.3	169.0	29.6
Group D	**Protein molar mass**	285.3	148.4	4.8
	DNA molar mass	24.7	24.6	32.3
	Total molar mass	310.1	172.9	37.1

c) ITC

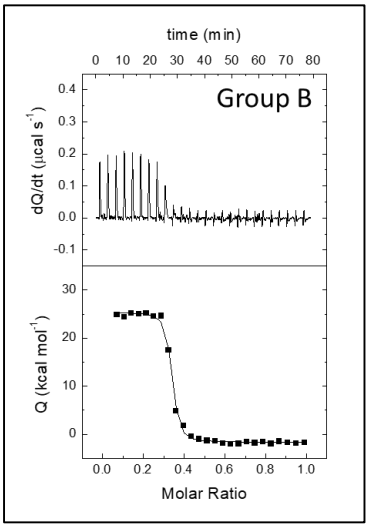

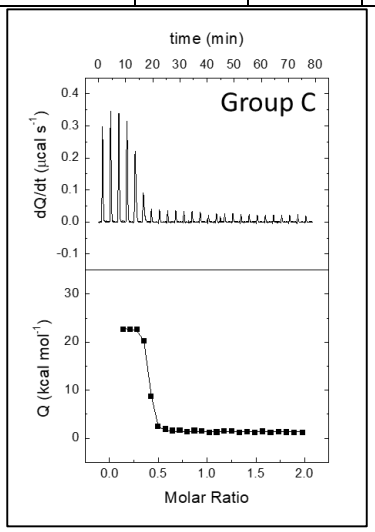

	K (M^{-1})	K_D (nM)	ΔH (kcal/mol)	n
Group B	$3.4\ 10^8$	3.0	27.1	0.32
Group C	$2.3\ 10^9$	4.3	21.7	0.37

d) BLI: Group AB and Group CD

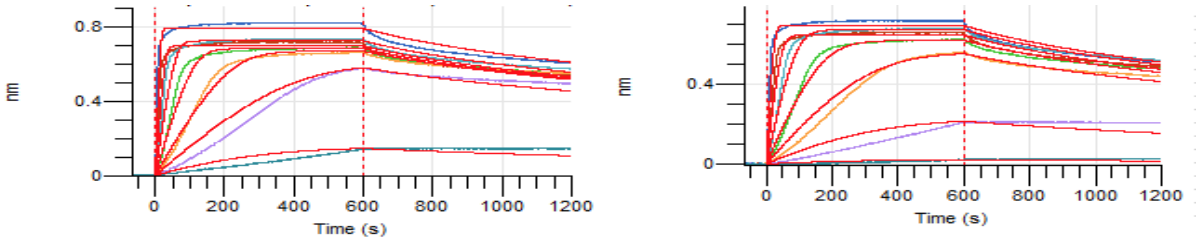

e) switchSENSE

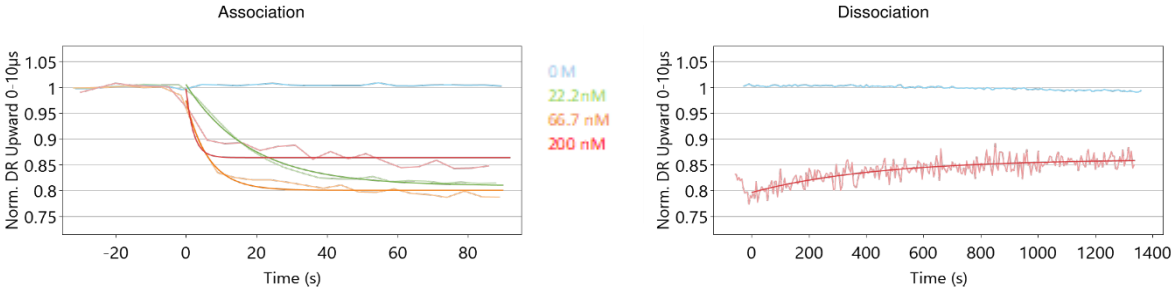

f) AUC-FDS

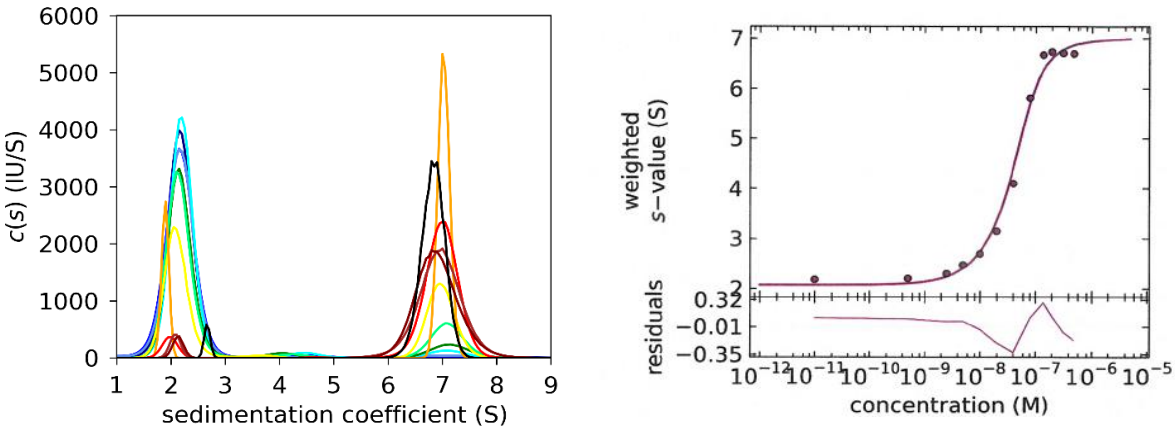

g) MST

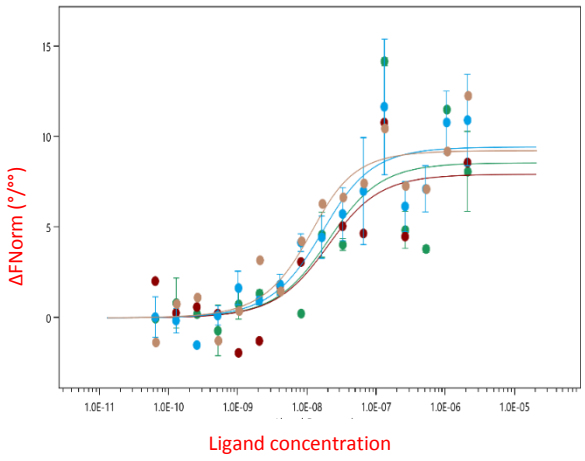

GROUPS	Excitation Power	K_D	K_D Confidence	Std. Error of Regression	Signal to Noise
A1-B1	60	$1.53\ 10^{-08}$	$1.86\ 10^{-08}$	2.77	3.33
A2	40	$1.49\ 10^{-08}$	$1.73\ 10^{-08}$	2.01	4.33
B2-C2-D2	100	$1.14\ 10^{-08}$	$7.26\ 10^{-09}$	1.61	6.31
D1	100	$6.15\ 10^{-09}$	$4.3\ 10^{-09}$	1.56	6.37

a) Crystal structure of the Ku- DNA complex (PDB: 1JEQ). View down the DNA helix (left) and side view (right), with Ku70 colored in red, Ku80 in yellow cartoons and DNA in grey spheres. b) SEC-MALS elution profiles and molar masses of Ku-DNA complex in duplicate. Representation of elution volumes in mL and molar mass in g/mol. c) VP-ITC data in duplicate. d) Octet RED96e BLI kinetics data in duplicate. Colors code of Ku concentration: 3.13

nM (teal), 6.25 nM (purple), 12.5 nM (orange), 25 nM (green), 50 nM (cyan), 100 nM (red), 200 nM (blue). e) switchSENSE dynamic mode data for three Ku concentrations. F) AUC-FDS measurement of Ku-DNA interaction. AUC-FDS distribution of sedimentation coefficients (left) with labeled DNA at 60 nM and increasing concentrations of Ku from 0.5 nM to 0.5 µM, obtained with the program SEDFIT (Schuck, 2000) and GUSSI (Brautigam, 2015). Colors code of Ku concentration: 0 µM (navy blue), 0.5 nM (blue), 1 nM (cornflower blue), 2 nM (cyan), 4 nM (green), 8 nM (springgreen), 16 nM (yellow), 32 nM (orange), 64 nM (red), 128 nM (maroon), 256 nM (brown) and 0.5 µM (black). AUC-FDS K_D calculation by fitting with isotherm tool in the program SEDPHAT (right). g) MST analysis. Representation of ligand concentration against ΔFNorm °/°° (left). Superposition of several run in the similar conditions, but different excitation power and students. Summary of MST data (right).

In summary, for the Ku-DNA project, the students also obtained consistent results of stoichiometry, kinetic rates and affinity (Fig. 3, Table S2). As for the alphaRep project, the quantity of sample required varies between the different approaches. ITC, SEC-MALS and AUC-FDS were very efficient for measuring the stoichiometry of Ku on DNA with one Ku molecule bound every 18-21bp DNA. They observed that measurements on surfaces, either by BLI or switchSENSE, were successful only when the DNA was immobilized. They could observe that switchSENSE allows a quite accurate estimation of the Ku size (Fig. S3d, bottom). Oligonucleotides with a fluorescent probe in 5' or 3' are inexpensive and allow to follow the interaction between a fluorescent DNA and a protein quite easily by MST or AUC-FDS, without major steric hindrance between the fluorescent probe and the interaction sites.

Discussion

The study presented here compares six different *in vitro* biophysical approaches to characterize the architecture (in terms of size or stoichiometry) and binding parameters (k_{ON}, k_{OFF}, K_D) of two different types of complexes (protein-protein and protein-DNA). It was designed to provide a rather complete overview of six different techniques in a short period. During a week, 20 participants performed this study in the context of the MoSBio Training School (ARBRE-MOBIEU COST Action). During the first day of the training school, experts of each field presented the projects, the theory and examples of applications for the three classical techniques (AUC, SEC-MALS, ITC), and the three more recent ones (MST, BLI, switchSENSE). An additional presentation about, sample quality control, a relevant subject regarding reproducibility of experimental measurements, completed the first day of the training (Raynal et al., 2014). The remainder of the week was dedicated fulltime to practical sessions where the participants could perform experiments on instruments, analyze results and discuss with experts. All six approaches, except AUC, and SEC-MALS for the alphaRep interaction, were successfully used during the training school to study two important types of macromolecular interactions (alphaReps and Ku-DNA). The training allowed the students,

first, to compare the quantity of material consumed for each technique, and, second, to understand the parameters that can be measured by each of them (Fig. 4). This first edition of the MoSBio Training School was positively assessed both by trainers and trainees. It was a unique opportunity to compare advantages and limitations of this large ensemble of techniques. A new edition will be scheduled soon. The participants were able to use all instruments quite easily by themselves, with the exception of AUC, which requires a little more expertise and longer run times. Finally, this study showed that a nanomolar range affinity can be easily assessed with most tested techniques. The students could observe that the K_D vary significantly with the technique used, though the K_D measured were all in the nanomolar range. The maximal and minimal values of K_D measured between the alpharep and the different techniques differ by a factor 21. The extreme K_D differ by a factor 13 for the K_D measured between Ku and DNA. We observed that in these two systems the presence of a label on one partner, in MST and AUC-FDS approaches, comes with a higher K_D than without label. During the training school, the students could observe the variability on the K_D values measured in the different groups or with the different approaches (see Fig. 2 and Fig. 3). The training was also an opportunity to discuss on the techniques that are more favorable to measure lower (pM) or higher (µM) K_D values.

The results presented here for the alphaRep-proteins and Ku-DNA complexes highlight the advantages and drawbacks of each approach. The quantity of required sample was not limited in our case, but the participants clearly observed that the amounts of protein and DNA used for each approach are very different (Fig. 4). AUC, SEC-MALS and ITC are the most sample-consuming techniques. The ITC200 and PEAQ-ITC instruments were an important progress for ITC in this regard, but we observed that for interactions with very weak heat exchange like Ku-DNA, the more sensitive, but more sample-consuming VP-ITC was still needed to obtain good results. Surface methods like BLI and switchSENSE require only small amounts of the immobilized protein. For the study of high affinity systems (in the nM range) like those characterized here, the consumption of analyte is small too. For weaker affinities (higher K_D in the µM range) the required quantity of analyte will however rise significantly to cover concentrations from 1/10 of the K_D to 10 times the K_D. The MST technique consumes very small volumes of material once the labeling step is successfully achieved. Anyway, the time and sample consumption for a given technique must be evaluated not just for a single

646 successful experiment, but must also take into account he experimental design and
647 optimization stage.

648 **Figure 4. Comparison of results obtained for the alphaReps and the Ku-DNA interaction with**
649 **the six approaches.**

Alpha Reps	**SEC-MALS**	**200 µg A3, 200 µg Rep2** Molar mass Stoichiometry: (A3-dimer): 2 Rep2	**ITC**	**80 µg A3, 130 µg Rep17** Biphasic curve Cooperativity (A3 dimer) K_{D1}, K_{D2}, ΔH, -TΔs
	BLI	**8 µg A3, 2 µg Rep17** A3-monomer K_D, k_{ON}, k_{OFF}	**Switch-SENSE**	**150 ng A3, 2-20 µg Rep17** A3-monomer Size (D_h) K_D, k_{ON}, k_{OFF}
	AUC-FDS	**1 µg A3, 8 µg Rep17** Sedimentation coefficient Stoichiometry K_D	**MST**	**620 ng A3, 6 µg Rep17** (One labeling failed) K_D
Ku-DNA	**SEC-MALS**	**40µg of DNA, 200 µg Ku** Molar mass Stoichiometry: 1 Ku /18-21 bp	**ITC**	**990 µg Ku, 320 µg DNA** Biphasic curve Stoichiometry: 1 Ku /18-21bp K_D, ΔH,-TΔS
	BLI	**400 ng DNA, 14 µg Ku** (Failed with Ku immobilized) K_D, k_{ON}, k_{OFF}	**Switch-SENSE**	**150 ng DNA, 2-20 µg Ku** (Ligand is the nanolever) Size (D_h) K_D, k_{ON}, k_{OFF}
	AUC-FDS	**3.5 µg DNA, 80 µg Ku** (DNA easily labeled) Sedimentation coefficient Stoichiometry K_D	**MST**	**50 µg DNA, 12 µg Ku** (DNA easily labeled) K_D

The experiments performed by the students on the two systems of study with the six approaches were successful. The sample quantities used for the different approaches are indicate, as well as the parameters that can be deduced from the different approaches.

All experimental approaches used in this study can provide K_D values of the interaction. Interestingly, they also provide additional information that may orient the users to one or the other according to the main questions raised in their specific projects. In the two examples we studied, the stoichiometry issue is an important point, since the A3 alphaRep is a dimer when its concentration is in the µM range, while it is a monomer in the nM range. According to this oligomeric state, we can observe some cooperative binding of its partner, which influences the binding parameters. In this regard, ITC, SEC-MALS and AUC allow characterizing the ratio between the dimeric alphaRep target and its binders or between Ku and DNA of increasing

lengths, and confirm the information provided by the crystal structures of the complexes. The sizing measurement in switchSENSE can also provide some information regarding the stoichiometry or conformation.

Kinetic parameters are important data to estimate the half-time of a complex, which is an important interaction parameter. BLI and switchSENSE (as well as SPR) proved to be efficient in this study to determine k_{ON} and k_{OFF}. We observed that the switchSENSE allows to characterize tight interactions with small k_{OFF} values (k_{OFF} about 10^{-4} s) by monitoring the dissociation over a long time period (5000 s). Thermodynamic parameters (enthalpy, entropy and Gibbs free energy) also provide key information about macromolecular interactions, notably about the polar/apolar nature of the interface between a protein and its ligand. The Ku-DNA thermograms for example indicate that the interaction is entropically driven with a positive and unfavorable enthalpy probably linked to desolvation of the DNA and Ku surface upon binding.

The choice of one technique over another depends mainly on the questions one wants to answer. Some practical issues can also guide the choice of the method, such as the quantity and solubility of protein and ligands available, the possibility to immobilize or to label one of the interaction partners, and the time available. The presence of an instrument and experts in house or nearby the user is another criterion. Noteworthy, all these approaches are available in many research institutions in Europe, especially in those engaged in Structural Biology studies. If needed, these approaches are also available through research infrastructures, like MOSBRI and Instruct in Europe or FRISBI in France. Finally, there are research networks, like ARBRE-MOBIEU, allowing to foster fruitful exchanges with experts in the different fields. The MoSBio training school over a week with 20 students proved to be a very rich occasion for such discussions.

Studying macromolecular interactions *in vitro* is extremely complementary to *in cellulo* analyses. Interactions observed in cells or in cellular extracts often need further *in vitro* characterization of target engagement. Training schools, as the one described in this article, are central to further disseminate the importance of biophysical studies in cell biology laboratories. This training school contributed to initiate students from various fields to biophysical approaches and showed in a short period the added-value of quantitative measurements of protein interactions.

By mutagenesis, Nuclear Magnetic Resonance (NMR) shift or Hydrogen-Deuterium Exchange Mass Spectrometry (HDX-MS), one can determine the residues involved in the interaction, and structural analysis can yield information about their topology. One can play with the experimental conditions (pH, ionic strength, temperature) to expand the knowledge about the nature of the interaction under study (electrostatic and/or hydrophobic, exo- or endothermic, presence/absence of conformational changes, coupling with additional binding equilibria). Furthermore, pharmacological studies require this kind of biophysical approaches. Finally, molecular scale biophysics data can also be used to implement *in silico* simulations to predict other interactions in basic research. A second edition of this Training School will be held as soon as possible. The extremely positive feedback from the students, as well as from the academic experts and industrials participating in this school, highlights the need for a better understanding of the theoretical bases of such a panel of biophysical methods coupled to hands-on experimental practice.

References

Abdiche Y, Malashock D, Pinkerton A, Pons J.(2018) Determining kinetics and affinities of protein interactions using a parallel real-time label-free biosensor, the Octet. *Anal Biochem*. 377(2):209-17

Andreani J, Guerois R. (2014) Evolution of protein interactions: from interactomes to interfaces. *Arch Biochem Biophys*. 554:65-75

Asmari M, Ratih R, Alhazmi HA, El Deeb S. (2018) Thermophoresis for characterizing biomolecular interaction. *Methods* 146:107-119

Brautigam, CA. (2015) Chapter Five - Calculations and Publication-Quality Illustrations for Analytical Ultracentrifugation Data. In *Methods in Enzymology*, Cole, J. L., Ed. Academic Press: Vol. 562, pp 109-133

Campanacci V, Urvoas A, Consolati T, Cantos-Fernandes S, Aumont-Nicaise M, Valerio-Lepiniec M, Surrey T, Minard P, Gigant B. (2019) Selection and Characterization of Artificial Proteins Targeting the Tubulin α Subunit. *Structure*. 27(3):497-506

Chang HHY, Pannunzio NR, Adachi N, Lieber MR. (2017) Non-homologous DNA end joining and alternative pathways to double-strand break repair. *Nat Rev Mol Cell Biol* 18(8):495-506

Chevrel A, Mesneau A, Sanchez D, Celma L, Quevillon-Cheruel S, Cavagnino A, Nessler S, Li de la Sierra-Gallay I, van Tilbeurgh H, Minard P, Valerio-Lepiniec M, Urvoas A. (2018) Alpha repeat proteins (αRep) as expression and crystallization helpers. *J Struct Biol*. 201(2):88-99

Di Meo T, Ghattas W, Herrero C, Velours C, Minard P, Mahy JP, Ricoux R, Urvoas A. (2017) αRep A3: A Versatile Artificial Scaffold for Metalloenzyme Design. *Chemistry*. 23(42):10156-10166

Fernandez M, Urvoas A, Even-Hernandez P, Burel A, Mériadec C, Artzner F, Bouceba T, Minard P, Dujardin E, Marchi V. (2020) Hybrid gold nanoparticle-quantum dot self-assembled nanostructures driven by complementary artificial proteins. *Nanoscale*. 12(7):4612-4621

Folta-Stogniew E. (2006) Oligomeric states of proteins determined by size-exclusion chromatography coupled with light scattering, absorbance, and refractive index detectors. *Methods Mol. Biol. 328*, 97-112

Freire E, Schön A, Velazquez-Campoy A. (2009) Isothermal titration calorimetry: general formalism using binding polynomials. *Methods Enzymol*. 455:127-55

Frit P, Ropars V, Modesti M, Charbonnier JB, Calsou P. (2019) Plugged into the Ku-DNA hub: The NHEJ network. *Prog Biophys Mol Biol*. 147:62-76

Gontier A, Varela PF, Nemoz C, Ropars V, Aumont-Nicaise M, Desmadril M, Charbonnier JB. (2021) Measurements of Protein-DNA Complexes Interactions by Isothermal Titration Calorimetry (ITC) and Microscale Thermophoresis (MST). *Methods Mol. Biol. 2247*, 125-143

Guellouz A, Valerio-Lepiniec M, Urvoas A, Chevrel A, Graille M, Fourati-Kammoun Z, Desmadril M, van Tilbeurgh, Minard P. (2013) Selection of Specific Protein Binders for Pre-Defined Targets from an Optimized Library of Artificial Helicoidal Repeat Proteins (alphaRep). *PLoS One*. 8(8):e71512

Holdgate GA. (2001) Making cool drugs hot: isothermal titration calorimetry as a tool to study binding energetics. *Biotechniques* 31(1):164-170

Jerabek-Willemsen M, Wienken CJ, Braun D, D, Baaske P, Duhr S. (2011) Molecular interaction studies using microscale thermophoresis. *Assay Drug Dev Technol* 9(4):342-353

Knezevic J, Langer A, Hampel PA, Kaiser W, Strasser R, Rant U. (2012) Quantitation of Affinity, Avidity, and Binding Kinetics of Protein Analytes with a Dynamically Switchable Biosurface *J. Am. Chem. Soc.* 134 (37), 15225–15228

Krell T. (2008) Microcalorimetry: a response to challenges in modern biotechnology. *Microb Biotechnol* 1(2):126-136

Léger C, Di Meo T, Aumont-Nicaise M, Velours C, Durand D, Li de la Sierra-Gallay I, van Tilbeurgh H, Hildebrandt N, Desmadril M, Urvoas A, Valerio-Lepiniec M, Minard P. (2019) Ligand-induced conformational switch in an artificial bidomain protein scaffold. *Sci Rep*. 9(1):1178

Léger C, Yahia-Ammar A, Susumu K, Medintz IL, Urvoas A, Valerio-Lepiniec M, Minard P, Hildebrandt N. (2020) Picomolar Biosensing and Conformational Analysis Using Artificial Bidomain Proteins and Terbium-to-Quantum Dot Förster Resonance Energy Transfer. *ACS Nano*. 14(5):5956-5967

Loiseau L, Fyfe C, Aussel L, Hajj Chehade M, Hernández SB, Faivre B, Hamdane D, Mellot-Draznieks C, Rascalou B, Pelosi L, Velours C, Cornu D, Lombard M, Casadesús J, Pierrel F, Fontecave M, Barras F. (2017) The UbiK protein is an accessory factor necessary for bacterial ubiquinone (UQ) biosynthesis and forms a complex with the UQ biogenesis factor UbiJ. *J Biol Chem.* 292(28):11937-11950

Nemoz C, Ropars V, Frit P, Gontier A, Drevet P, Yu J, Guerois R, Pitois A, Comte A, Delteil C, Barboule N, Legrand P, Baconnais S, Yin Y, Tadi S, Barbet-Massin E, Berger I, Le Cam E, Modesti M, Rothenberg E, Calsou P, Charbonnier JB. (2018). XLF and APLF bind Ku at two remote sites to ensure DNA repair by non-homologous end joining. *Nat Struct Mol Biol.* 25(10):971-980

Prasad J, Viollet S, Gurunatha KL, Urvoas A, Fournier AC, Valerio-Lepiniec M, Marcelot C, Baris B, Minard P, Dujardin E. (2019) Directed evolution of artificial repeat proteins as habit modifiers for the morphosynthesis of (111)-terminated gold nanocrystals. *Nanoscale*. 11(37):17485-17497

Raynal B, Lenormand P, Baron B, Hoos S, England P. (2014) Quality assessment and optimization of purified protein samples: why and how? Microb Cell Fact. 13:180

Schuck, P. (2000) Size-distribution analysis of macromolecules by sedimentation velocity ultracentrifugation and lamm equation modeling. *Biophys. J.* 78, 1606-1619

Tadi SK, Tellier-Lebegue C, Nemoz C, Drevet P, Audebert S, Roy S, Meek K, Charbonnier JB, Modesti M. (2016) PAXX Is an Accessory c-NHEJ Factor that Associates with Ku70 and Has Overlapping Functions with XLF. *Cell Rep* 17(2):541-555

Valerio-Lepiniec M, Urvoas A, Chevrel A, Guellouz A, Ferrandez Y, Mesneau A, de la Sierra-Gallay IL, Aumont-Nicaise M, Desmadril M, van Tilbeurgh H, Minard P. (2015) The αRep artificial repeat protein scaffold: a new tool for crystallization and live cell applications. *Biochem Soc Trans*. 43(5):819-24

Vega S, Abian O, Velazquez-Campoy A. (2015) A unified framework based on the binding polynomial for characterizing biological systems by isothermal titration calorimetry. *Methods. Apr.* 76:99-115

Velazquez-Campoy A, Freire E. (2006) Isothermal titration calorimetry to determine association constants for high-affinity ligands. *Nat Protoc* 1(1):186-191

Walker JR, Corpina RA, Goldberg J. (2001) Structure of the Ku heterodimer bound to DNA and its implications for double-strand break repair. *Nature* 412(6847):607-614

Wyman J, Gill SJ. (1990) Binding and linkage: Functional chemistry of biological macromolecules. *Mill Valley, CA: University Science Books*

797 Zhao H, Brautigam CA, Ghirlando R, Schuck P. (2013) Overview of current methods in
798 sedimentation velocity and sedimentation equilibrium analytical ultracentrifugation. *Curr*
799 *Protoc Protein Sci*. Chapter 20
800

Declarations

Funding JBC is supported by ARC program (SLS220120605310), ANR-12-SVSE8-012, ANR-18-CE44-0008, INCA DomRep (PLBIO 2012-280) and by the French Infrastructure for Integrated Structural Biology (FRISBI) ANR-10-INBS-05.

Conflicts of interest/Competing interests The authors declare no competing interest. Pierre Soule (NanoTemper) and Christophe Quétard (FortéBio) helped during the training without commercial interest

Ethics approval Not applicable.

Consent to participate The authors consent to participate to this project.

Consent for publication The authors consent to publish the work reported in this paper.

Availability of data and material Data can be obtained by requesting the corresponding author.

Code availability Not applicable.

Authors' contributions PFV, PE, SU, CE, AVC, AR, JBC authors contributed to the study conception and design. Material preparation, data collection and analysis were performed by CV, MAN, SU, PE, AVC, DS, GB, PS, CQ, CE, AR. The first draft of the manuscript was written by PFV and all authors commented on previous versions of the manuscript. All authors read and approved the final manuscript.

Acknowledgments

We thank: members of Philippe Minard's and Jean-Baptiste Charbonnier's teams at I2BC for the sample preparation, Bruno Baron and Bertrand Raynal from *Institut Pasteur, Paris* for all their expert advices in molecular scale biophysics, and Eric Ennifar from *Institut de Biologie Moléculaire et Cellulaire, Strasbourg* for sharing its expertise in the study of biomolecular machineries using biophysical approaches. Friederike Möller and Hanna Müller-Landau from *Dynamic Biosensors*, Aymeric Audfray from Malvern Panalytical, Mathilde Belnou from *NanoTemper technologies*, and Stephanie Bourgeois and coworkers from *Fluidic Analytics* for their availability and all the fruitful discussion. We kindly thank all the participants to the MoSBio Training School, all the sponsors without whom this successful event had not been possible, and finally the keynote speakers, Julie Ménétrey and Terence Strick who shared their projects with us. Most of preparatory experiments were performed in the I2BC, PIM platform (https://www.pluginlabs-universiteparissaclay.fr/fr/results/keywords/PIM), while some others were performed in Institut Pasteur, PFBMI platform.

Supplementary material

Figures

Figure S1. Unfolding profile plot of Ku70/Ku80.

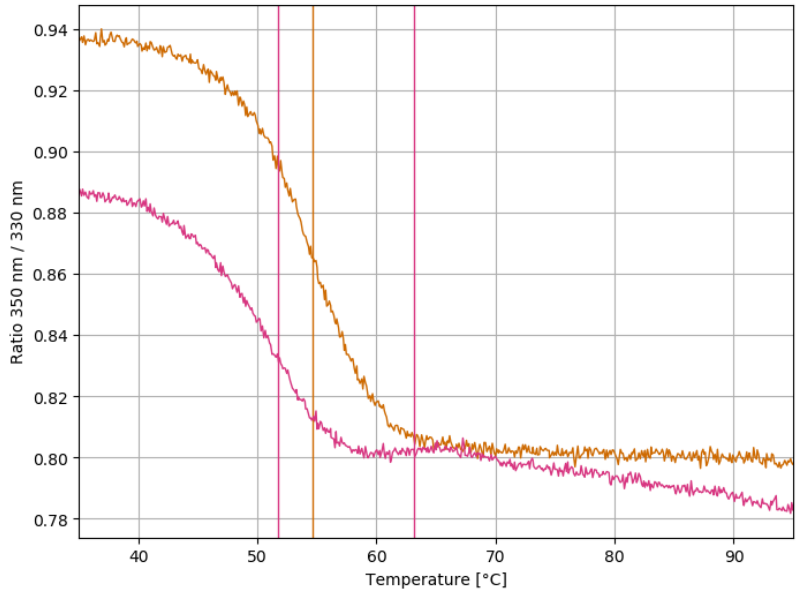

Quality and stability of samples are crucial to obtain accurate biophysical data. For all the biophysical studies shown in this manuscript, we used a full-length version of Ku (called KuFL), but for structural studies we used a shorter version where the C-terminus of each monomer is deleted (called KuCC). We took advantage of the new technology of *NanoTemper*, the Tycho NT.6 instrument, present during the training, to compare the thermal stability of these two versions of Ku protein by a fast measurement. Fluorescence intensity is recorded at 330 nm and 350 nm (emission profile of the Tryptophan residues). The brightness ratio 350 nm / 330 nm plotted against the temperature is called the unfolding profile plot and inflexion temperatures can be derived representing unfolding events. Tryptophan fluorescence of KuFL (orange) and KuCC (pink) were follow during a ramp of temperature of 35-95°C. KuFL showed a higher temperature of unfolding than KuCC (vertical bars). Thus, KuFL appears to be more stable than KuCC by a few degrees.

Figure S2. Additional biophysical measurements of alphaRep interactions.

a) ITC

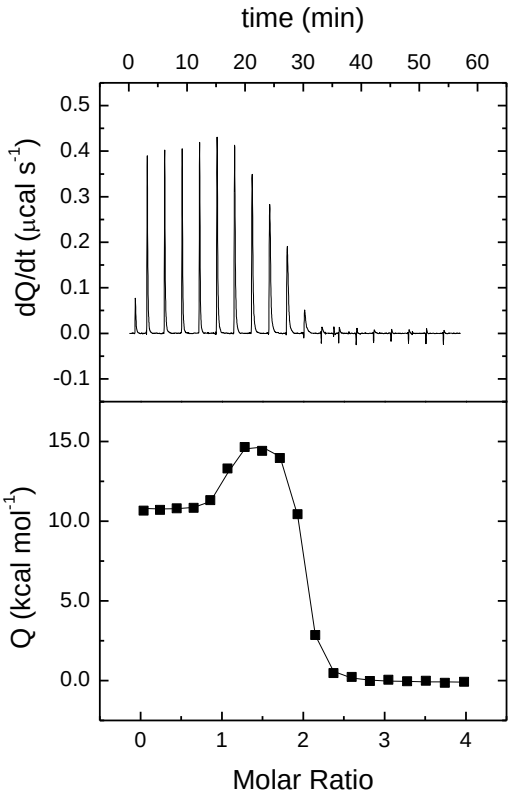

K (M^{-1})	K_D (nM)	ΔH (kcal/mol)	α	Δh (kcal/mol)	n
$1.4 \cdot 10^9$	0.71	10.9	0.024	4.4	0.95

b) SPR

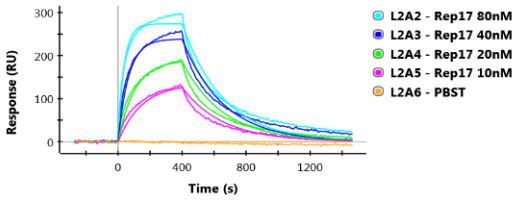

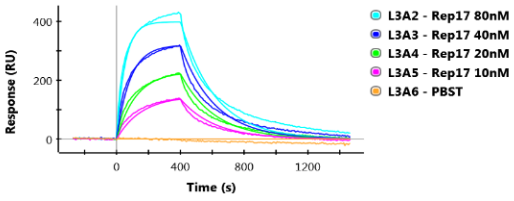

c) **BLI**

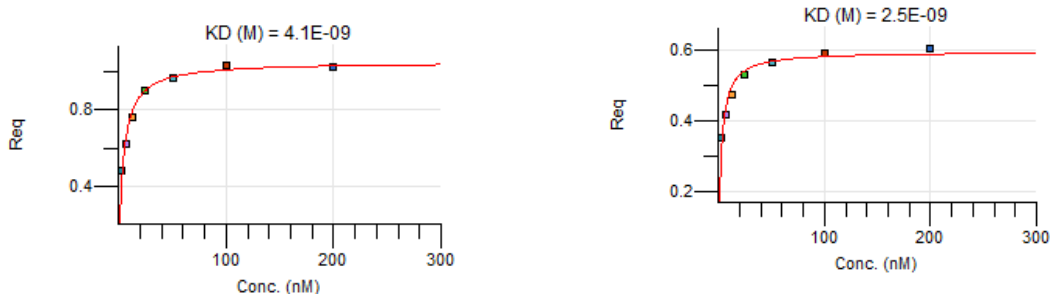

d) **switchSENSE**

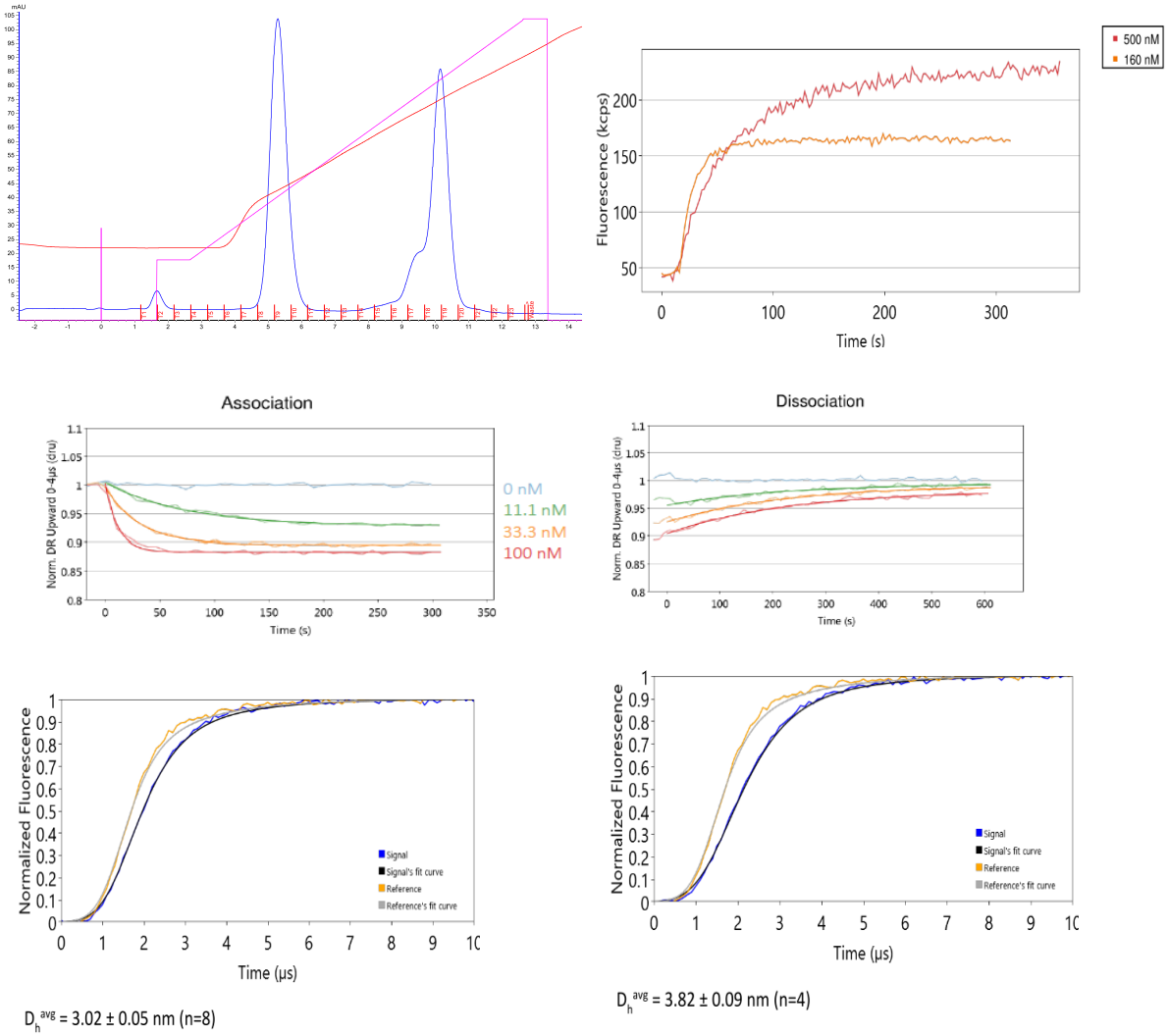

D_h^{avg} = 3.02 ± 0.05 nm (n=8)

D_h^{avg} = 3.82 ± 0.09 nm (n=4)

a) PEAQ-ITC data obtained before the training in our laboratory. K, K_D, and ΔH were the association constant, the dissociation constant, and the interaction enthalpy of either of the two binding sites when the dimer was unoccupied. α and Δh were the cooperative interaction constant and the cooperative interaction enthalpy, which modulate the binding cooperative phenomenon (a factor that modulates the binding affinity and a term that modulates the binding enthalpy to the second site when there was a site already occupied, respectively). n was the active (or binding-competent) fraction of protein, since the stoichiometry was already included in the model. K_{D1} and ΔH_1 were the intrinsic site-specific dissociation constant and binding enthalpy for the first binding site

(K_{D1} = K_D, ΔH_1 = ΔH). K_{D2} and ΔH_2 were the intrinsic site-specific dissociation constant and binding enthalpy for the second binding site ($K_{D2} = K_{D1} / \alpha$, $\Delta H_2 = \Delta H_1 + \Delta h$). b) Sensograms of alphaRep A3-Rep17 interaction measured in duplicate on a ProteON XPR36 instrument from *Biorad*. For this experiment, association and dissociation times were 400 s and 1000 s, respectively with a flow rate of 50 µL/min in phosphate buffered saline with 0.1 % Tween-20 (PBST) using His-Tag capturing (HTG) chip to immobilized A3 at 6.25 or 12.5 µg/mL during 80 s (inducing 60 RU and 95 RU, respectively). Rep17 ranges from 10 to 80 nM concentration. A k_{ON} of 2.8 10^{+5} $M^{-1}s^{-1}$, a k_{OFF} of 3.9 10^{-3} s^{-1} and a K_D of 13.8 nM were measured in the first run, and a k_{ON} of 1.8 10^{+5} $M^{-1}s^{-1}$, a k_{OFF} of 4.6 10^{-3} s^{-1} and a K_D of 25.9 nM in the second one. c) Octet RED96e BLI steady-state analysis in duplicate. Colors code of Rep17 concentrations: 3.13 nM (teal), 6.25 nM (purple), 12.5 nM (orange), 25 nM (green), 50 nM (cyan), 100 nM (red), 200 nM (blue). d) Sample preparation for switchSENSE experiments. Anion-exchange chromatogram of the A3 cross-linked protein (up, left). The cross-linked protein was the shoulder of the final peak that correspond to the free DNA. Hybridization of the cross-linked ssDNA-A3 on the chip, which carries a red fluorescent probe (up, right). Red profile corresponds to the control (free cNLB48 without protein) and the orange one to the cross-linked cNLB48-A3 conjugate. switchSENSE dynamic mode data of A3-Rep2 at three concentrations (middle, left). Normalized association (left) and dissociation (right) data were represented in function of time. switchSENSE sizing measurement of A3 hydrodynamic diameter (D_h) (bottom, left), and of the A3-Rep17 complex (bottom, right). Measured signal curve is in blue (conjugated DNA), the associated fitted curve in blank, reference signal (cNLB48) is in orange, and the associated fitted curve in grey.

Figure S3. Additional biophysical measurements of Ku-DNA interactions.

a) SEC-MALS

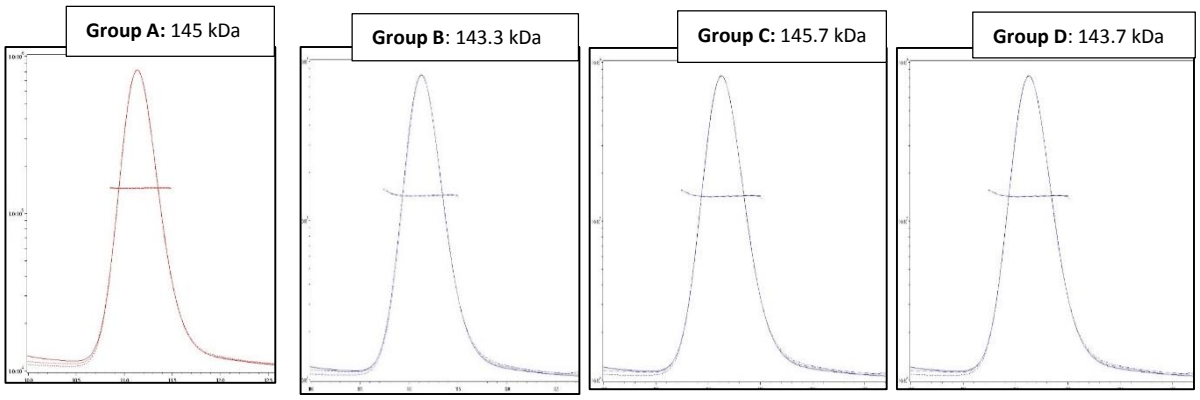

b) BLI

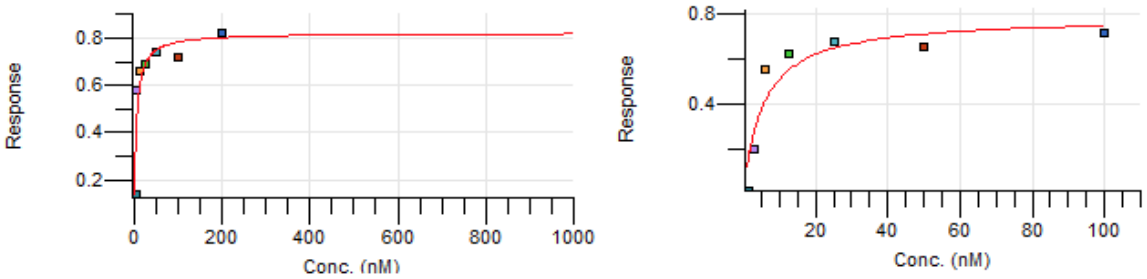

c) switchSENSE

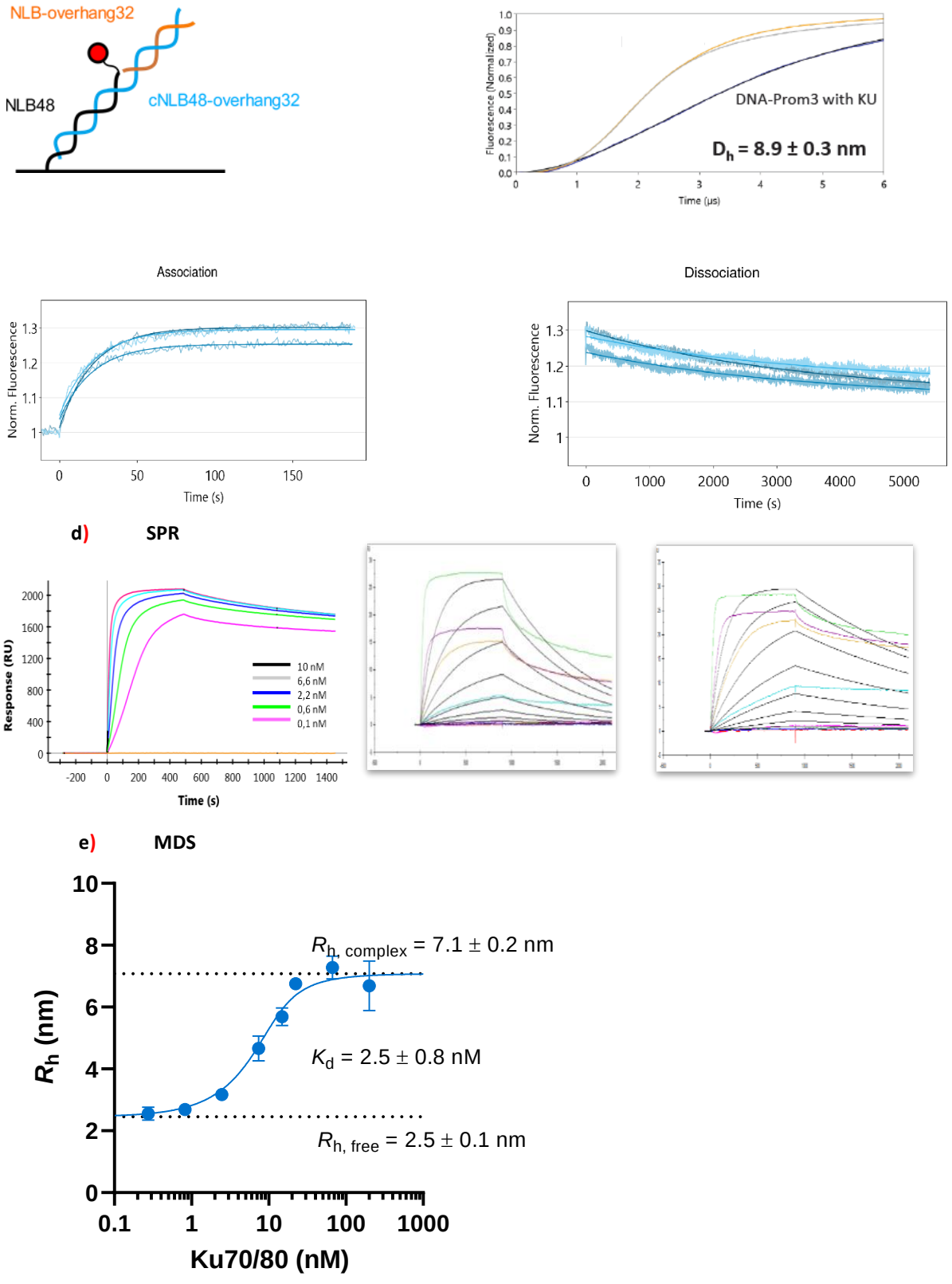

874 a) SEC-MALS elution profiles and molar masses of Ku alone in quadruple. b) Octet RED96e BLI steady-state data
875 in duplicate. Colors code of Ku concentration: 3.13 nM (teal), 6.25 nM (purple), 12.5 nM (orange), 25 nM (green),
876 50 nM (cyan), 100 nM (red), 200 nM (blue). c) switchSENSE measurement set up (top, left). By hybridization of
877 complementary DNA carrying the target sequence as overhang, the surface is functionalized with the sequence

of interest. switchSENSE static mode data of 1 Ku concentration in duplicate (bottom). switchSENSE sizing data (top, right). Reference (bare DNA) is depicted in yellow. DNA-protein-complex is depicted in blue. d) SPR sensograms by ProteON XPR36 of Ku-200 bp dsDNA interaction measured (right). A 200 bp biotinylated DNA was immobilized on a Streptavidin (NLC) chip. Ku70/Ku80 ranged from 0.1 to 10 nM concentrations, one heterodimer may induce 200 RU. A k_{ON} of 7.8 ± 4 10^{+6} $M^{-1}s^{-1}$, a k_{OFF} of 1.5 ± 0.8 10^{-4} s^{-1} and a K_D of 7.3 ± 3 nM were measured. This experiment showed the threading of Ku on DNA, approximately 10 heterodimers bound to this 200 bp DNA. SPR sensograms by BIAcore T200 of Ku-42 bp dsDNA (middle) and, Ku-60 bp dsDNA (left) interaction measured by biotinylated DNA immobilized in a serie S sensor chip SA at 10 nM concentration. Same buffer as in switchSENSE experiment adding 0.2 mg/mL of BSA, flow rates of 20 to 100 µL/min, and Ku at 5 nM as higher concentration for 900 s of association and dissociation. A k_{ON} of 1.0 10^{+6} $M^{-1}s^{-1}$, a k_{OFF} of 11.7 10^{-4} s^{-1} and a K_D of 1.2 nM (R_{max} of 32.9 RU) were measured for the 42 bp DNA and, a k_{ON} of 1.4 10^{+6} $M^{-1}s^{-1}$, a k_{OFF} of 5.0 10^{-4} s^{-1} and a K_D of 35.4 nM (R_{max} of 31.6 RU) for the 60 bp DNA. Colors code of Ku concentrations: 5 nM (light green), 2.5 nM (purple), 1.25 nM (orange), 0.625 nM (cyan), 0.3125 nM (pink), 0.156 nM (dark green), 0.078 nM (blue) and 0.039 nM (red). The differences observed in the results depend mainly on the setup strategy of the experiment. Nevertheless, open questions remain to answers: the purity of dsDNA and the stability of the protein will affect the results, but there is also the possibility of different ways of DNA fixation by Ku. e) In collaboration with *Fluidic Analytics*, we collected preliminary data to test their new instrument, Fluidity One-W with the Ku-DNA interaction. This is a novel technique in solution based in diffusional sizing of a complex in a microfluidic system. For this experiment we used the 18 bp dsDNA-FAM as before (AUC, MST) at 10 nM concentration, and 1/3 dilution of Ku70/Ku80 from 200 to 0.09 nM concentration. We were able to measure R_h (DNA alone, complex) and K_D values.

Tables

Table S1. Summary of the results for the interaction between alphaRep proteins using different techniques.

	AUC-FDS	SEC-MALS*	ITC		MST	switchSENSE		BLI		SPR*
His-A3	**Blue-NHS**	**Dimer**	**Monomer /high affinity**	**Dimer /low affinity**	**Red-His**	**Rep2***	**Rep17**	**Monomer**		**Monomer**
Ratio	1:1	1:1	1:1	1:1	N/A	1:1	1:1	N/A		N/A
K_D (nM)	13.4 ± 1.8	N/A	0.6 ± 0.1	21.3 ± 7.5	8.0	0.29 ± 0.01	0.98 ± 0.16	3.2 ± 1.1	3.3 ± 0.8	3.97 ± 1.38
k_{ON} ($M^{-1}s^{-1}$) k_{OFF} (s^{-1})	N/A	N/A	N/A	N/A	N/A	2.4 ± 0.1 10^{+6} 6.9 ± 0.2 10^{-4}	2.4 ± 0.2 10^{+6} 2.3 ± 0.3 10^{-3}	2.6 ± 0.7 10^{+5} 7.6 ± 0.7 10^{-4}	Steady-state	2.31 ± 1.79 10^{+5} 4.28 ± 0.36 10^{-3}
Other information	S (A3) = 2.2 ± 0.1 S (A3/Rep 17) = 3.0 ± 0.1	Mw (Rep2) = 11.6 kDa Mw (A3) = 44.8 kDa R_h (A3) dimer = 3nm Mw (A3/Rep2) = 65.5 kDa R_h (A3/Rep2) = 3.8 nm	ΔH = 11.6 ± 0.6 kcal/mol	ΔH = 15.5 ± 1.0 kcal/mol	N/A	D_h (A3) monomer = 3 nm D_h (A3-Rep2) = 3.8 nm	N/A	N/A	N/A	N/A

In the last column in grey, previous SPR data obtained by P. Minard's team.*Rep2

Table S2. Summary of the results for the interaction Ku-DNA using the different techniques.

	AUC-FDS	ITC		SEC-MALS	BLI		MST	switch SENSE		SPR	MDS
DNA(bp)	**18***	**18**	**42**	**42**	**42****		**18***	**48**	**80**	**200****	**18***
Ratio Ku vs DNA	1:1	1:1	2:1	2:1, 1:1	N/A		N/A	1:1		20:1	1:1
K_D (nM)	12.9 ± 3.2	0.71	3.7 ± 0.7	N/A	0.4 ± 0.1	5.2 ± 0.2	11.9	1.0 ± 0.2	3.1 ± 0.1	7.3 ± 3.0	2.5 ± 0.8
k_{ON} ($M^{-1}s^{-1}$) k_{OFF} (s^{-1})	N/A	N/A	N/A	N/A	$1.9 \pm 0.1\ 10^{+6}$ $7.2 \pm 0.3\ 10^{-4}$	N/A	N/A	$2.6 \pm 0.2\ 10^{+6}$ $2.3 \pm 0.3\ 10^{-3}$	$9.3 \pm 0.1\ 10^{+4}$ $2.8 \pm 0.1\ 10^{-4}$	$7.8 \pm 4.0\ 10^{+6}$ $1.5 \pm 0.8\ 10^{-4}$	N/A
Other information	S (DNA) = 2.2 ± 0.1 S (1:1) = 7.3 ± 0.2	ΔH = 10.9 kcal/mol n = 0.95	ΔH = 24.4 ± 2.7 kcal/mol n = 0.34 ± 0.02	Mw (DNA) = 26.1 kDa Mw (Ku) = 144.4 kDa Mw (1:1) = 171.0 kDa Mw (2:1) = 306.2 kDa	N/A	N/A	N/A	N/A	D_h = 8.9nm	N/A	Rh = 7.1 ± 0.2 nm

The last two columns came from additional data: Preliminary SPR obtained by Charbonnier's team, and MDF in collaboration with Fluidic Analytics. DNA modified *FAM or **Biotin.

Cover Letter

Click here to access/download

Supplemental Files

Cover Letter.docx